Spring 5-2013

Biological and Biologically Inspired Polymers for Interface Modification

Lea Clayton Paslay
University of Southern Mississippi

The University of Southern Mississippi

BIOLOGICAL AND BIOLOGICALLY INSPIRED POLYMERS FOR INTERFACE MODIFICATION

by

Lea Clayton Paslay

Abstract of a Dissertation
Submitted to the Graduate School
of The University of Southern Mississippi
in Partial Fulfillment of the Requirements
for the Degree of Doctor of Philosophy

May 2013

ABSTRACT

BIOLOGICAL AND BIOLOGICALLY INSPIRED POLYMERS

FOR INTERFACE MODIFICATION

by Lea Clayton Paslay

May 2013

Naturally occurring macromolecules are produced for a specific function and have the selectivity to accomplish objectives with little waste in energy. The scientific community strives to develop smart, efficient molecules on an economical scale, thus lessons can be learned from nature and applied to cost effective synthetic systems. First, the mimicry of naturally occurring antimicrobial peptides (AMPs) will be described. AMPs show great potential as alternatives to conventional antibiotics as they can selectively bind and eliminate pathogenic bacteria without harming eukaryotic tissues. Aqueous reversible addition−fragmentation chain transfer (RAFT) polymerization was utilized to prepare primary and tertiary amine containing AMP polymer mimics with precise polymerization control. The detailed synthetic strategy along with an outline of *in vitro* cell studies will be discussed in order to elucidate the effect of polymer composition on antimicrobial activity and selectivity.

The second section of this work will discuss a highly surface active protein from filamentous fungi called hydrophobin. Hydrophobins are small proteins that spontaneously self-assemble into polymeric films at interfaces. They are amphipathic in nature and form tightly bound membranes that shift the polarity of interfaces at which they assemble. This research focuses on elucidating the mechanisms and driving forces

for assembly of the ABH1 hydrophobin protein from the edible white button mushroom *Agaricus bisporus*.

The University of Southern Mississippi

BIOLOGICAL AND BIOLOGICALLY INSPIRED POLYMERS FOR INTERFACE MODIFICATION

by

Lea Clayton Paslay

A Dissertation
Submitted to the Graduate School
of The University of Southern Mississippi
in Partial Fulfillment of the Requirements
for the Degree of Doctor of Philosophy

Approved:

____Sarah Morgan_____
Director

____Robert Lochhead_____

____Charles McCormick_____

____Sabine Heinhorst_____

____Gordon Cannon_____

____Sergi Nazarenko_____

____Susan Siltanen_____
Dean of the Graduate School

May 2013

ACKNOWLEDGMENTS

First, I would like to thank my advisor, Sarah E. Morgan, for her continued guidance and support. Dr. Morgan has pushed me to be the best person, scientist, writer, communicator, and professional that I can be, and I will forever be grateful for my time as a student at The University of Southern Mississippi. I would also like to thank Dr. Morgan for all of the opportunities that were made available to me. I have had the opportunity to present my research 12 times at conferences around the country. Also, I was given the chance to pursue a three-month international research experience at the Indian Institute of Technology in New Delhi, India.

This work was supported primarily by the U.S. Department of Education GAANN Fellowship Program under Award Number P200A090066. This work was partially supported by the MRSEC Program of the National Science Foundation (NSF) under Award Number DMR 0213883 and by the National Science Foundation Award Number OISE-1132079. I would especially like to thank my committee members, Drs. Sabine Heinhorst, Gordan Cannon, Sergei Nazarenko, Charles McCormick, and Robert Lochhead, at The University of Southern Mississippi their consultation and guidance. Also, I would like to thank Professors Anushree Malik, Veena Koul, and Veena Choudhary and the rest of our collaborators at IIT Delhi for their hospitality and guidance. The NSF award DMR 1005127 supported several REU students who assisted with this project, of which I would like to acknowledge Leo Falgout, Scott Kanas, and Charlene Keyes for their contributions. I would also like to thank Lacey Harris, Chelsea Wahl, and Courtney Irby for their role in the early stages of ABH1 research and Brooks Abel and Tyler Brown for their contributions to antimicrobial polymer work.

TABLE OF CONTENTS

LIST OF TABLES

Table

LIST OF SCHEMES

Scheme

LIST OF ILLUSTRATIONS

Figure

CHAPTER I

INTRODUCTION

This dissertation is a compilation of research focused in two areas: (1) the design and synthesis of an amine containing poly(methacrylamide) system that mimics naturally occurring antimicrobial peptides and (2) the isolation and characterization of ABH1, a hydrophobin protein from the edible white button mushroom. The unifying theme of this work is interface modification. Antimicrobial peptides modify, interact with, and/or disrupt the surface of bacterial cells leading to cell death. This is interesting behavior as their cell toxicity is specific to bacterial cells. Hydrophobins are another class of protein that has high surface activity. They are amphipathic, which facilitates their self-assembly at interfaces, minimizing the tension between unlike phases. Both naturally occurring molecules fulfill complex roles in nature, however their function seems to be governed by simple interactions. It is the goal of this research to develop a better understanding of these biological systems in hopes that a fundamental knowledge will lead to the control and possible manipulation of their activities.

In the first section, a series of poly(methacrylamide) (co)polymers were designed and synthesized containing monomer units that mimic naturally occurring amino acids that are prevalent in antimicrobial peptides. In doing so, factors influencing antimicrobial and eukaryotic cell toxicity were outlined. A fundamental understanding of the factors that affect biocidal activity allows for the development of novel systems with tunable activities towards specific agents.

In the second section, ABH1 was isolated and characterized. The self-assembly behavior of the protein was investigated as a function of varying solution and

environmental factors. These studies yielded fundamental insight into the mechanisms of self-assembly and helped define methods to manipulate ABH1 activity.

CHAPTER II

ANTIMICROBIAL PEPTIDES AND THEIR POLYMER MIMICS

Chapter Overview

This chapter provides an overview of the literature regarding antimicrobial peptides (AMPs) and polymer systems that have been developed to mimic their activities. The overuse of antibiotics is a major problem in America today and it is of immense importance that novel antimicrobial therapeutics are developed. It is also well known that bacteria have begun to develop resistance to conventional antibiotics, a fact that poses a great challenge to medical providers around the world. A previous study concluded that approximately 5% of the 2,000,000 people who contract a hospital-associated infection this year will lose their lives.[1] With conventional antibiotics as the only line of defense, that number is likely to grow as bacterial strains continue to mutate. Naturally occurring AMPs show great promise as alternative therapeutics, as bacterial resistance has not been shown to readily occur.[2] AMPs show selective toxicity towards bacterial cells and remain non-toxic to eukaryotic tissues within a certain concentration range. Interest has developed in mimicking AMPs activity with synthetic polymer systems in order to provide a more economical approach to addressing the problem. AMPs are produced naturally at low levels and peptide synthesis using current laboratory techniques is arduous and expensive. The remainder of this chapter will outline the foundation for our research and discuss current limitations in the knowledge base that we intend to address.

Antimicrobial Peptides

AMPs are small biopolymers of amino acids (~20-50 amino acids in length) that selectively bind and eliminate pathogenic bacteria without harming eukaryotic cells

within a certain therapeutic range.[2-4] They are produced naturally by many complex, multi-cellular organisms and play a role in immunity processes. AMPs have diverse amino acid sequences; however, they typically display a net positive charge at physiological pH. This cationic net charge results from an abundance of basic lysine and arginine residues (Figure 1).

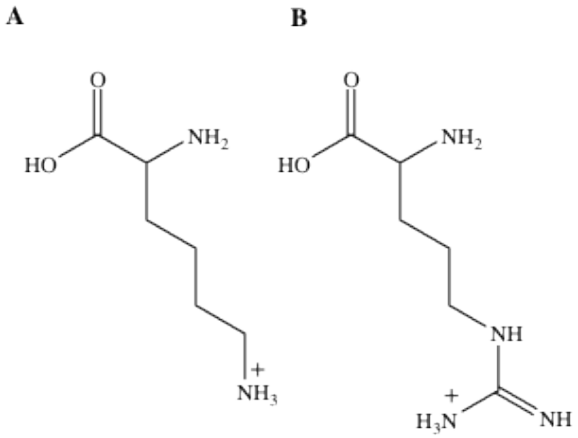

Figure 1. Structure of the amino acids (A) lysine and (B) arginine. At physiological pH (~7.4), lysine and arginine residues are protonated and positively charged.

The AMPs' ability to selectively attack bacterial pathogens rather than their own natural host tissues is governed by fundamental differences in the composition and structure of the phospholipid bilayers found in cell membranes. Bacterial cell membranes typically contain significant concentrations of phosphatidylglycerol, cardiolipin, and phosphatidylserine phospholipids that contribute anionic head groups to the outer membrane surface.[3] In contrast, eukaryotic cells are commonly rich in zwitterionic phospholipids such as phosphatidylethanolamine, phosphatidylcholine, and sphingomyelin. The net positive charge of AMPs and the net negative charge of bacterial cell membranes drives the initial attraction of the peptide to the cell surface.[3, 5] Specifically, lysine and arginine residues interact strongly with negatively charged phospholipids, allowing electrostatic interactions to govern initial binding to target cell

membranes.[3, 6] Welling et al.[7] showed that in vivo, AMPs accumulated at sights of infection very rapidly. This is important as it is critical that AMPs bind to their target before being renally cleared, a process which also occurs rapidly for small molecules.[8] After binding to the negatively charged phospholipid, hydrophobic moieties of the peptide interact with the inner hydrophobic core of the bacterial membrane leading to a disruption in integrity and subsequent cell death. One commonly accepted model for the membrane disruption process is depicted in Scheme 1.

Other that membrane disruption, AMPs have been shown to cause membrane depolarization which corrupts cell processes such as water and ion transport.[9] AMPs can also inhibit extracellular protein synthesis[10] and intracellular functions by binding nucleic acids.[11] It is possible that an individual peptide could work simultaneously via several mechanisms or that multiple peptides could work in unison to reach appropriate target-cell toxicity.

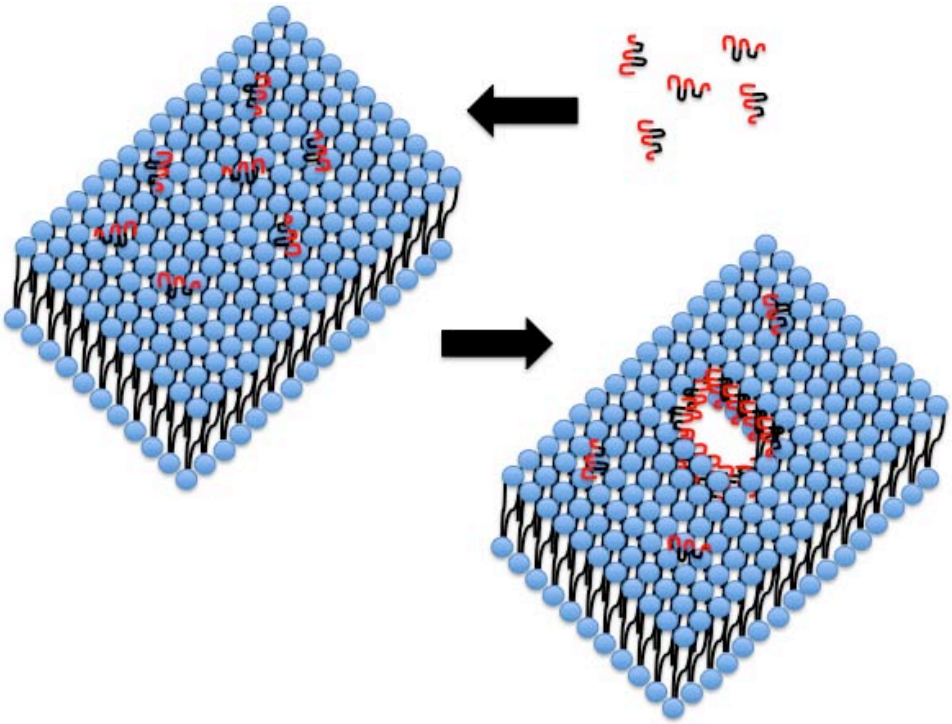

Scheme 1. The barrel-stave model of AMP biocidal mechanism. Modified from Brogden et al.[4]

Research has shown that a balance between the ratio of cationic and hydrophobic residues (amphiphilic balance) of AMPs is important in realizing antimicrobial behavior. Wieprecht et al.[12] concluded that tuning the amphiphilicity of AMPs plays a major role in their antimicrobial activity and that shifting the balance towards excessive hydrophobicity leads to mammalian cell toxicity. In addition to maintaining a proper amphiphilic balance, the conformations that AMPs adopt often indicate whether or not they will be toxic to eukaryotic cells. Typically, AMPs that form structures with a high degree of helicity or amphiphilicity, which causes segregation into domains, lead to an increased toxicity to mammalian cells.[13] An example of domain segregation would be a facially amphipathic helix. Interestingly enough, many AMPs exist as unstructured random coils in extracellular solution, however upon binding to their target cell, they organize into functional, *active* secondary structures.

AMPs show great promise as therapeutic agents for infections and in general biocidal applications; however, they are produced naturally at low levels and synthesizing them in the laboratory is quite expensive. For this reason, there is extensive interest in developing synthetic systems that mimic AMP behavior.

Synthetic AMP Mimics

Several research groups have synthesized low molecular weight oligomers which possess antimicrobial properties.[14-17] However, this research will focus on polymers which mimic the natural size of AMPs.

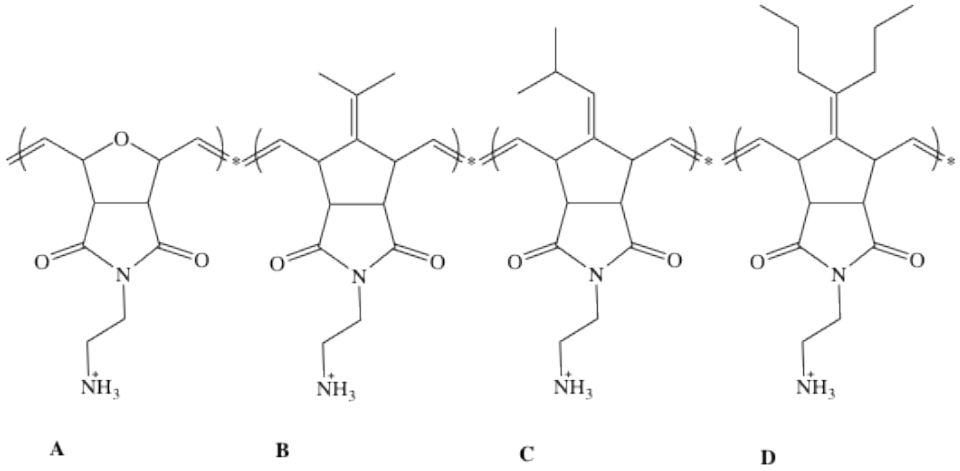

Figure 2. Shifting the amphiphilic nature of polynorbornene derivatives.[18]

Ilker et al.[18] utilized polynorbornene derivatives in an attempt to mimic AMPs. The polymers shown in Figure 2 were polymerized via ring opening metathesis polymerization (ROMP). The primary amine attached to polymers A-D resembles the functional side chain (R group) of lysine and enables electrostatic binding to anionic phospholipids. In order to control the amphiphilicity, the authors varied the monomer hydrophobic alkyl chain length and structure. In moving from polymer A to polymer D an increase in hydrophobic character is observed. The authors found polymer A to be ineffective at eliminating bacteria (*inactive*), but that increasing the hydrophobic content

(i.e., polymers B-D) increased the antimicrobial nature. Unfortunately, as the hydrophobicity was increased so too was toxicity toward eukaryotic cells. Polymer B presented weak bacterial toxicity, but excellent eukaryotic red blood cell (RBC) compatibility. Polymer C presented exceptional antimicrobial activity; however, it was also toxic to eukaryotic cells. The authors, in an attempt to fine tune the amphiphilic balance, polymerized a statistical copolymer, poly(B-co-C) at a B_{90}:C_{10} ratio. With this formulation, selective synthetic mimics were produced that possessed the antimicrobial properties of polymer C with the biocompatibility of polymer B.

In a later communication, Gabriel et al.[19] replaced the primary amine of polymer A with a guanidinium moiety (Figure 3A). This substitution caused the *inactive* polymer A to become both antimicrobial and non-disruptive to eukaryotic cell membranes. It is important to note that the incorporation of the guanidinium moiety shifted the hydrophobic character of the system, making it slightly more hydrophobic; therefore, the authors not only changed the cation structure, but also shifted the amphiphilic nature of the system. Both the structure/nature of the cation and the overall amphiphilicity of the polymer seem to be important variables that contribute to polymer activity. Polymer C (antimicrobial and toxic to eukaryotic cells) caused cell mimics to aggregate and leak internal components via membrane disruption while the guanidinium-substituted polymer A caused no apparent membrane disruption or cell aggregation. This was attributed to the fact that the guanidinium moiety facilitated polymer transport through the membrane, and it was hypothesized that it induced bacterial cell death by binding internal cellular targets such as anionic nucleic acids.

Al-Badri et al.[20] also monitored the effect of charge density on selectivity. The number of pendant primary amines was increased on polymer C from 1 to 3 (Figure 3B). Increasing the charge density led to retained antimicrobial activity while improving biocompatibility. While not observed in this study, there may be an upper limit at which increasing the cationic character has no beneficial affect on selectivity.[21]

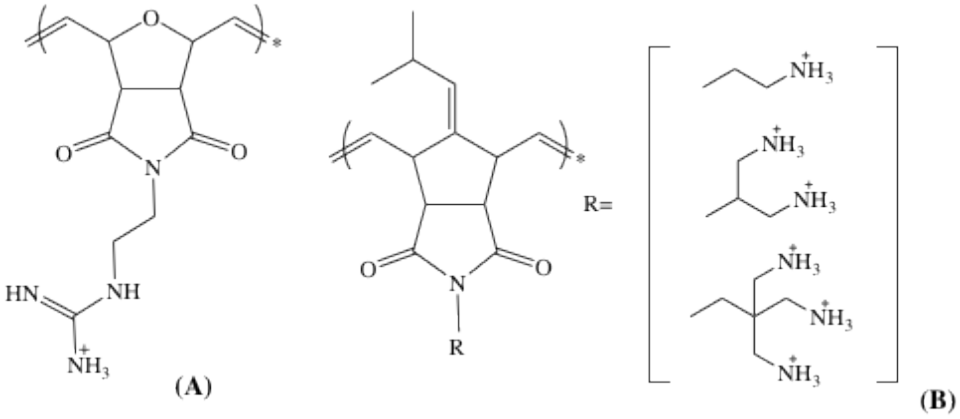

Figure 3. (A) Guanidinium substituted polymer A[19] and (B) polymer C with varying charge density.[20]

Tuning the amphiphilicity is extremely important in obtaining molecules that selectively eliminate bacterial cells over eukaryotic cells. The relative hydrophobicity of the polymer played a primary role in determining its antimicrobial nature and its eukaryotic biocompatibility.

Lienkamp et al.[22] took another approach at creating tunable polymer systems by utilizing a norbornene derivative that contained a reactive anhydride group to which a hydrophilic cation and hydrophobic alkyl chain could be attached. Figure 4 shows the polymer system post anhydride reaction and polymerization.

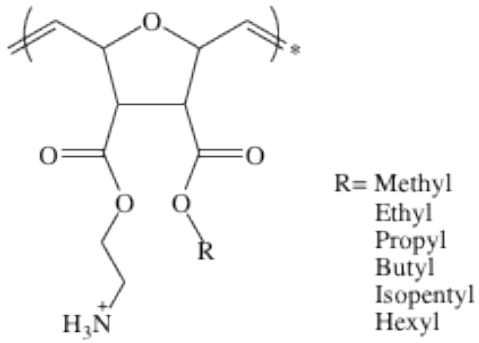

Figure 4. Amphiphilic polynorbornene derivatives with tunable antimicrobial properties.[22]

From this polymer design, the authors were able to create a library of polymers with tunable amphiphilicities and molecular weights, from which selective polymers were obtained. Not only were the polymers generally selective towards bacteria over eukaryotic RBCs, but they could also be tuned to show activity towards individual bacteria species such as *Staphylococcus aureas*.

In a recent communication Mowery et al.[23] prepared statistical copolymers of β-lactams to form the amphipathic, antimicrobial polymer shown in Figure 5.

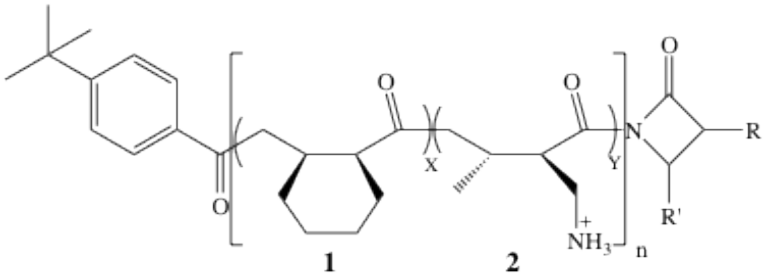

Figure 5. Polymerization of novel β-lactams to produce tunable antimicrobial polymers.[23]

The authors varied the ratio of monomer 1 and monomer 2 in an attempt to tune the antimicrobial and hemolytic (i.e., causing red blood cell destruction) behavior, and found that polymers containing less than 50% of monomer 2 were extremely hemolytic. A DP of 15-20 was targeted and PDIs ranging from 1.3-1.7 were obtained. At a monomer 2

content of 60%, the polymer showed toxicity towards a range of bacterial species; however, it was still hemolytic at relatively low concentrations. In a later study, Epand et al.[24] concluded that these β-lactam polymers were able to penetrate through the lipid membranes of vesicles mimicking of Gram-positive and Gram-negative bacteria at low concentration; however, when the concentration was raised the polymers remained bound to the membrane and caused vesicle aggregation. This fact indicates a concentration dependent mechanism of activity.

Venkataraman et al.[25] used RAFT polymerization to create antimicrobial pegylated polymers from methacrylate derivatives. The authors statistically polymerized 3-(dimethylamino)ethyl-methacrylate (DMAEMA) and oligo(ethylene glycol)methylether-methacrylate (OEGMA) and then performed post polymerization quaternization of the DMAEMA nitrogen with different halide functional species, testing the relationship of chain length and chemical group to antimicrobial properties. It was concluded that shorter hydrophobic chain lengths (i.e., methyl and ethyl) produced polymers with the best antimicrobial properties. As observed with other systems, it was concluded that tuning the amphiphilic nature of the polymer had a large impact on its antimicrobial characteristics.

Kuroda et al.[26] synthesized poly(methacrylate) derivatives via free radical polymerization. Figure 6A depicts the polymer structure.

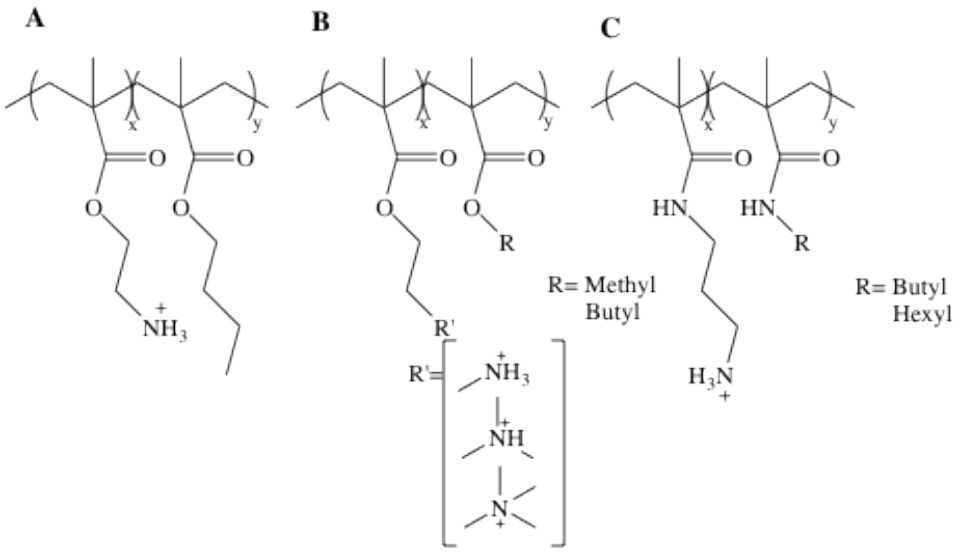

Figure 6. Free radical polymerization of methacrylate (A)[26] and (B)[27] and methacrylamide (C)[28] derivatives to form membrane active polymers.

The authors obtained reasonable antimicrobial properties; however, these polymers were relatively hemolytic compared to the other systems discussed. This is attributed to the fact that the amphipathic balance of the overall polymer system could not be tuned, as the butyl alkyl chain is the only hydrophobic component studied. The effect of pendant amine structure on antimicrobial activity was described for low molecular weight (DP = 6-10) random copolymers prepared from similar methacrylate derivatives (Figure 6B).[27] Within this system, it was concluded that primary amines helped to maximize antimicrobial properties, while quaternary ammonium-containing polymers required the addition of excess hydrophobic functionality to realize potent activity. It was reported that, in general, as polymer hydrophobicity increased so too did hemotoxicity. To decrease the overall hydrophobicity, primary amine-containing poly(methacrylamide) derivatives of the above system were prepared in order to replace acrylate linkages with amide linkages for all side chains (Figure 6C).[28] The homopolymer of the primary amine-containing methacrylamide monomer was found to provide significantly higher

antimicrobial activity than that of the poly(methacrylate) version, reportedly due to improved hydration of the polymer backbone. Recent work by Palermo et al. on poly(methacrylate) systems discussed the effect of the spacing of cations from the backbone main chain on antimicrobial properties[29] and the preparation of self-degrading polymers[30] that exploit the inherent properties of acrylate linkages to promote hydrolysis.

From previous research performed on AMPs and AMP mimics, it is clear that any attempts at creating novel systems must meet a few main requirements.[31] The system must contain cationic charges, which facilitate binding to anionic bacterial phospholipids, and its amphiphilic balance must be highly tunable in order to achieve microbial toxicity while maintaining hemo-compatibility.

Current Limitations and Objectives of Research

While creating polymers that are toxic to bacterial cells has not been a problem, achieving selective toxicity has proven to be a challenge. Great care must be taken in order to fine tune the amphiphilic balance so that electrostatic interactions govern initial cell binding. Once hydrophobicity reaches a certain threshold, hydrophobic interactions dominate cell binding and the polymers lose their selectivity. Along with the need for complex design strategies, the polymerization of primary amine containing polymers often requires the use of protecting group chemistry which adds additional unwanted reaction steps.

Based on the report of Palermo et al.[28] showing increased antimicrobial activity for methacrylamide-containing polymers, we were interested in determining the degree to which selective toxicity could be controlled in poly(methacrylamide) (co)polymers through changes of the cation structure and the placement of hydrophobic moieties. In

contrast to the poly(methacrylate) systems explored previously,[27] all of the methacrylamide monomers employed in our study are fully water soluble, with the direct incorporation of hydrophobic moieties onto the hydrophilic monomer side chain. This methodology eliminates the need to add lipophilic comonomers and allows for controlled polymerization to be carried out in aqueous media via RAFT polymerization. Aqueous RAFT polymerization allows the production of statistical copolymers of precise molecular weight and narrow molecular weight distribution, mimicking those of natural AMPs. Low molecular weights were targeted for these AMP mimics to eliminate the need for biodegradation of polymers within the body, given that small macromolecules are removed from the body by the renal system.[32]

The following research involving polymers designed to mimic AMPs is split into 3 sections:

1. Antimicrobial poly(methacrylamide) derivatives prepared via Aqueous RAFT polymerization exhibit biocidal efficiency dependent upon cation structure;

2. Polymerization and characterization of poly(methacrylamide) polymer brushes;

3. Synthesis of poly(methacrylamide) derivatives containing varying ratios of primary amine and guanidinium moities.

In the first section, we describe the use of aqueous RAFT polymerization to copolymerize N-(3-aminopropyl)methacrylamide (APMA), which mimics the cationic amino acid lysine, with N-[3-(dimethylamino)propyl]methacrylamide (DMAPMA) or N-[3-(diethylamino)propyl]methacrylamide (DEAPMA), both of which impart hydrophobic character to the amines while maintaining water-solubility of each of the individual

monomers. The rational for imparting hydrophobic character while maintaining overall hydrophilicity of each monomer is that we hypothesize that eukaryotic cytotoxicity will be decreased as compared to that exhibited by previously reported AMP mimics. To our knowledge, aqueous RAFT polymerization has not previously been reported for preparation of AMP-mimicking antimicrobial polymers. Aqueous RAFT facilitates the polymerization of primary amines without the need for protecting group chemistry or organic solvents.[33, 34] A series of copolymers was prepared with systematic variation of (1) the ratio of primary to tertiary amine and (2) the concentration and structure of hydrophobic groups (DMAPMA and DEAPMA comonomers) in order to gain greater understanding of the effects of the individual components on selective toxicity. The controlled polymerization of APMA and DMAPMA has been demonstrated previously by our research team.[35, 36] However, using aqueous RAFT to polymerize DEAPMA has, to our knowledge, not yet been reported. The true novelty of this system lies in its controlled distribution of cationic monomers which allows for a better definition of the structural characteristics necessary to obtain highly selective antimicrobial agents for a poly(methacrylamide) based system. The antimicrobial activity of the polymers against *E. coli* (EC) (Gram-negative) and *B. subtilis* (BS)(Gram-positive) was analyzed as a function of buffer type, salt concentration, pH, and time. Hemolytic behavior and cell viability studies with selected polymers were performed.

The second section serves as a continuation of the research in the first section. In order to determine the effectiveness of our poly(methacrylamide) system as an antimicrobial coating, silicon wafers were functionalized with free radical initiators and APMA polymer brushes were *grafted from* the surface. APMA polymer brushes were

synthesized via two methods. Silicon wafers were functionalized with either an azobisisobutyronitrile (AIBN) or an Irgacure derivative using silane chemistry. APMA was then polymerized from the functionalized substrate by thermal or photo-initiated processes, dependent upon the initiator. The surfaces were characterized via ATR-FTIR, ellipsometry, water contact angle goniometry, and AFM.

The third section focuses on the on the synthesis and characterization of poly(methacrylamide) (co)polymers that contain a second amino acid mimicking moiety, guanidinium. As noted previously, the incorporation of a guanidino moiety has been shown to change the antimicrobial mechanism.[19] Utilizing the statistical, well-defined control of aqueous RAFT polymerization, a series of (co)polymers was prepared with systematic variation in composition (i.e., primary amine versus guanidino containing monomers). We hypothesize that detailing the activity of this well-defined distribution will allow for the determination of critical monomer ratios that result in the onset of biocidal mechanism shift. A better understanding of mechanistic shift could allow for the specific targeting of individual bacteria types. For this research, APMA and 3-(guanidino)propyl methacrylamide (GPMA) were chosen as the monomer units to mimic the amino acids lysine and arginine, respectively.

CHAPTER III

EXPERIMENTAL DETAIL FOR ANTIMICROBIAL PEPTIDE POLYMER MIMICS

Research Overview

The major goal of the study was to define the roles of cation structure and distribution of hydrophobic moieties surrounding protonated amines in determining the selective toxicity behavior of poly(methacrylamide) derivatives. The synthesis of amine containing methacrylamide polymers was performed via aqueous RAFT polymerization. Structure/property relationships were developed for relating pendant amine type to antimicrobial activity and eukaryotic biocompatibility. In a follow-up study, poly(methacrylamide) derivatives were *grafted from* a silicon substrate with the future goal of evaluating this systems functionality as an antimicrobial coating. Also, the synthesis of statistical poly(methacrylamide) (co)polymers containing varying ratios of primary amine and guanidino moieties was performed via aqueous RAFT polymerization with the future goal outlining the role that each moiety plays in determining the antimicrobial mechanism.

Materials

Triethylamine, 99.5% (Sigma Aldrich), methacryloyl chloride, >97% (Fluka) and N-[3-(dimethylamino)propyl]methacrylamide, 99% (Sigma Aldrich) were purchased and further purified via distillation prior to use. 3-diethylaminopropyl-amine, 99+% (Acros Organics), ethyl acetate (Fisher Scientific), 4,4’-azobis(4-cyanovaleric acid) (Sigma Aldrich), methanol, anhydrous, 99.8% (Sigma Aldrich), sodium acetate anhydrous (Fisher Scientific), acetic acid, glacial (Fisher Scientific), deuterium oxide, 99.9 atom % D (Sigma Aldrich), chloroform-d, 99.8 atom % D (Cambridge Isotope Laboratories,

Inc.), N-(3-aminopropyl)methacrylamide (Polysciences, Inc.), sodium sulfate, powder, >99%, A.C.S. reagent, anhydrous (Sigma Aldrich), *Escherichia coli (αDH5) and Bacillus subtilis* (obtained from the central microbial culture facility, Department of Biotechnology & Biochemical Engineering, Indian Institute of Technology, Delhi, India), Luria broth (Himedia, India), Luria agar (Himedia, India), tris(hydroxymethyl)aminomethane (Sisco Research Laboratories PVT. LTD., India), potassium dihydrogen phosphate (Merck, India), disodium hydrogen orthophosphate (Qualigens, India), sodium chloride (Qualigens, India), hydrochloric acid (Merck, India), sterile discs, diameter 6 mm (Sigma–Aldrich, India), Triton-X 100 (Merck, India), MCF-7 cells (NCCS, Pune, India), Dulbecco's Modified Eagle Media (DMEM) (Himedia, India), fetal bovine serum (Himedia, India), Trypsin-EDTA Solution 1X (Himedia, India), Antibiotic Solution 100X Liquid (Himedia, India), (3-(4,5-dimethylthiazol-2-yl)-2,5-diphenyltetrazolium bromide (MTT) (Sigma-Aldrich, India), dimethyl sulfoxide (DMSO) (Merck, India), silicon wafers (Silicon Inc.), acetone (Fisher), anhydrous toluene (Sigma), potassium carbonate (Sigma) and N,N'-Di-Boc-1H-pyrazole-1-carboxamidine (Aldrich) were purchased and used as received.

Methods

Synthesis of N-[3-(Diethylamino)Propyl]Methacrylamide (DEAPMA).

To an ice cooled solution of triethylamine (90 mL) 3-(diethylamino)propyl-amine (7.50 mL, 47.2 mmol) and ethyl acetate (30 mL) were added. Methacryloyl chloride (9.24 mL, 94.5 mmol) was added dropwise over the course of 10 min. An additional 50 mL of ethyl acetate was added and the reaction progressed for 2 hr. After the reaction was completed, the mixture was further diluted with ethyl acetate to a final volume of 1

L. The solution was filtered of insoluble salts and the solvents were removed by rotary evaporation. DEAPMA was purified by distillation (115 °C, 0.38 mm Hg) and isolated as a light yellow oil (see Figure 7 for ^{1}H NMR spectrum). The reaction yield calculated after distillation was approximately 54%, however it is expected that yield can be significantly increased through optimization of the distillation procedure. ^{1}H NMR (300 MHz, CDCl3): δ [ppm] 8.12 (s, 1H), 5.67 (s, 1H), 5.25 (s, 1H), 3.45-3.32 (m, 2H), 2.61-2.43 (m, 6H), 1.91 (s, 3H), 1.74-1.57 (m, 2H), 1.00 (t, 6H).

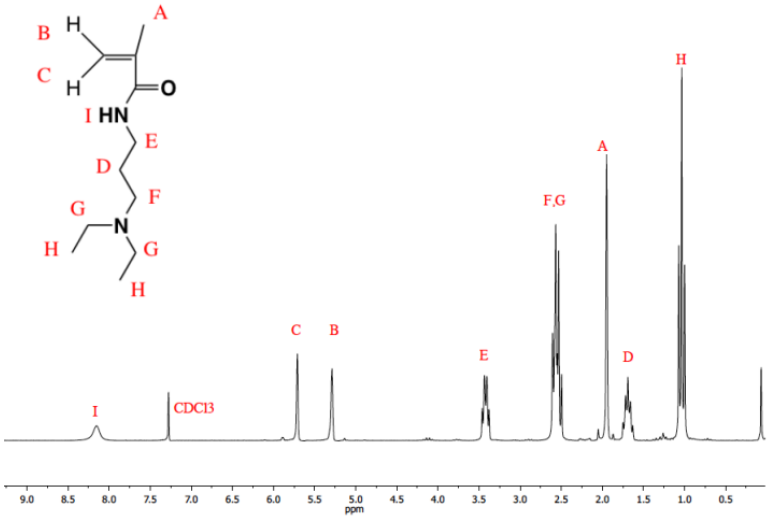

Figure 7. ^{1}H NMR spectrum of DEAPMA after distillation.

Polymerization of Antimicrobial Peptide (AMP) Mimics

By way of aqueous RAFT polymerization, polymer molecular weights were targeted by selecting appropriate initial monomer and CTA concentrations. The ratio of M_0:CTA_0 was set to be approximately 30:1 to yield a degree of polymerization of ~30, which mimics the size of naturally occurring AMPs. 4-cyano-4-(ethylsulfanylthiocarbonylsulfanyl)pentanoic acid (CEP) was used as the CTA and was synthesized via previously published procedures,[37] while 4,4'-Azobis(4-cyanopentanoic

acid) was used as the initiator. For all polymerizations, CTA_0/I_0=5. The polymerization took place in aqueous acetate buffer (pH 5) at 70 °C[38] for 6 hr (see Scheme 2). Methanol was added in low quantities (~30%) to improve the solubility of CEP in the aqueous media. After the reactions were completed the solutions were exposed to air and quenched in liquid nitrogen. The solutions were then dialyzed against water for 72 hr followed by lyophilization for 72 hr and the samples were then stored in desiccant. A representative yield was calculated to be 75% of the theoretical yield. Some polymer is lost in dialysis due to excessive swelling of the dialysis tubing as a result of internal osmotic pressure. This loss can be minimized by making the water slightly acidic during the dialysis procedure to reduce the extent of swelling.

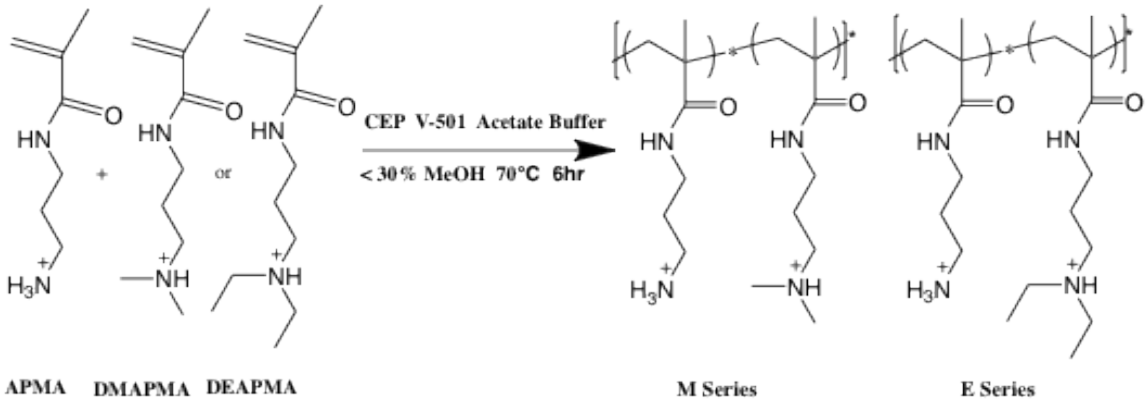

Scheme 2. Statistical polymerization of APMA with DMAPMA or DEAPMA to vary amine structure and hydrophobic functional group size.

Nuclear Magnetic Resonance (NMR)

^{1}H NMR was performed with a Varian Mercury^{PLUS} 300 MHz spectrometer in $CDCl_3$, utilizing delay times of 5 s to determine monomer purity. A 500 MHz NMR equipped with a standard 5 mm ^{1}H/^{13}C probe and operating at 499.77 MHz (^{1}H) was used to identify the homopolymer structures of PAPMA, PDMAPMA, PDEAPMA and the statistical structures of the PAPMA-*stat*-PDMAPMA (M Series) and the PAPMA-*stat*-

PDEAPMA (E Series) copolymer series in D_2O. Sixty-four scans were taken for each experiment with a 3.1 second recycle delay. For each of the homopolymers, unique peak assignments were made, and the copolymer compositions were calculated for the statistical polymers via peak integration (see Figures 8 and 9 for representative spectra).

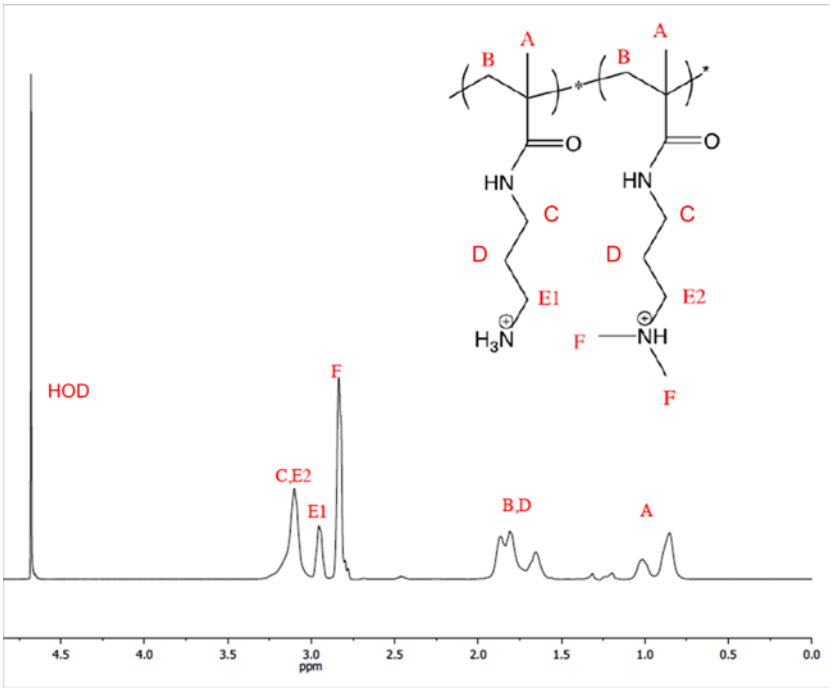

Figure 8. ^{1}H NMR spectrum of a representative PAPMA-***stat***-PDMAPMA copolymer. Peak integration values indicate 49.7% contribution from APMA (Target = 50%).

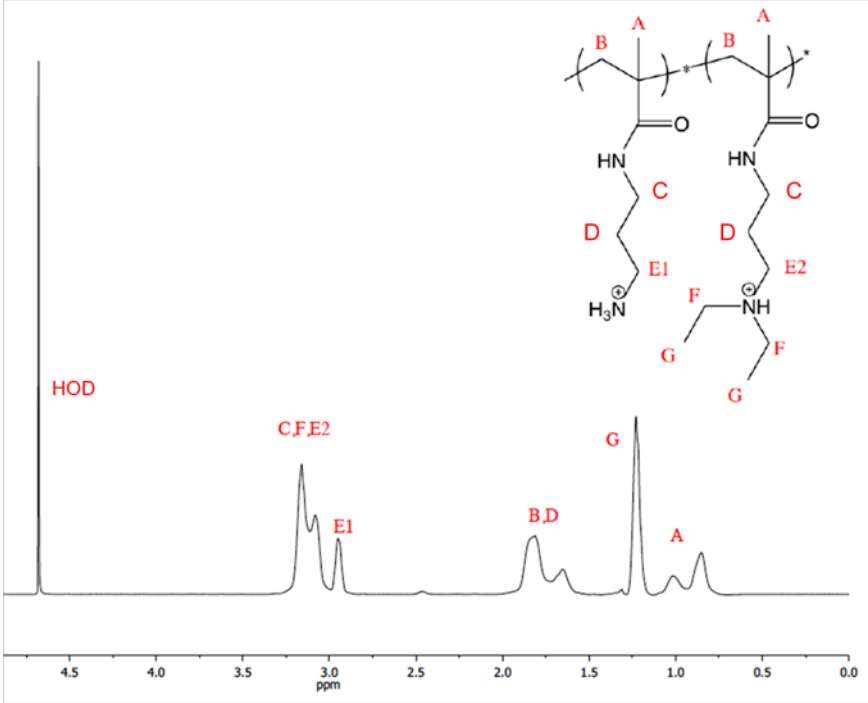

Figure 9. ^{1}H NMR spectrum of a representative PAPMA-***stat***-PDEAPMA copolymer. Peak integration values indicate 48.2% contribution from APMA (Target = 43%).

Aqueous Size Exclusion Chromatography

The molecular weight and polydispersity index (PDI) of the polymers were determined by aqueous size exclusion chromatography (ASEC) coupled with multi-angle laser light scattering (MALLS). Eprogen CATSEC columns (100, 300 and 1000 Å) were used in combination with a Wyatt Optilab DSP interferometric refractometer (k = 690 nm) and a Wyatt DAWN DSP MALLS detector (k = 633 nm). 1 wt% acetic acid/ 0.1 M Na_2SO_4 (aq) was used as the eluent at a flow rate of 0.25 mL/min. The interferometric refractometer was utilized off-line to determine dn/dc values for PAPMA, PDMAPMA and PDEAPMA at 25 °C in the eluent (0.2000 mL/g, 0.2086 mL/g and 0.1930 mL/g, respectively) in order to assign absolute molecular weight values to all polymers. For the statistical polymers the dn/dc values were calculated as the mole fraction-averaged composites of the measured homopolymer dn/dc values using the copolymer

compositions determined by NMR. Wyatt ASTRA SEC/LS software was used for molecular weight and PDI calculations.

Determining Antimicrobial Activity of Polymers

Broth Microdilution Method. Polymer antimicrobial activity was determined against EC (Gram-negative) and BS (Gram-positive) bacteria by modifications of previously published procedures.[19] Bacteria glycerol stocks were inoculated into Luria broth (LB) and allowed to grow overnight at 37 °C under shaking conditions. Polymer stock solutions (4-6 mg/mL) for all polymers were prepared in tris(hydroxymethyl)aminomethane (TRIS) (10 mM), TRIS buffered saline (TBS) (10 mM TRIS, 150 mM NaCl) and phosphate buffered saline (PBS) (12 mM NaH_2PO_4, 1 mM K_2HPO_4, 140 mM NaCl). Each buffer was titrated to a pH of either 6.8 or 7.4 with 6 N HCl and further diluted via serial dilution to afford a range of polymer concentrations. The overnight cultures of bacteria were diluted with fresh LB to an optical density of 0.001 at 600 nm (OD_{600}) and mixed 1:1 with buffered polymer dilutions in a 96 well plate. These mixtures were then incubated under shaking conditions at 37 °C for 24 hr. The OD_{600} was measured using a BioTek PowerWave XS2 UV-Visible plate reader after 6 and 24 hr of incubation. Minimum inhibitory concentrations (MIC) are reported for each measurement time as the concentration at which no bacterial growth was observed.

Agar Plate Conformation of MIC. Utilizing the broth microdilution method, polymer solutions (TBS, pH 7.4) at concentrations above and below the observed MIC were inoculated with EC and BS for 24 hr at 37 °C (shaking). Inoculums from each well were streaked onto sterile LB agar plates and incubated for an additional 18 hr at 37 °C. Viable bacteria cells present in the wells are observed as visible bacteria colonies on the

agar plates. All experiments were run in duplicate and photographs were taken using a digital camera.

Zone of Inhibition Method. Disc susceptibility tests were used to determine antimicrobial activity as a corroborating test to the broth microdilution method.[39] Sterile LB agar plates were prepared, and 100 μL of bacteria inoculums (either EC or BS at an OD_{600} of 0.001) were spread evenly on the surface. Samples were allowed to dry for 5 min. Three sterile discs were fixated on the top of the agar and impregnated with either 10 or 20 μL polymer solution from an initial 6 mg/mL stock (TBS pH 7.4). The plates were allowed to incubate for 18 and 48 hr for BS and EC, respectively, at 30 °C. All experiments were run in duplicate and photographs were taken using a digital camera.

Determining Eukaryotic Biocompatibility

Hemolysis. Hemolysis experiments were performed according to previously published procedures[18] with slight modifications. Human blood was obtained from AIIMS hospital in New Delhi, India. Red blood cells (RBCs) were separated from the whole blood via centrifugation at 1500 rpm for 10 min. RBCs (30 μL) were suspended in 10 mL TBS (pH 7.4), rinsed 3 times by centrifugation (10 min at 1500 rpm), and then re-suspended in 10 mL TBS. Polymers were dissolved in TBS (pH 7.4) to create 6.0 mg/mL stock solutions. These solutions were further diluted to 0.1, 0.2, 2.0, 4.0, and 6.0 mg/mL. RBC suspensions were incubated 1:1 at 37 °C (light shaking) for 30 min with polymer dilutions in microcentrifuge tubes to afford final polymer concentrations of 0.05, 0.1, 1.0, 2.0, and 3.0 mg/mL within the total volume of solution. After incubation, the tubes were centrifuged at 1500 rpm for 10 min. The supernatant from each tube was transferred to individual wells in a 96 well plate and the absorbance was measured at 540

nm. Positive and negative controls for 100 and 0% hemolysis were obtained by 1% TRITON-X and TBS, respectively.

MTT Assay (Cell Viability). An MTT assay was performed on MCF-7 cell lines using standard procedures[40] with slight modification. Cells were cultured on tissue culture polystyrene flacon flasks in DMEM media supplemented with 10% fetal calf serum and 1% antibiotic solution (Penicillin and Streptomycin) at 37 °C in a 5% CO_2 incubator. After obtaining ~80% confluence the cells were trypsinized and counted on a hemocytometer. The cells in fresh media were seeded into a 96 well plate ($8x10^3$ cells/well) and incubated for 24 hr at 37 °C in a 5% CO_2 incubator. Next, the media was removed from each well and 100 μL of fresh media was added. To select wells (in triplicate) were added 50 μL of polymer solutions at various concentrations (90, 225, 375, and 6000 μg/mL). The resulting solutions had final polymer concentrations of 30, 75, 125, and 2000 μg/mL, respectively. For a positive control, 50 μL TBS (pH 7.4) was used, while 50 μL 3% Triton-X was used as a negative control. Reported data is normalized for viability observed in the positive control (taken as 100% viability). The plate was incubated for 6 or 12 hr at 37 °C in a 5% CO_2 incubator. After incubation, the media was removed from each well and 100 μL of fresh media was added. Next, 10 μL of MTT reagent (MTT dissolved in TBS at 5 mg/mL concentration) was added to each well and samples were incubated for an additional 4 hrs. The media from each well was then removed and replaced with 100 μL of DMSO to solubilize the formed formazan crystals. Absorbance readings at 570 nm were recorded using a BioTek PowerWave XS2 UV-Visible plate reader.

Silicon Substrates Cleaning

Silicon wafers were cleaned using a previously developed procedure.[41] Wafers were cut into 1.2 in x 1.0 in rectangles and subsequently sonicated twice for 5 min each in DI water, acetone, ethanol and toluene. Wafers were then dried under a stream of N_2 gas and exposed to UV-ozone treatment for 45 min. The substrates were stored in a 120°C oven until use.

Silicon Functionalization with AIBN-Trichlorosilane Initiator

AIBN-trichlorosilane was synthesized via a previously developed procedure[41] and supplied as a part of collaborative research. Substrates (two wafers oriented back-to-back, polished side out) were transferred into a dry, septum-sealed test tubes containing a toluene solution of AIBN-trichlorosilane (4 mmol, 13 mL) and triethylamine (Et_3N, 0.2 mL). Substrates were allowed to react for 45 min and were then rinsed and sonicated in toluene and dried with a stream of N_2 gas. If not used immediately, initiator substrates were stored in the dark at -20 °C in dry toluene.

Silicon Functionalization with Irgacure-Trichlorosilane Initiator

HPP-trichlorosilane (the Irgacure initiator) was synthesized as previously described[42] and in toluene (4 mM) was immobilized on the SiO_2 surface at room temperature using excess triethylamine as an acid scavenger for ~ 1 hr. The samples were then cleaned by rinsing with toluene and methanol and dried under a stream of N_2 gas. The functionalized silicon wafers were stored in dry toluene at -20°C until use.

Deprotection of the Irgacure-Initiator Functionalized Surface[42]

The acetate protection group was removed by immersing the wafers prepared above in a suspension of 240 mg K_2CO_3 in 12 mL methanol containing 150 µL H_2O for 1

hr. The substrate was subsequently washed with water, methanol, and toluene, followed by drying with a stream of N_2.

Thermal Polymerization of PAPMA Brushes

In a typical thermal polymerization of PAPMA brushes, an AIBN initiator functionalized substrate was placed in a test tube that contained a 1M solution of APMA in DMSO. The solution was degassed by purging with N_2 for 1 hr before being placed in an oil bath at 120°C. After 24h the substrate was removed, sonicated in DMSO and H_2O and dried under N_2 flow. The substrates were stored in desiccant until they were characterized.

Photopolymerization of PAPMA Brushes

In a typical photopolymerization of APMA, an Irgacure-functionalized substrate was placed in a test tube that contained a solution of 1 M APMA in DMSO. The solution was purged with N_2 for 1 hr. The reaction was carried out under the UV intensity of 330mW/cm^2 for 2 hr. The substrate was removed, sonicated in DMSO and H_2O and dried under N_2 flow. The substrates were stored in desiccant until they were characterized.

Ellipsometry

Ellipsometry measurements were carried out using a Gaertner Scientific Corporation LSE ellipsometer with a 632.8 nm laser at 70° from the normal. Refractive indices of 3.89 for silicon, 1.46 for silicon oxide, 1.43 for initiator, and 1.5 for the polymer were used in the calculation of film thickness.

Contact Angle Goniometry

Contact angle measurements were conducted via the sessile drop technique using a Ramé-Hart goniometer coupled with DROP-image® data analysis software to monitor

the change in water contact angle upon modification of the silicon substrates. The static contact angle formed by drops of HPLC grade water (11 μL) was measured on each surface immediately after deposition.

Attenuated Total Reflectance Fourier Transform Infrared Spectroscopy (ATR-FTIR)

IR spectra of surface polymers were obtained using a ThermoScientific FTIR instrument (Nicolet 8700) equipped with a VariGATR™ accessory (grazing angle 65°, germanium crystal; Harrick Scientific). Spectra were collected with a resolution of 4 cm^{-1} by accumulating a minimum of 128 scans per sample. All spectra were collected while purging the VariGATR™ attachment and FTIR instrument with N2 gas along the infrared beam path to minimize the peaks corresponding to atmospheric moisture and CO_2.

Atomic Force Microscopy (AFM)

The surface coverage, topography and morphology of PAPMA brush functionalized substrates were studied using a Bruker Dimension Icon scanning probe microscope in Scan Asyst mode in a temperature (25 °C) and humidity (50% RH) controlled room with a standard Bruker SCANASYST-AIR probe (nominal force constant: 0.4 N/m and resonance frequency: 70 kHz). Height, phase and amplitude images were collected simultaneously. The resolution was held constant at 512 x 512 data points. The images shown were chosen to best represent the samples as multiple scans were taken for each sample on macroscopically separated regions of the substrate. All standard image processing techniques were performed on Bruker image analysis software.

Synthesis of Boc-Protected GPMA

In a 250 mL round bottom flask, APMA HCl was dissolved in a mixture of 12 mL DI H_2O and 20 mL (148 mmol) TEA and stirred at 25 °C. 10 g (32 mmol) N,N'-di-boc-1H-pyrazole-1-carboxamidine (PCA) was dissolved in 108 mL acetonitrile and added dropwise to the stirring APMA solution via an addition funnel over the course of 30 min. The reaction progressed for 24 hr. The product was obtained via filtration and then washed three times with 50 mL DI water (yield = 91%).

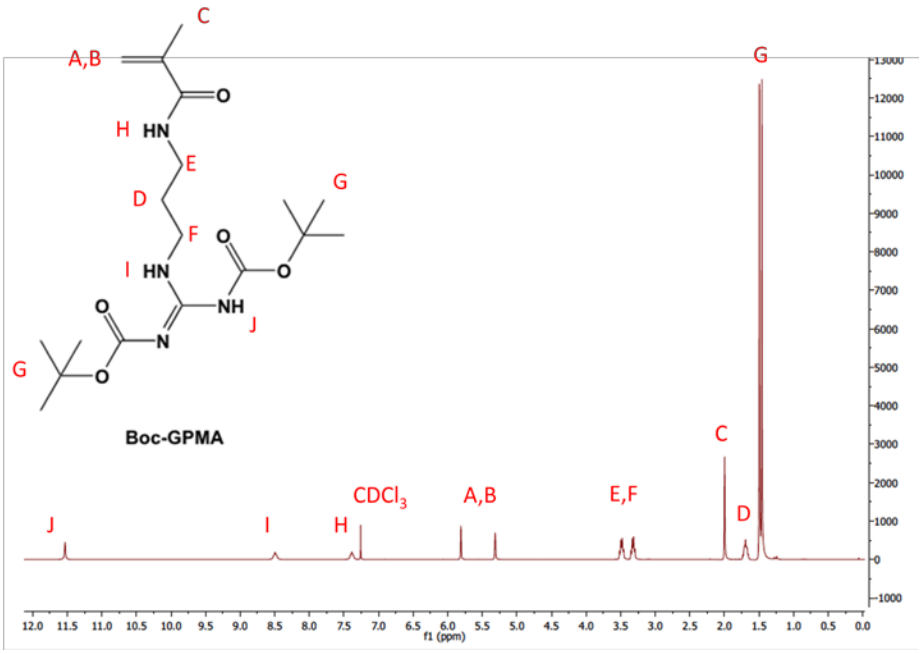

Figure 10. ^{1}H NMR spectrum of boc-protected GPMA.

Deprotection of Boc-Protected GPMA

In a 250 mL round bottom flask, 10.96 g (28.48 mmol) boc-protected GPMA was dissolved in 87 mL CH_2Cl_2 stirring at 0 °C. 87 mL (1.14 mol) (20 equivalences per boc-protecting group) trifluoroacetic acid (TFA) was then added to the solution dropwise via an addition funnel and the reaction was allowed to progress for 16 hr warming from 0 °C to 25 °C. The solvents were removed via rotary evaporation, and the resulting clear

viscous oil was dissolved in 250 mL DI H_2O, frozen in liquid N_2 and lyophilized for 48 hr. The product was obtained as a white solid.

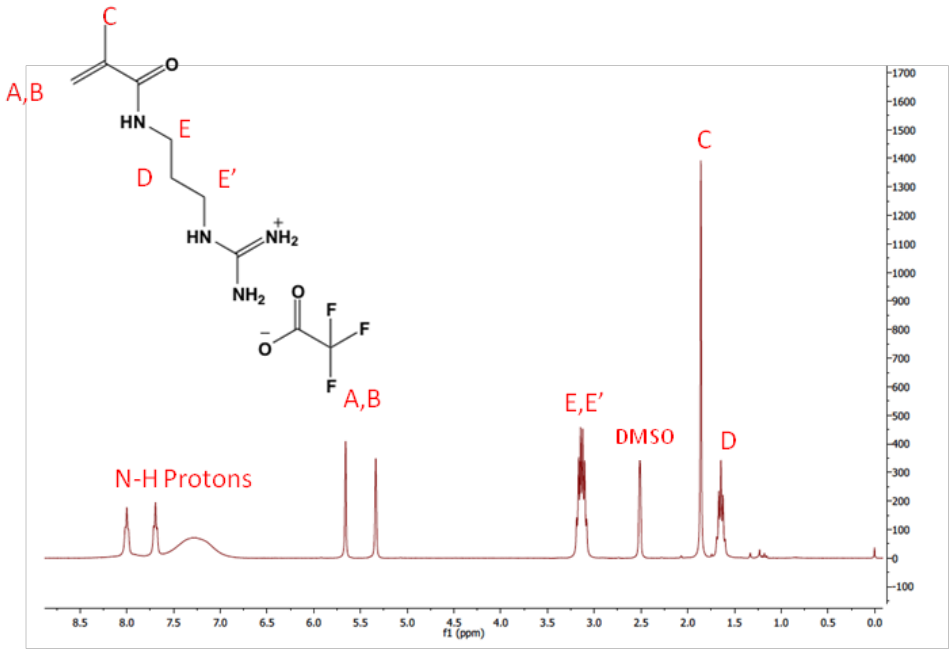

Figure 11. ^{1}H NMR spectrum of GPMA after boc-deprotection with TFA.

Synthesis and Characterization of APMA-stat-GPMA (Co)Polymers

The synthesis and polymer characterization of APMA-***stat***-GPMA (co)polymers was carried out as described for APMA-***stat***-DMAPMA and APMA-***stat***-DEAPMA (co)polymers with minor modifications.

CHAPTER IV

ANTIMICROBIAL POLY(METHACRYLAMIDE) DERIVATIVES PREPARED VIA AQUEOUS RAFT POLYMERIZATION EXHIBIT BIOCIDAL EFFICIENCY DEPENDENT UPON CATION STRUCTURE

Chapter Overview

Antimicrobial peptides (AMPs) show great potential as alternative therapeutic agents to conventional antibiotics as they can selectively bind and eliminate pathogenic bacteria without harming eukaryotic cells. It is of interest to develop synthetic macromolecules that mimic AMP behavior, but that can be produced more economically at commercial scale. The goal of the study was to define the roles of cation structure and distribution of hydrophobic substituents on protonated amines in determining the selective toxicity behavior of poly(methacrylamide) derivatives. N-(3-aminopropyl)methacrylamide (APMA) was statistically copolymerized with N-[3-(dimethylamino)propyl]methacrylamide (DMAPMA) or N-[3-(diethylamino)propyl]methacrylamide (DEAPMA) to afford a range of (co)polymer compositions. Analysis of antimicrobial activity against *E. coli* (EC)(Gram-negative) and *B. subtilis* (BS)(Gram-positive) as a function of buffer type, salt concentration, pH, and time indicated that polymers containing large fractions of primary amine were most effective against both strains of bacteria. Under physiological pH and salt conditions, the polymer with the highest primary amine content caused complete inhibition of bacterial growth at low concentrations, while negligible hemolysis was observed over the full range of concentrations tested, indicating exceptional selectivity. The cytotoxicity of select polymers was evaluated against MCF-7 cells.

Synthesis of Antimicrobial Peptide Mimics

For this work, methacrylamide monomers were chosen due to their hydrolytic stability, structural similarity to amino acids found in naturally occurring AMPs, incorporation of hydrophobic and hydrophilic moieties, and pKa values. APMA was chosen due to its similarity to lysine. Many research groups have demonstrated that in addition to electrostatic attraction, hydrophobic functionality is required to realize antimicrobial activity. While ionic bonding facilitates initial polymer-cell interactions, it is the hydrophobic substituents that act to disrupt the lipid membrane of bacteria. DMAPMA and DEAPMA were chosen due to their hydrophobic dimethyl and diethyl amino groups, respectively. Previous literature reports suggested that tuning the amphiphilic balance is important in obtaining selective antimicrobial agents,[18] thus DMAPMA and DEAPMA monomers were selected to allow manipulation of the relative hydrophobicity of the system. Simultaneously, systematic variation of the copolymer composition utilizing these monomers facilitates study of the effect of cation structure on antimicrobial efficiency in (poly)methacrylamide systems. Additionally, all comonomers studied are expected to remain charged at physiological pH. PAPMA was reported to be essentially fully protonated over a pH range of 6-8.[28] PDMAPMA has been shown to have a pKa of approximately 8.8,[43] and, thus, following the Henderson – Hasselbalch equation, it is expected that >96% of the monomers will be charged at physiological pH. PDEAPMA is expected to follow a similar trend as PDMAPMA with a slightly higher pKa. In the poly(methacrylate) copolymers studied previously,[27] because of the lower pKa values in these systems, partial protonation of the amine groups (and thus greater hydrophobicity) occurred under physiological pH test conditions. As the PDEAPMA and

PDMAPMA copolymers in the present study remain essentially fully charged under the test conditions, it is possible to separate the effects of cation structure from those of charge density on antimicrobial efficiency.

Eleven polymers were synthesized using identical polymerization conditions with varying monomer type and monomer feed ratio. APMA, DMAPMA, and DEAPMA were each homopolymerized and unique ^{1}H chemical shifts were assigned. Copolymers were formed by copolymerizing APMA with DMAPMA and APMA with DEAPMA at varying ratios (Scheme 2). For simplicity of nomenclature, each (co)polymer was given a letter based on its composition of tertiary amine. For example, Polymer 1, composed of 70 % APMA and 30 % DMAPMA is named M30 with "M" representing the di-methyl tertiary amine and the "30" representing its mole percent. Similarly, the letter "E" represents the di-ethyl tertiary amine (DEAPMA) comonomer. Table 1 summarizes polymer molecular weights and monomer compositions.

Table 1

Molecular Weight and Composition Data for Synthesized (Co)polymers

Polymer	mol% DMAPMPA (theory)	mol% DEAPMA (theory)	mol% APMA (theory)	mol% APMA (exp)[a]	$M_{n,th}$ (g/mol)[b]	$M_{n,exp}$ (g/mol)[c]	PDI[c]	dn/nc[d]
1 (M30)	37	-	63	70	4905	5343	1.06	0.2026
2 (M41)	56	-	44	59	5032	5023	1.06	0.2036
3 (M50)	50	-	50	50	5100	5110	1.04	0.2045
4 (M72)	79	-	21	28	5187	5601	1.05	0.2062
5 (M100)	100	-	-	0	5328	6006	1.06	0.2086
6 (PAPMA)	-	-	100	100	4656	5194	1.05	0.2000
7 (E39)	-	37	63	61	5287	6674	1.08	0.1973
8 (E43)	-	47	53	57	5177	6292	1.11	0.1970
9 (E52)	-	57	43	48	5560	6369	1.12	0.1965
10 (E71)	-	78	22	29	5844	5263	1.09	0.1950
11 (E100)	-	100	-	0	6150	7124	1.10	0.1930

[a]Determined by ^{1}H NMR. [b]Based upon 80% conversion of [M_0]. [c]Determined by ASEC-MALLS. [d]Determined by a Wyatt Optilab DSP interferometric refractometer.

Antimicrobial Activity

The biocidal nature of the polymers was probed first by the broth microdilution method. All polymers were tested against EC and BS, and minimum inhibitory concentration (MIC) values were reported as a function of saline concentration, incubation time (6 and 24 hours), polymer concentration (0-2 mg/mL), polymer composition (effect of hydrophobic functionality and cation architecture), and bacterial cell line. The presence of salt is known to induce the anti-polyelectrolyte effect;[44] thus, it was necessary to determine if physiological salt conditions would influence polymer-cell electrostatic interaction. Table 2 provides a summary of MIC data after 24 hr of incubation.

Table 2

Twenty-Four Hour Minimum Inhibitory Concentration Values

	MIC μg/mL					
Polymer	E. coli (Tris)	E. coli (TBS)	E. coli (PBS)	B. subtilis (Tris)	B. subtilis (TBS)	B. subtilis (PBS)
1 (M30)	10	10	25	50	100	100
2 (M41)	10	25	25	75	125	125
3 (M50)	10	25	25	75	250	125
4 (M72)	10	25	25	100	500	250
5 (M100)	10	25	25	250	500	500
6 (PAPMA)	5	25	25	50	50	100
7 (E39)	10	25	25	75	250	500
8 (E43)	10	25	25	75	250	250
9 (E52)	10	25	25	100	250	250
10 (E71)	10	50	125	250	2000	2000
11 (E100)	5	25	50	500	>2000	>2000

Note. Minimum Inhibitory concentration (MIC) = concentration of polymer required to completely inhibit bacterial growth. Values determined by microdilution assays. The addition of salt to the solution media weakens polymer / cell interactions. Against BS, as the amount of tertiary amine increases within each copolymer series the amount of polymer needed to achieve complete inhibition also increases. (pH=6.8)

The data show that activity depends on the bacterium studied, the buffer solution in which the test was performed, and, for the tests using BS, the copolymer composition.

In general, high antimicrobial activity (defined as an MIC value of 100 μg/mL or lower) was exhibited by all of the polymers against EC. Exceptionally high activity was observed in TRIS buffer, which does not contain additional NaCl. In the TBS buffer system (TRIS plus 150 mM NaCl), the MIC values increased slightly; however, all polymers demonstrate very high activity against EC. Similar trends were observed when the polymers were dissolved in PBS buffer. Against the Gram-positive bacteria, BS, on the other hand, generally lower antimicrobial efficiency is observed. Other than the obvious difference in outer cell structure (Gram-positive vs Gram-negative), the most observable difference between EC and BS was their speed of growth in microdilution assays. BS control samples consistently displayed higher OD_{600} values after 6 hr incubations, indicating a faster growth rate. This will be discussed further in later sections. Biocidal activity against BS was influenced to a large extent by polymer composition and buffer type. Polymers M30 and PAPMA ($PAPMA_{20}$-stat-$PDMAPMA_9$ and the $PAPMA_{25}$ homopolymer, respectively) showed the lowest MIC values against BS in each of the three buffers. As the concentration of tertiary amine-containing monomer (DMAPMA or DEAPMA) increased within each copolymer series the effectiveness against BS decreased. Figure 12 provides a more detailed analysis of the relationship of the activity against BS.

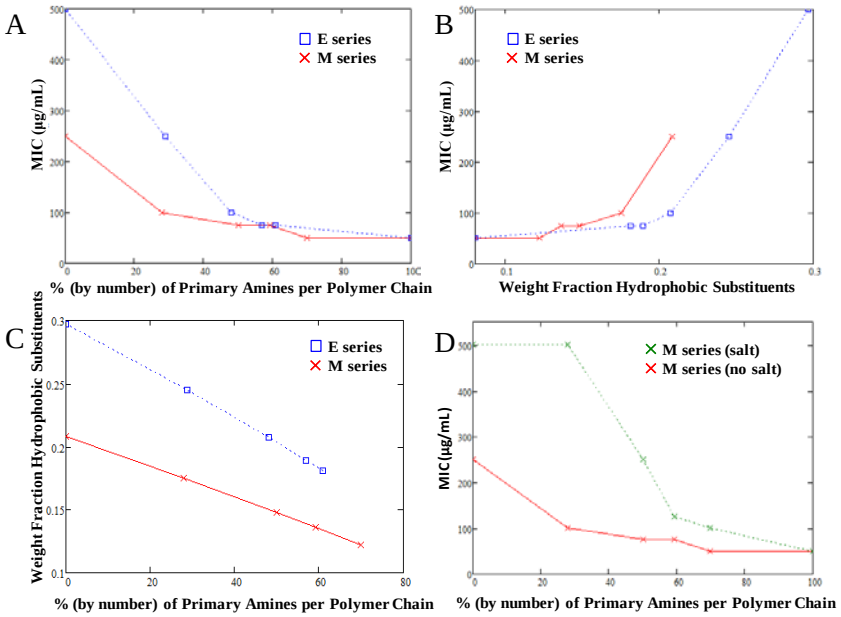

Figure 12. Analysis of activity against BS as a function of copolymer composition. M series is PAPMA-stat-PDMAPMA copolymers while E series is PAPMA-stat-PDEAPMA copolymers. The solvent for (A), (B) and (C) is Tris buffer, while Tris buffer and Tris buffered saline were used for (D). (A) represents the relationship between MIC and primary amine content. (B) represents the relationship between the weight fraction of hydrophobic groups of each polymer and the observed MIC. (C) Depicts the linear relationship between % primary amine and the weight fraction of hydrophobic groups for each polymer system. (D) Isolates the role of amine structure on MIC by the introduction of salt into the solution media.

Both series show a decrease in MIC with an increase in primary amine content (Figure 12A**)**. Series E (PAPMA-stat-PDEAPMA copolymers) shows a sharp increase in MIC below 48% (by number) APMA, whereas Series M (PAPMA-stat-PDMAPMA copolymers) shows a less severe increase below 28% APMA. We attribute the differences in MIC behavior to the weaker association of the diethyl-substituted tertiary amine of the DEAPMA copolymers with the bacterial membrane than the association of the dimethyl-substituted tertiary amine of the DMAPMA copolymers, primarily due to greater steric hindrance. This leads to a requirement for higher primary amine ratios in the DEAPMA polymers to achieve comparable MIC values. Figure 12B shows MIC as a function of the weight fraction of hydrophobic groups, calculated as the total molecular

weight of alkyl chains on the polymer available to interact with the bacterial membrane (defined as the methyl groups pendant to the polymer backbone and the methyl and ethyl substituents of the tertiary amines) divided by the total molecular weight of the polymer (determined by ASEC-MALLS). This parameter provides a relative value for the degree of hydrophobic modification (by weight) in our methacrylate copolymers as the copolymer composition shifts. The observation made clear in Figure 12B is that as the weight fraction of hydrophobic substituents is increased within each series, MIC increases. However, there is no direct correlation between hydrophobic substituent weight fraction and MIC when comparing M and E series. At equivalent weight fractions of hydrophobic substituents, E series has a lower fraction of tertiary amine, as its substituents are of a larger mass. Therefore, since a lower MIC is observed for E series than M series at equivalent hydrophobic substituent fractions, the evidence suggests that amine type is the primary factor influencing MIC. However, it is difficult to completely separate the contributions of hydrophobicity and cation structure on antimicrobial activity, as they are linearly correlated in our copolymer systems, as shown in Figure 12 C. To further define the effects of cation structure on antimicrobial activity, MIC was evaluated in the presence of added salt. The addition of salt is known to weaken or shield electrostatic interaction. Figure 12D shows that the introduction of NaCl causes an increase in MIC for M series polymers. This shift is greatest when the primary amine fraction (by number) drops below 60%, indicating that the tertiary amine moieties are more susceptible to electrostatic shielding. PAPMA (100% primary amine) is unaffected by added NaCl, indicating a strong attraction to BS. A similar trend was observed for E series polymers (graph not shown).

Steric hindrance, due to the bulky methyl and ethyl substituents on the tertiary amines, limits interactions between the polymers and the bacteria. It is likely that the primary amine of the APMA monomer is more effective at binding (and staying bound) to negatively charged phospholipids. Palermo et al.[45] reported a similar finding, in which they concluded that ammonium containing poly(methacrylate) derivatives interacted more strongly with lipid membranes than did tertiary or quaternary amines. Since the PAPMA homopolymer shows the highest level of activity, it appears that the methyl group on the PAPMA backbone adds sufficient lipophilic character to cause membrane disruption and the additional hydrophobic groups of the PDMAPMA and PDEAPMA pendant amines are not necessary. Conversely, if the biocidal activity for this system is realized through a cellular aggregation mechanism,[24] then the additional hydrophobic groups may not influence antimicrobial activity. In this case, the strong binding affinity between negatively charged phospholipids and protonated primary amines,[6] serving to agglomerate cells, is the main driving force.

Against BS, under all buffering conditions, DEAPMA-containing (co)polymers show reduced biocidal activity compared to DMAPMA-containing polymers. Previous systems reported in the literature rarely show a decrease in activity with increasing hydrophobicity as long as the system maintains solubility; therefore, we attribute the observed decrease in activity towards BS to the tertiary amine's weakened ability to interact with the bacterial membrane. All polymers are effective against the relatively slower growing EC, yet when the rate of growth is increased, the polymers with the highest content of primary amine show higher performance. It appears that the rapidity

and strength of the initial polymer ionic attachment to the bacteria controls the biocidal effectiveness against BS.

MIC levels were evaluated for each polymer against BS after 6 and 24 hr incubation (TBS pH 6.8) in order to gain a better understanding of activity as a function of time (Table 3). In all cases, the concentration required to inhibit growth for only 6 hr was lower. This indicates that inhibiting growth or at least keeping growth below an observable level for a given period of time does not necessarily mean that complete bacterial death is obtained.

Table 3

MIC Values Measured After 6 and 24 Hours

	MIC (μg/mL)	
Polymer	B. subtilis (6 hr)	B. subtilis (24 hr)
1 (M30)	25	100
2 (M41)	25	125
3 (M50)	25	250
4 (M72)	75	500
5 (M100)	50	500
6 (PAPMA)	25	50
7 (E39)	50	250
8 (E43)	25	250
9 (E52)	25	250
10 (E71)	250	2000
11 (E100)	100	>2000

Note. Buffer = TBS pH 6.8

While it is difficult to compare reported antimicrobial activity of copolymers analyzed in separate studies because of differences in testing protocols (i.e., buffer conditions, bacterial strain, and bacterial concentration), it is clear that the most potent (co)polymers in our study yield MIC values at least as effective as those of other successful systems presented in the literature. Polymers M30, PAPMA, and E39 were chosen for further characterization because they demonstrated the greatest antimicrobial activity in the above studies. Using the microdilution method, antimicrobial activity was determined for the polymers after they had been dissolved in TBS at a more physiologically relevant pH of 7.4 (the pH of blood). Table 4 summarizes the MIC values determined for EC and BS at 6 and 24 hr time intervals. Against EC, the MIC for polymers M30 and PAPMA was 30 μg/mL, while polymer E39 showed a MIC of 40 μg/mL after 24 hr. For the same time of incubation, polymers M30 and PAPMA exhibited a MIC of 70 μg/mL, while polymer E39 showed a MIC of 170 μg/mL against BS. MIC values obtained at pH 6.8 and pH 7.4 were similar, indicating that within the chosen pH range, the polymers maintain activity.

Table 4

MIC Values After 6 and 24 Hours for a Physiologically Relevant pH

	MIC (μg/mL)			
Polymer	E. coli (6 hr)	E. coli (24 hr)	B. subtilis (6 hr)	B. subtilis (24 hr)
1 (M30)	30	30	20	70
6 (PAPMA)	30	30	20	70
7 (E39)	40	50	30	170

Note. Buffer = TBS pH 7.4

To illustrate the biocidal activity of polymers M30, PAPMA, and E39, inoculums from 24 hr incubations with polymer concentrations ranging from below to above their respective MICs were streaked onto freshly prepared agar plates and incubated for 24 hr at 37 °C. Figure 13 gives pictorial evidence that live colony forming units are not present in inoculums derived from broth microdilutions above the determined MIC values. Thus, it can be concluded that the polymers induce cell death rather than solely inhibit cell growth. In the case of BS, polymer PAPMA showed slight growth at 60 μg/mL; thus, the MIC is reported as 70 μg/mL to be conservative.

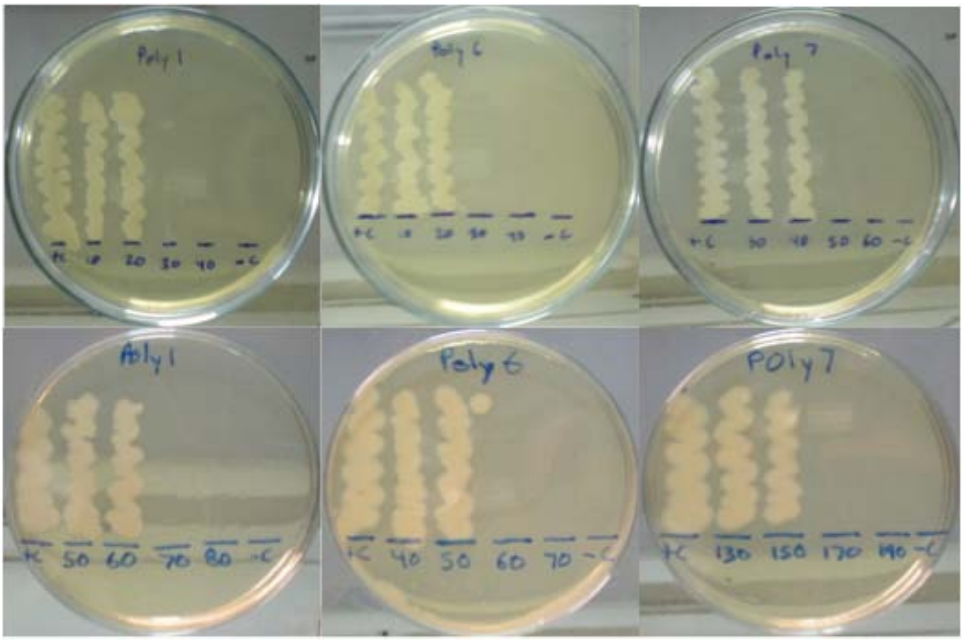

Figure 13. MIC confirmation via agar plate visualization (polymer solvent = TBS pH 7.4). +C is positive control (bacteria in growth media plus TBS without polymer) and –C is negative control (polymer in TBS and bacterial growth media without the presence of bacteria). Numbers refer to final polymer concentration in μg/mL. EC (top) and BS (bottom) growth is observed below MIC, however complete cell death is obtained above MIC. As observed in microdilution assays, polymers 1 (M30) and 6 (PAPMA) show similar MIC levels where polymer 7 (E39) requires a slightly higher concentration to cause complete inhibition. Each experiment was run in duplicate.

To confirm antimicrobial activity by a secondary technique, zone of inhibition measurements were performed. Sterile agar plates were prepared and inoculated with either EC or BS and sterile disks loaded with varying amounts of polymer were fixated onto the top of the agar and incubated at 30 °C. Figure 14 shows the results of disk susceptibility tests.

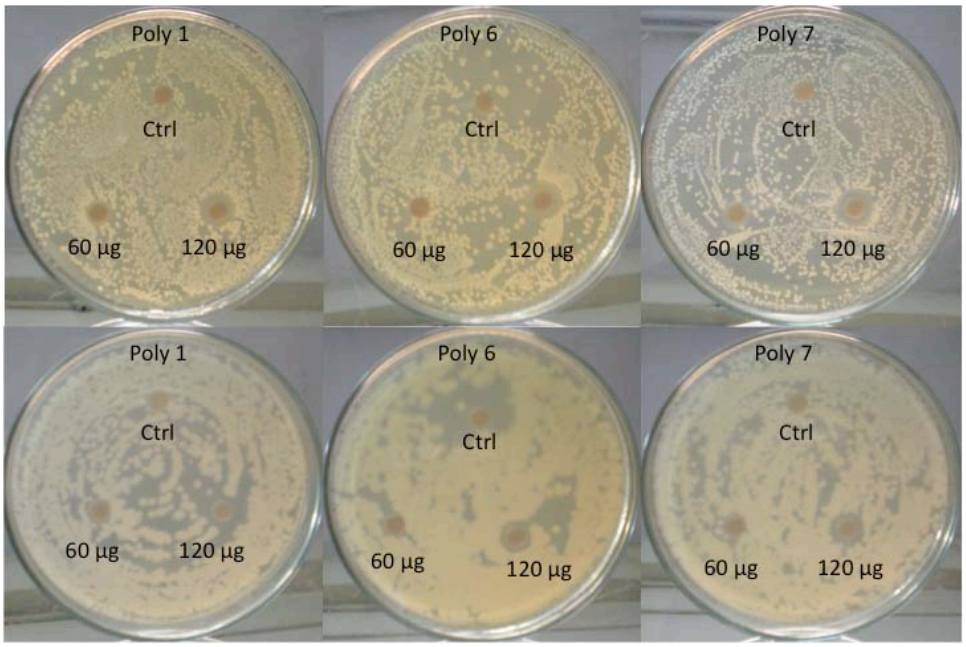

Figure 14. Zone of inhibition. Against EC (top) and BS (bottom), polymers 1 (M30), 6 (PAPMA) and 7 (E39) show similar zone of inhibition patterns. The control discs, where no polymer was present, come into contact with bacteria. When the disc was loaded with 60 µg polymer, little inhibition zone was evident, however when 120 µg polymer was used, an additional zone of inhibition was observed. Each experiment was run in duplicate.

Against EC, (top images) obvious inhibition zones were observed for all polymers when 120 µg of material were deposited. Against BS (bottom images), smaller zones were observed at equivalent concentrations. The amount of growth observed for EC (top images) was reached after 40 hr of incubation where BS shows overgrowth in the plates after only 18 hr under the same incubation condition and starting OD_{600}. Thus, not only did BS show faster growth rates in the microdilution assays, but also in zone of inhibition

studies. The immobilization of the polymers onto sterile discs demonstrate that they need not be free-floating in solution to realize antimicrobial activity, indicating potential application in surface modification and wound dressings where immobilization is required.

In summary, polymers M30, PAPMA, and E39 demonstrate antimicrobial activity against EC and BS over a broad range of conditions. In microdilution assays, polymers M30 and PAPMA (polymers with the highest content of primary amine) display the highest potency against BS. Against the faster growing BS, cation structure is important to the resulting activity in solution assays. Increasing the amount of tertiary amine or the size of hydrophobic functional groups surrounding the amine leads to weaker interaction between the polymers and microorganisms. Weakened interactions, caused by either the cation structure or the addition of saline, give bacteria with high turnover rates an edge in overwhelming the antimicrobial agent.

Hemolysis

An effective way to test eukaryotic cell toxicity is to study the hemolytic behavior of a system. While not conclusive, hemolysis experiments are used to indicate the possibility of eukaryotic cell toxicity.[46] Polymers M30, PAPMA, E39, and E100 were dissolved in TBS at pH 7.4 and incubated with isolated red blood cells for 30 min at 37 °C. It was found that at the highest concentration tested (3 mg/mL), minimal hemolysis was observed (Figure 15). E100 has the highest weight fraction of hydrophobic groups (Figure 12B) of the polymers synthesized; however, hemolysis was avoided. The high selectivity of these polymers is attributed to the use of fully water soluble monomers,

which allow incorporation of hydrophobic moieties while maintaining water solubility of the polymer.

A common practice within the antimicrobial polymer community is to report polymer selectivity towards bacterial cells over eukaryotic cells as a ratio of HC_{50}/MIC, where HC_{50} is the polymer concentration required to lyse 50% of red blood cells. At 3 mg/mL, percent hemolysis was near 5% for each polymer, which is well below 50%. Table 5 provides a summary of polymer selectivity towards EC and BS.

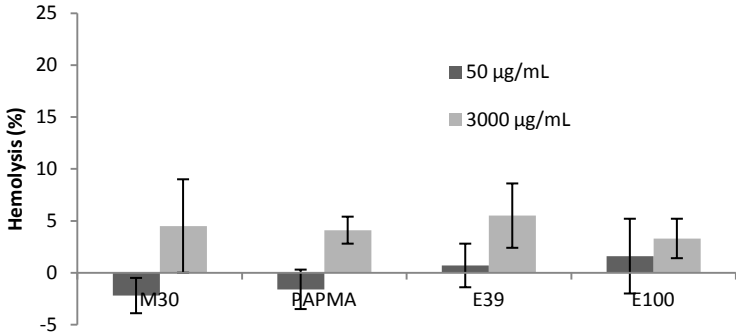

Figure 15. Polymers cause negligible hemolysis up to 3000 µg/mL. HC_{50} is reported as >3000 µg/mL to estimate polymer selectivity. Negative values are interpreted as zero hemolysis and are considered within the error of the experiment.

Table 5

Hemolysis and MIC Data Suggest that Polymers M30, PAPMA, and E39 Display Selective Toxicity.

	MIC (µg/mL)			Selectivity (HC_{50}/MIC)	
Polymer	E. coli	B. subtilis	HC_{50} (µg/mL)	E. coli	B. subtilis
1 (M30)	30	70	>3000	>100	>42
6 (PAPMA)	30	70	>3000	>100	>42
7 (E39)	50	170	>3000	>60	>17

Note. Buffer = TBS pH 7.4

Cell Viability

MTT assays were performed to further investigate the eukaryotic cytotoxicity of polymers M30 and E39. Figure 16 shows cell viability as a function of polymer concentration after 6 and 12 hr for polymers M30 and E39. Although these polymers caused little hemolysis, a reduction in MCF-7 cell viability was observed. At 30 μg/mL the reduction is minimal at each incubation time, however viability decreases with increasing concentration. In the lower concentration range, polymer E39 appears to be less toxic than polymer M30. It is difficult to compare MIC data for bacterial toxicity with eukaryotic cell viability results because each testing procedure utilizes different techniques to compare the number of living cells. For antimicrobial assays, OD_{600} is monitored to visualize the presence of bacterial growth directly, whereas in a MTT assay, the conversion of MTT to purple formazan by mitochondrial reductase is utilized to quantify the mitochondrial activity of the cells rather than directly visualizing the number of living cells. Also, bacterial cells have a much faster growth rate than MCF-7 cells in vitro. Under optimal growth conditions the number of EC cells doubles approximately every 40 min,[47] whereas MCF-7 cells (29 hr doubling time)[48] do not have an opportunity to multiply within the given time frame of polymer incubations. This fact puts MCF-7 cells at a disadvantage in a direct comparison. The goal of future work should be to outline a therapeutic concentration range in which these polymers are considered safe.

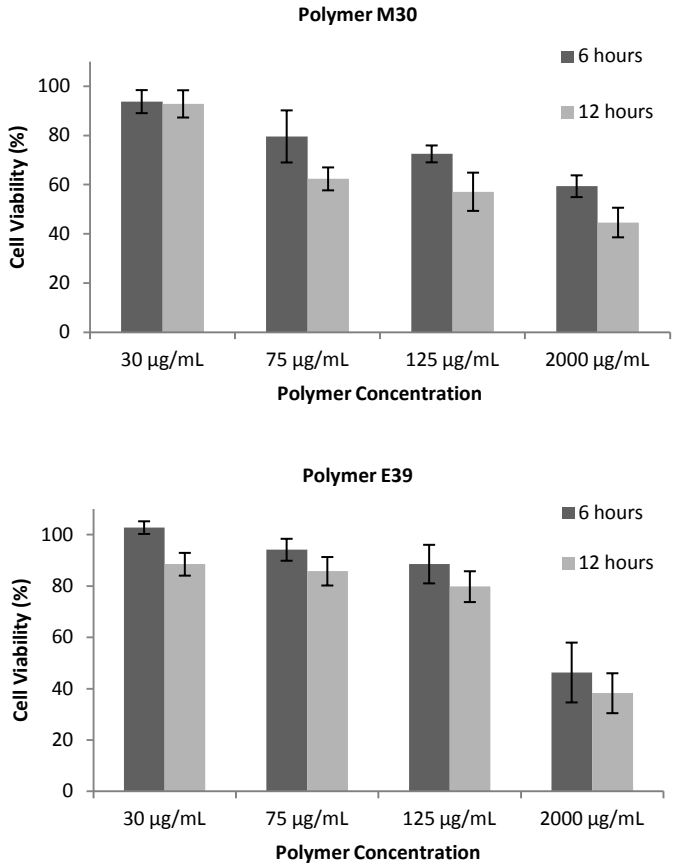

Figure 16. Cell viability of MCF-7 cells after incubation with polymers M30 (top) and E39 (bottom) for 6 and 12 hours. Data were normalized based on (+) and (-) controls. For 12 hr samples, (+) control = 100 ± 5% and (-) control = 0 ± 0%.

Chapter Summary

A series of amine-functionalized methacrylamide (co)polymers with systematic variation of the ratio of primary/tertiary amines and hydrophobic content was synthesized via aqueous RAFT polymerization. As the PDEAPMA and PDMAPMA copolymers produced remain positively charged and fully water-soluble at physiological pH, it was possible to study the effects of cation structure on antimicrobial efficiency independently from those of charge density. Very low MIC values ($\leq$ 100µg/mL) were observed against both Gram-negative EC and Gram-positive BS in a range of buffers for those

polymers having the highest primary amine content and the lowest concentration of hydrophobic groups. Approximately 50% primary amine content was required when evaluated in TRIS buffer and approximately 60% when evaluated in TRIS with 150 mM NaCl to achieve the highest levels of antibacterial activity. Bacterial toxicity was observed both when polymers were allowed to float freely in solution and when they were immobilized on surfaces. The excellent biocidal performance of these AMP mimics is attributed to high binding efficiency of the primary amines with bacterial phospholipids and a resultant high rate of bacterial cell destruction. The reduced performance of the copolymers with high tertiary amine content is attributed to the bulky methyl and ethyl amine substituents, which limit interactions between the cations and the bacteria. Greater reductions in antimicrobial activity were observed for the bulkier DEAPMA copolymers. The degree of hydrophobicity of the copolymers appeared to be of lower importance than the concentration of primary amine groups in determining antibacterial effectiveness. Selective toxicity performance was also observed. Polymers M30 and PAPMA ($PAPMA_{20}$-stat-$PDMAPMA_9$ and $PAPMA_{25}$, respectively) displayed excellent toxicity towards EC and BS while showing little disruption in membrane integrity of red blood cells. In cell assays polymer M30 killed 100% of EC and BS cells at 30 and 70 μg/mL, respectively, while approximately 50% of MCF-7 cells remained viable at 2,000 μg/mL. In order to authenticate the results from eukaryotic cell viability studies, MTT assays using additional cell lines should be performed. These studies demonstrate the importance of cation structure and solution environment in the design and performance of polymeric biocidal agents.

CHAPTER V

POLYMERIZATION AND CHARACTERIZATION OF POLY(METHACRYLAMIDE) POLYMER BRUSHES

Chapter Overview

The previous chapter discussed the development of a fully water-soluble, AMP-mimicking, polymer system composed of APMA that exhibited excellent biocidal selectivity. As a continuation of this research, this chapter details the polymerization of APMA from a surface with the future goal of determining its viability as a biocompatible antimicrobial coating. Silicon wafers were functionalized with azobisisobutyronitrile (AIBN) or Irgacure derivatives and thermally or photo initiated free radical polymerization was utilized, respectively, to create PAPMA polymer brushes. After polymerization, the brush thickness and morphology were characterized via ellipsometry and atomic force microscopy (AFM). Polymer brush composition was characterized via grazing angle infrared spectroscopy.

Thermally Initiated Surface Polymerization of an APMA Polymer Brush from a Silicon Substrate

Silicon wafers were functionalized with a chlorosilane derivative of AIBN and APMA was polymerized from the surface as shown in Scheme 3. After the polymerization had concluded, the substrate was removed from solution, sonicated in DMSO, and dried. Grazing angle IR analysis (Figure 17) indicated the presence of characteristic absorptions at 1650 cm^{-1} (s, amide C=O stretch) and 3350 cm^{-1} (s, amine N-H stretch).

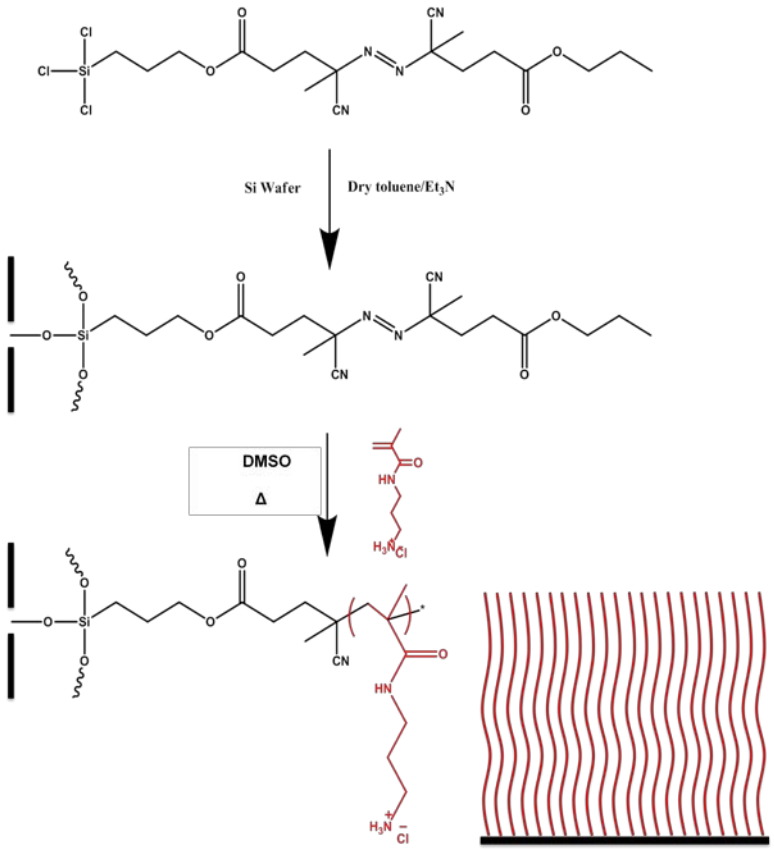

Scheme 3. Thermally initiated free radical polymerization of APMA from a silicon substrate.

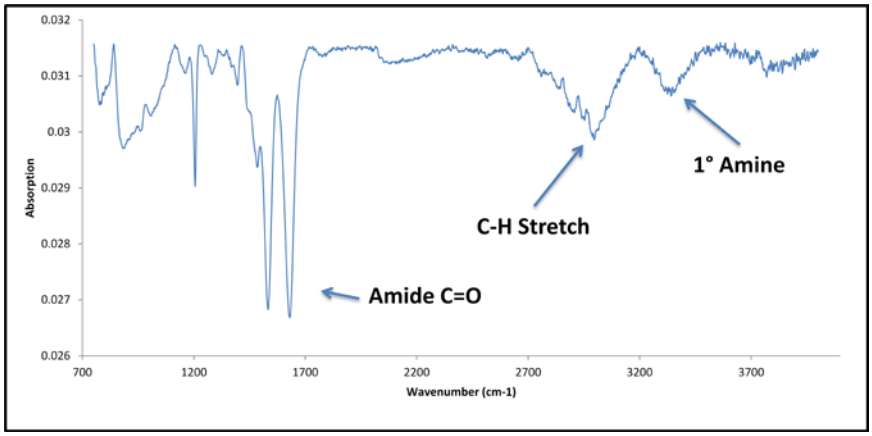

Figure 17. IR spectrum of PAPMA polymer brush prepared via AIBN surface initiated free radical polymerization of APMA.

AFM analysis (Figure 18) of the substrate indicated a smooth, one phase morphology at the nano scale; however, wave-like undulations (ripples) in the film can be

observed on the micron scale (top of Figure 18A). The film produced had a gray tint that was observable without optical enhancement. Ellipsometry could not be used for film thickness determination due to the large thickness of the brush layer. To determine film thickness, a razor blade was used to remove a portion of the PAPMA film, and AFM stepheight analysis was performed. The water contact angle of the PAPMA film was measured to be 66.5°.

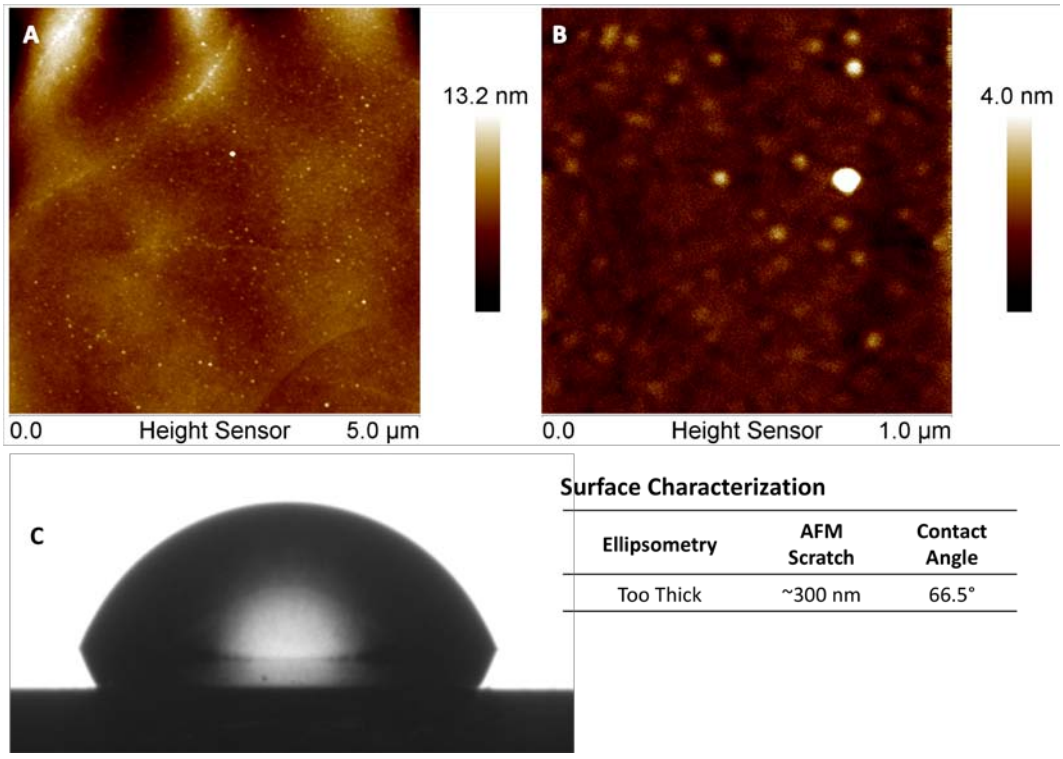

Figure 18. Thermally-initiated PAPMA brush characterization (sonicated in DMSO). AFM height images (A, 5X5 µm; B, 1X1 µm) and water contact angle images (C) of AIBN surface initiated free radical polymerization of APMA after sonication with DMSO. A brush + initiator thickness of ~300 nm was calculated via AFM scratch analysis. Assuming an extended polymer chain, a C-C bond length of 1.54 Å and a bond angle of 109.5°, the law of cosine was used to estimate the degree of polymerization required to reach a brush thickness of ~300 nm. The estimated DP for this thickness is 1167 (~208,000 g/mol).

After characterization, the stability of the PAPMA brush in H_2O was determined. Upon sonication in H_2O for 5 min, the gray film visibly disappeared from the substrate.

Figure 19 summarizes the characterization of the substrate after exposure to H_2O. A polymer layer thickness of 8 nm was measured by ellipsometry. Although the film was no longer visible un-magnified, a small fraction of the polymer remained on the substrate. The water contact angle did not change after sonication in H_2O, also indicative of the presence of PAPMA. The majority of PAPMA was liberated from the substrate upon sonication in H_2O, presumably due to hydrolysis of the ester linkage of the AIBN derivative. It should also be noted that when the polymerization was attempted in H_2O, no brush was formed. Although this polymer brush proved to be unstable, the surface cleavage of PAPMA in aqueous media could have potential applicability as a one-time-use antimicrobial coating. The polymer would remain stable on the substrate until it comes in contact with water, causing a release of the antimicrobial agent. In order to produce a polymer brush with long term water stability, a different synthetic strategy must be employed.

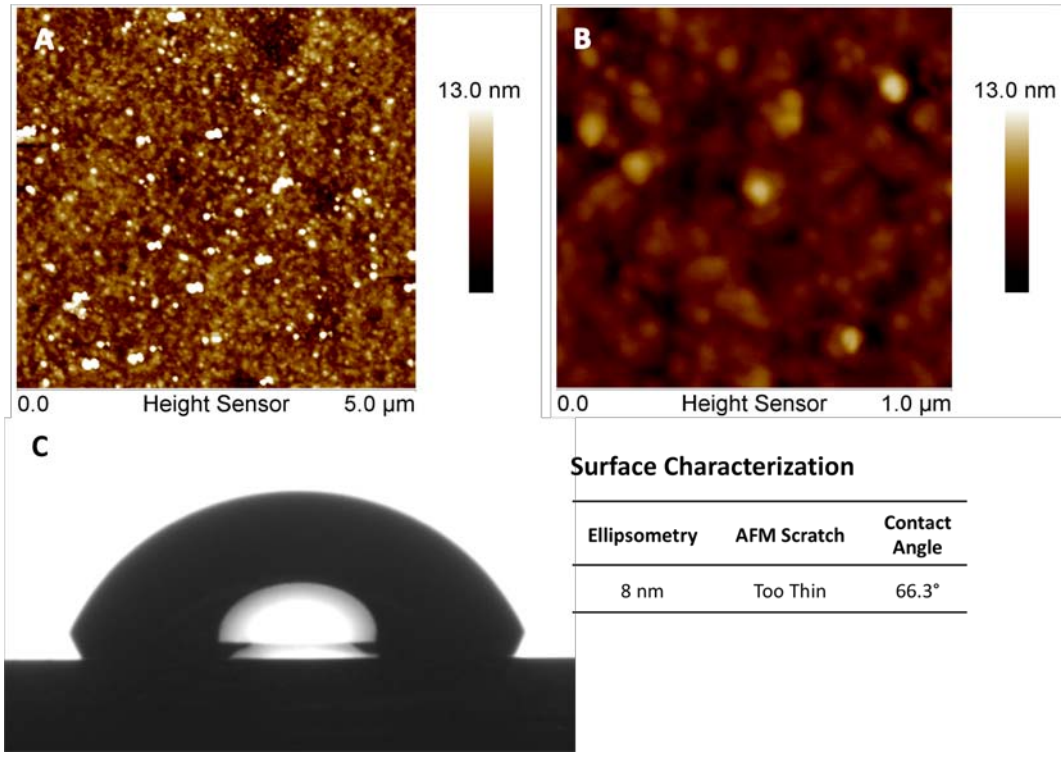

Figure 19. Thermally-initiated PAPMA brush characterization (sonication in H_2O). AFM height images (A, 5X5 µm; B, 1X1 µm) and water contact angle images (C) of AIBN surface initiated free radical polymerization of APMA after sonication with H_2O. A brush thickness of ~8 nm was calculated via ellipsometry.

Photo-Initiated Surface Polymerization of an APMA

Polymer Brush from a Silicon Substrate

A second strategy was constructed to produce a hydrolytically stable PAPMA brush. AIBN was replaced with an ester-free Irgacure photoinitiator derivative and APMA was polymerized from the substrate as described in Scheme 4.

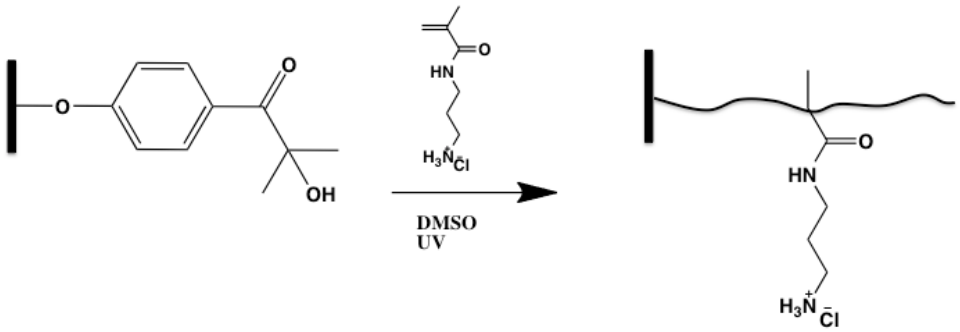

Scheme 4. UV-initiated free radical polymerization of APMA from a silicon substrate.

Using this synthetic strategy, no change in film thickness was observed after sonication in H_2O. **Figure 20** details the brush characterization after it had been sonicated in DMSO and H_2O. The UV-initiated process produced a visible smooth film. The AFM images suggest that the brush formed is uniform at the nano scale. The thicknesses determined via ellipsometry and AFM stepheight analyses were in good agreement and the water contact angle measured similar to that observed for the thermally initiated brush.

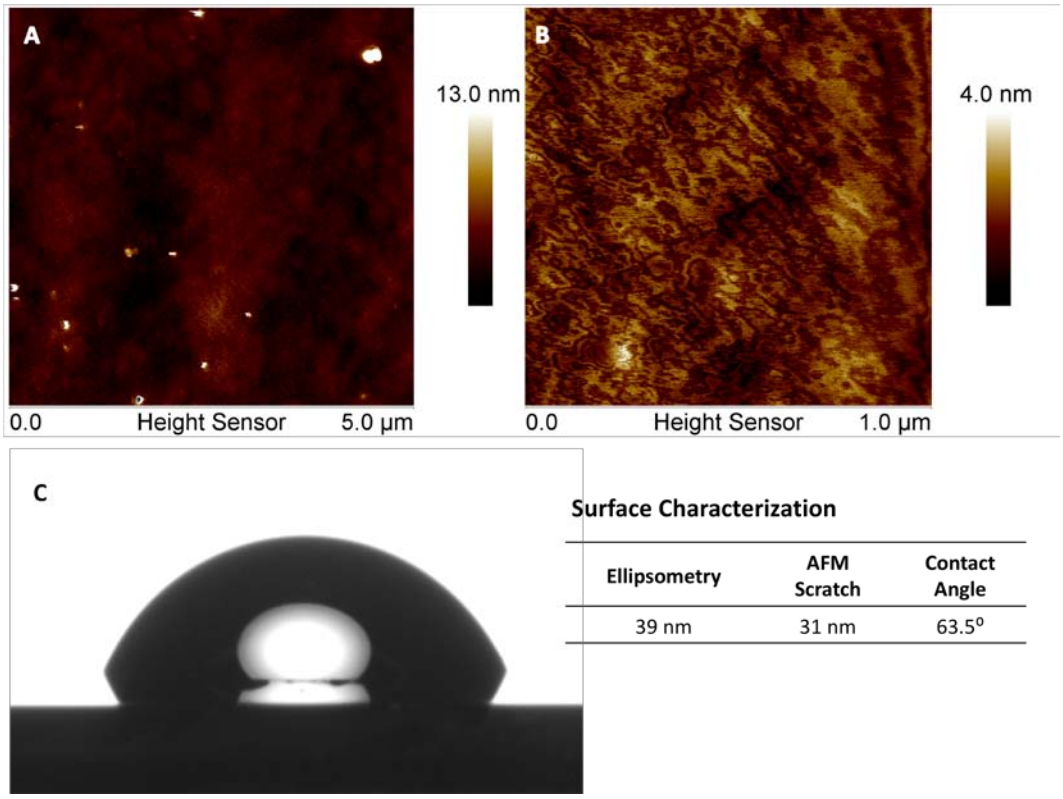

Figure 20. UV-initiated PAPMA brush characterization. AFM height images (A, 5X5 µm; B, 1X1 µm) and water contact angle images (C) of Irgacure surface initiated free radical polymerization of APMA after sonication with DMSO and H_2O. A brush thickness of ~35 nm was calculated via ellipsometry and AFM scratch analysis.

Chapter Summary

APMA was polymerized from a silicon substrate via two methods. PAPMA brushes that were produced using the thermal, AIBN initiated method were stable to sonication in DMSO, however upon exposure to H_2O the polymer chains were liberated from the surface. PAPMA brushes created via UV, Irgacure initiated polymerization were stable to sonication in both DMSO and H_2O. Follow-up studies are planned by the research group to determine the effectiveness of bound PAPMA as an antimicrobial coating.

CHAPTER VI

SYNTHESIS OF POLY(METHACRYLAMIDE) DERIVATIVES CONTAINING VARYING RATIOS OF PRIMARY AMINE AND GUANIDINIUM MOITIES

Chapter Overview

This chapter details the synthesis and polymer characterization of antimicrobial peptide polymer mimics containing varying ratios of primary amine and guanidinium, lysine and arginine mimicking moieties, respectively. Naturally occurring antimicrobial peptides have been known to eliminate a broad range of bacterial cells. These amphipathic peptides incorporate two key amino acid moieties, lysine and arginine. Literature has shown that the mechanism of cell death differs based upon the predominance of either lysine or arginine. This research utilizes APMA and GPMA to investigate the possibility of tuning the mechanism of biocidal action. In order to achieve this, boc-protected GPMA was synthesized, deprotected, and subsequently statistically copolymerized in varying ratios with APMA via aqueous RAFT polymerization. These statistical copolymers were characterized via ^{1}H NMR and ASEC-MALLS for compositional analysis, molecular weight, and PDI.

Synthesis of APMA-**stat**-GPMA (Co)polymers

In the previous chapters, the structure/property relationship between amine type within our poly(methacrylamide) system and biocidal efficiency was discussed. In this chapter, another amine-containing moiety, guanidinium, is considered. Figure 21 compares the pendent R group of naturally occurring lysine and arginine to APMA and GPMA.

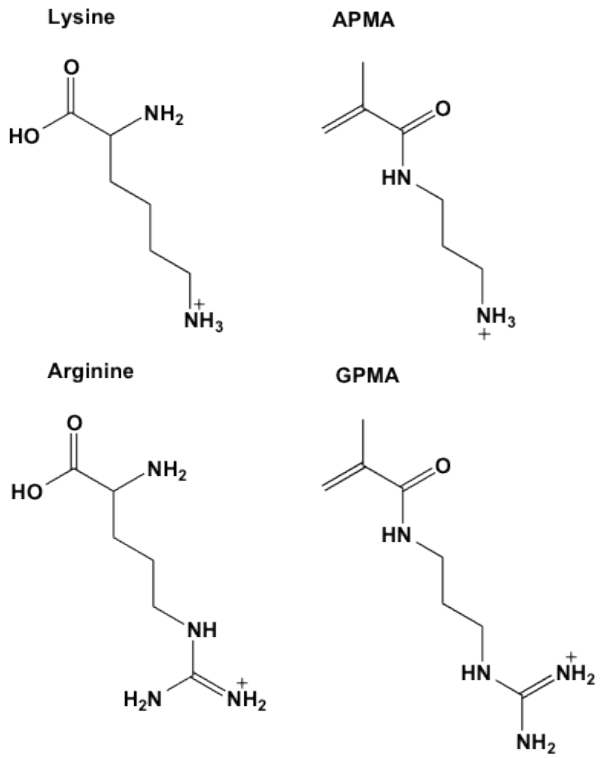

Figure 21. Comparison of lysine and arginine to APMA and GPMA.

Previous research has shown that peptides containing high quantities of arginine exhibit cell penetrating behaviors.[49] Our ultimate goal is to take advantage of this phenomenon and to develop a system that allows for manipulation of the biocidal mechanism[4] via tuning of (co)polymer composition. Previous research performed by Treat et al.[50] details the synthesis of GPMA; however, this research utilizes a modification of another synthetic route[19] to improve yield and simplify purification and handling.

APMA-***stat***-GPMA copolymers were synthesized via aqueous RAFT polymerization as described previously with minor modifications. The objective of this synthetic strategy was to polymerize (co)polymers containing a range of APMA:GPMA ratios. A highly controlled statistical distribution of monomers within our poly(methacrylamide) system will allow the outlining of the role of each, APMA and

GPMA, in determining the mechanism of biocidal action. Also, we hypothesize that detailing the activity of this well-defined distribution of (co)polymer compositions will allow the determination of critical monomer ratios that result in the onset of biocidal mechanism shift. Scheme 5 summarizes the polymerization reaction.

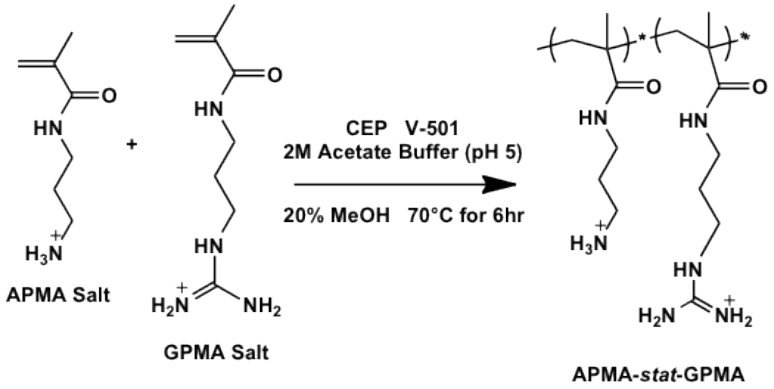

Scheme 5. Aqueous RAFT polymerization of APMA-***stat***-GPMA (co)polymers.

Monitoring the Kinetics of the Copolymerization of APMA and GPMA

The nomenclature PGT represents polyGPMA TFA and the corresponding number indicates its targeted mole fraction in the (co)polymer. For example PGT25 represents a copolymer composed of 25 mol% GPMA TFA and 75 mol% APMA. In order to monitor the polymerization reaction progress of APMA-***stat***-GPMA, aliquots were taken every hour from the PGT50 reaction vial. ^{1}H NMR was utilized to determine [M] at time (t) by comparing the vinylic hydrogen peak integrations to the integration of an internal standard (MeOH). A plot of $\ln([M_0]/[M])$ versus time (***Figure 22***) indicates that the reaction follows linear first order kinetics.

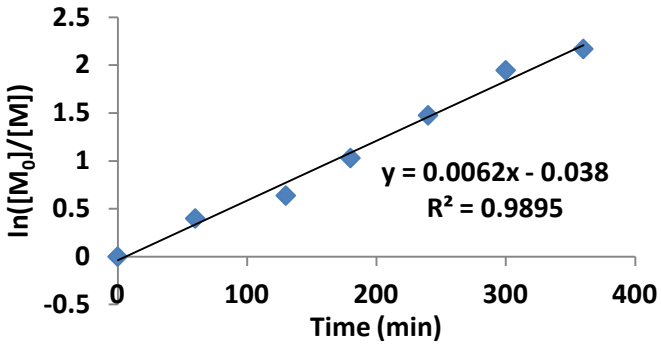

Figure 22. APMA-***stat***-GPMA reaction kinetics. ln([M_0]/[M]) vs time kinetic plot for the polymerization of 1:1 molar ratio of APMA:GPMA TFA. The linear relationship indicates that the polymerization follows a predictable behavior.

ASEC-MALLS was also utilized to monitor molecular weight as a function of time.

Figure 23 diagrams the refractive index (RI) response vs elution volume for aliquots taken at each time interval, and a summary of the molecular weight characterization data is given in Table 6.

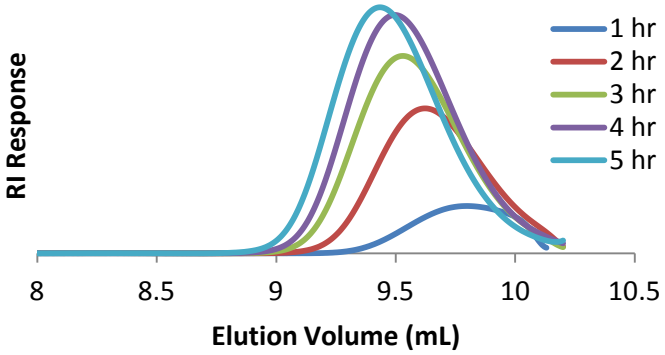

Figure 23. APMA-***stat***-GPMA molecular weight distribution as a function of reaction time. RI response vs elution volume at multiple time intervals during the polymerization reaction.

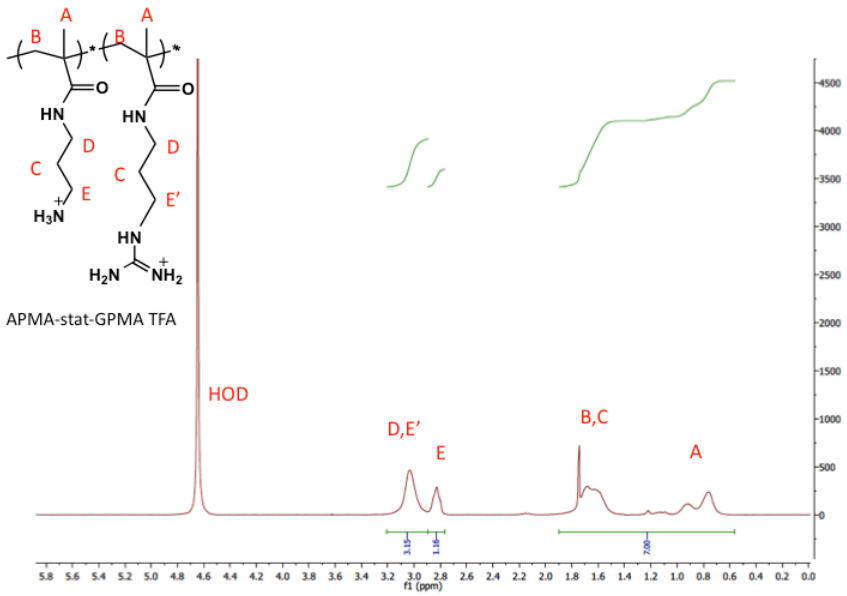

Figure 24. Representative ^{1}H NMR spectrum of APMA-***stat***-GPMA copolymer. The target APMA/GPMA composition for the above formulation was 50:50 mol %. Peak integration indicates 45 mol% GPMA in the copolymer.

Table 6

Molecular Weight and Composition Data for Synthesized (Co)polymers

polymer	mol % GPMA (theory)	mol % GPMA (exp)[a]	$Mn,_{th}$ (g/mol)[b]	$Mn,_{exp}$ (g/mol)[c]	PDI[c]	*dn/dc*[d]
1 (PAPMA)	0	0	5,600	6,500	1.06	0.200
2 (PGT25)	25	23	6,500	6,900	1.03	0.183
3 (PGT50)	50	45	7,400	6,100	1.06	0.169
4 (PGT75)	75	72	8,300	5,800	1.12	0.152
5 (PGT100)	100	100	9,200	8,100	1.04	0.132

Note. [a]Determined by ^{1}H NMR. [b]Based on 90% conversion of [M_0]. [c]Determined by ASEC-MALLS. [d]Determined by a Wyatt Optilab DSP interferometric refractometer.

Chapter Summary

GPMA was synthesized, purified and statistically polymerized with APMA via aqueous RAFT polymerization. The (co)polymers formed have a well-defined

distribution of monomers as well as a low polydispersity. This research will allow the outline of each monomer's role in determining the antimicrobial mechanism and reactivity. Future antimicrobial and biocompatibility tests are planned by the research group.

CHAPTER VII

HYDROPHOBIN PROTEINS

Chapter Overview

This chapter provides an overview of the literature of hydrophobin proteins. Hydrophobins are of great commercial interest as they have the ability to self-assemble at interfaces and serve as an intermediary layer between two incompatible phases. Much of the current knowledge base surrounding hydrophobins comes from research performed on a hydrophobin from the wood rotting fungus, *Schizophyllum commune.* This chapter outlines our current hydrophobin knowledge and our rationale for moving in the direction of a hydrophobin, ABH1, from the edible white button mushroom.

Introduction to Hydrophobins

Hydrophobins are small, amphipathic proteins secreted by fungi that are characterized by a conserved spacing of eight cysteine residues and a common hydropathy pattern.[51] The genes that code for hydrophobins were first discovered in the fungus *Schizophyllum commune.*[52, 53] Their role in the development of fungi is very diverse, ranging from lowering the surface tension of water, thus allowing the escape of aerial hyphae,[54] to protecting mushrooms from bacterial infection.[55] Hydrophobins are categorized into two classes based on stability. Class I hydrophobins are among the most surface-active molecules identified to date.[56] They spontaneously self-assemble upon exposure to hydrophobic/hydrophilic interfaces, including the air/water, oil/water, and substrate/water interfaces, to form stable, semi-permeable, amyloid films that are insoluble in boiling 2% sodium dodecyl sulfate (SDS) solutions, resistant to changes in temperature and pressure, and denatured only by harsh acids.[54] The self-assembled

hydrophobin membrane is generally characterized by a specific rod-like (rodlet) morphology of the aggregated protein similar in appearance to other amyloid proteinaceous deposits.[57] Wang et al.[58] discuss the biological implications of semi-permeable hydrophobin membranes as it allows for the transport of water vapor in and out of fungi. Due to these remarkable characteristics, their use has been suggested for a wide range of biomedical, personal care and technical applications.[59] Previous studies in our laboratories demonstrated that polymer substrates, as well as human hair, coated with the hydrophobin SC3 from *Schizophyllum commune* provide improved lubricity, adhesion, friction resistance, and hydrophilicity to surfaces.[60, 61] Class II hydrophobins self-assemble in a similar way; however, the film produced can be removed by boiling SDS solutions, 60% ethanol, heat, or pressure.

Their Role in Fungi

Amyloid peptides or proteins are most commonly described as misfolded proteins, which form insoluble self-assemblies and cause irreversible damage to the systems from which they were created. However, Gebbink et al.[62] discuss the role of hydrophobins as functional amyloid coatings. They coat fungal aerial structures including spores and fruiting bodies, thus making them water repellent.[63] In the grand scheme of fungal development, spores are produced by aerial structures, which arise from aerial hyphae. Aerial hyphae are often found in moist environments from which they must escape. Gebbink et al.[62] reported that hydrophobins play critical roles in all stages of this development. For the escape of aerial hyphae, hydrophobins are secreted into the medium and, through a process of self-assembly at the air/water interface, reduce the surface tension of water. This decrease in surface tension allows the hyphae to break

through the interface. Also, the self-assembled film coats the hyphae, shifting the polarity of its surface. Now hydrophobic, the hyphae can rest above the water interface.[64] As spores are released from aerial structures, they are coated by a hydrophobin monolayer as well, which in turn aids in their windborne dispersal. This hydrophobic coating also helps spores bind to hydrophobic substrates.

SC3 is the most characterized hydrophobin and is the subject of the majority of the published literature. Martin et al.[65] showed that as SC3 concentration approaches 0.4 μg/ml, the surface tension begins to drop from 72 mN/m, eventually reaching a value of 40 mN/m at 4 μg/ml. Wosten et al.[57] showed that the hydrophobic side of the film formed amyloid-like rodlets much like the ones observed coating aerial hyphae and spores.

Self-Assembly

In order to fully understand the driving forces of self-assembly, structural characteristics of hydrophobins must first be discussed. It is accepted that the eight cysteine residues of hydrophobins come together to form four disulfide bridges.[66] De Vocht et al.[67] sought to understand the functional role of disulfide bonds in hydrophobins. They discovered that SC3 was a very stable protein, and in order to disrupt these disulfide bridges, it was necessary to treat the native protein with both 10 mM dithiothreitol (DTT) and 5.4 M guanidine. DTT, guanidine, heat, or pH alone had no effect on the secondary structure of the protein. After concluding their studies, they felt that the disulfide bridges played an important role in stabilizing the protein in solution and reducing unwanted aggregation. Butko et al.[68] reported that the hydrophobin SC3 contains 48% β strands, 52% loops, and no α-helix. Based on fluorescence emission spectra of thioflavin T and

absorption spectra of Congo red, they concluded that the hydrophobin SC3 self-assembles at water/air interfaces through β-sheet stacking, a mechanism operating in amyloidogenic proteins. In a similar study performed by Wang et al.,[69] it was concluded that the rodlets of SC3 form from the β-sheet state at the substrate/solution interface when coated on hydrophilic surfaces. Rodlets can also be formed on hydrophobic surfaces, but the thin film must be washed with detergent at an elevated temperature in order to induce β-sheet formation.[69]

The mechanism by which hydrophobins self-assemble is somewhat debatable. Stroud et al.[70] presented evidence that confirmed unimeric SC3 assembles into different forms based on experimental conditions. They propose that SC3 can either self-assemble into functional films at air/water interfaces or that it can aggregate in solution over time. Wang et al.[71] studied SC3 oligomerization in water and various buffers. They found that, in water, the monomeric form is unstable and that dimers are rapidly formed; however, the monomeric form was more stable in water than in the buffer solutions. Under all conditions including changes in pH, SC3 aggregated in solution to form oligomers. As the ionic strength of the buffer was increased, the protein dimerization proceeded more rapidly. This dimeric form is thought to be the most stable form of oligomerization. They observed a larger than expected hydrodynamic radius, which might indicate that dimeric SC3 has an elongated shape. When the pH was raised above 9, larger oligomers were formed, which indicates that SC3's sole basic amino acid, histidine, may play an important role in keeping SC3 dimeric in solution. The only thing that seemed to have an affect on aggregation was concentration. At really low concentrations, more of the monomeric form was present. Below 4.5 μg/ml, there was a noticeable decrease in

aggregation. Although aggregation may prove to be important in regards to the ability of the protein to self-assembly, large-scale changes in the protein structure only occur upon self-assembly on surfaces or at hydrophobic/hydrophilic interfaces.

According to de Vocht et al.,[72] at the air/water interface, soluble state SC3 proceeds via an intermediate, called the α-helical state, to the stable end form called the β-sheet state. The β-sheet state is broken down into two mini states. At first, this β-sheet state has no clear structure, but after some time has passed (suggesting kinetics are important to self-assembly) rodlets are formed, which is a characteristic of cross β-sheets. SC3 is stalled in the intermediate α-helical state when self-assembled onto Teflon; however, treating with detergent at an elevated temperature allows the protein film to convert into the final β-sheet state. The secondary structure predictions suggest that a region in the second loop has a high tendency to form an amphipathic helix. The hydrophobic face of this helix was suggested to bind to hydrophobic solid surfaces.[72] Wang et al.[73] show that this part indeed strongly adsorbs to Teflon, which is accompanied by α-helix formation and a reduced accessibility to the solvent. They prove this by MALDI-ToF mass spectroscopy and circular dichroism spectroscopy via digestion of SC3 with ASP-N and found that only the peptides that make up this second loop stayed attached to the Teflon after washing with detergents. The authors then suspended colloidal Teflon beads in the peptide fragment mixture and found that these same peptides bind the beads and that the CD spectra are consistent with proteins in an α-helical conformation. One of the main differences between Class I and Class II hydrophobins is that Class I hydrophobins have a larger second loop (17-39 residues) compared to that of class II (11 residues).[54] The SDS-resistant nature of Class I

hydrophobins as opposed to the SDS-soluble Class II hydrophobins could by explained by this fact alone.

Potential Applications

Hektor and Scholtmeijer [59] discuss the potential of hydrophobins in the areas of anti-fouling, biomaterials, medical, personal care, emulsion stabilizers, biosensors, separation technologies, and gushing detectors. The use of hydrophobins as anti-fouling agents is of special interest. Bacteria, such as *Staphylococcus epidermidis* (SE), have been shown to have a unique affinity for hydrophobic polymer surfaces. SE is everywhere and typically shows little virulence to humans upon everyday contact, but it forms antibiotic resistant biofilms on hydrophobic polymer surfaces,[74] which is likely due to the hydrophobic effect.[75] Once these biofilms are formed, the infection is almost impossible to treat. It should be noted here that there are conflicting ideas on how best to prevent bacteria from attaching to surfaces. Some believe that increasing the hydrophobicity of the surface will prevent bacteria from attaching and others feel that this is best accomplished by increasing hydrophilicity. In reality, it is probably a combination of the two. Different bacteria, undoubtedly, will have high affinities for different types of surfaces. Pringle and Fletcher [76] tested freshwater bacteria attachment to solid surfaces and found that all bacteria studied had a higher affinity for hydrophobic surfaces. Also, bacteria seem to attach more efficiently to rough surfaces.[77]

In relation to biomaterials, research from Scholtmeijer et al.[78] and Janssen et al.[63] has shown that by changing the N-terminal region of SC3, the physiochemical nature of the hydrophilic side can be altered. SC3 is unique because of its N-terminal sequence preceding its first cysteine residue. Located in this region are 16 to 22 mannose residues

attached to the 12 threonine residues. The N-terminal third of the protein is probably exposed at the hydrophilic side of assembled SC3 and determines the degree hydrophilicity.[72] In this research, they coated Teflon with SC3 and Arg–Gly–Asp (RGD) tri-peptide modified SC3 to see if fibroblast cells could be grown on hydrophobins. RGD was added to the N-terminal region of SC3 along with a version where the first 25 amino acids were deleted. Their results show that the deleted amino acid-RGD version of SC3 was capable of growing cells. Wang et al.[79] used hydrophobins to immobilize biomolecules on the surface of poly(dimethylsiloxane) by pattering the self-assembly. This is an example of how hydrophobin research could lead to small-scale biosensors and the fictionalization of surfaces without causing irreversible damage.

Bilewicz et al.[80] modified electrodes with self-assembled hydrophobins. This study showed the permeability, or lack of permeability, of various electroactive molecules through the hydrophobin membrane. Wang et al.[58] show that functional amyloid fibrils spontaneously form not only at an air/water interface, but also at an oil/water interface. To test the permeability of the SC3 membrane they measured the transfer of pyrene from the hydrophilic side (buffer) to the hydrophobic side (paraffin oil). Pyrene is 202 g/mol. They note that pyrene rapidly transferred to the paraffin oil when no SC3 was present, but was blocked completely when SC3 was self-assembled overnight from a concentration of 100 μg/ml. In contrast to the transfer from buffer to oil, pyrene apparently still transferred at room temperature from paraffin oil to buffer after overnight assembly of 100 μg/ml SC3. The explanation of this phenomenon was that the pyrene was found to be in tiny emulsified oil droplets. They concluded that the SC3 membrane was permeable to water vapor but the diffusion of molecules greater than

200 Da was blocked. However, these larger molecules can pass through the membrane by emulsification. Much like the stabilization of oil droplets, hydrophobins can also stabilize gas bubbles. This phenomenon is important in the beer brewing industry. When too many hydrophobins are present in beer they self-assembly around CO_2 bubbles and can lead to gushing.[81] A series of patent applications has recently appeared from BASF claiming hydrophobin application in Pickering emulsions,[82] coatings for expandable polymer beads,[83] anti-foaming/defoaming additives,[84] and coatings for fibers.[85]

Class II hydrophobins have also been a source of great interest recently. The hydrophobin, HFBII, from *Trichoderma ressei*, for example, self-assembles at interfaces; however, the resulting amphipathic films of Class II hydrophobins can be removed by boiling SDS solutions, 60% ethanol, heat, or pressure.[54] A recent representation of HFBII's applicability is described in work by Bimbo et al.,[86] in which porous silicon nanoparticles were coated with HFBII for use as nano vessels for drug delivery. A minimal change in drug loading/release was observed after the particles had been coated with HFBII, and the overall biocompatibility of the system was improved. Sarparanta et al.[87] concluded that the presence of the HFBII coating also improved the retention time of the nanoparticles within of the body due to its mucoadhesive characteristic. The authors also cited a recent study that suggests hydrophobins have the ability to prevent immune recognition of fungal spores.[88] The subversion of an immune response or the ability to mask a substrate that the protein coats is intriguing when considering future application of hydrophobins in which they may come in contact with the body. In other biologically relevant studies, hydrophobins have also been shown to have the ability to either prevent or promote secondary protein adsorption via electrostatic interactions.[89-92] This

interfacial mediation was shown to be dependent on the isoelectric point of both the substrate immobilized hydrophobin and the secondary protein in solution.

Current Limitations and Objectives of Research

While research into hydrophobins has been steady for the past two decades, an area of exploration that is surprisingly absent is a detailed description of the self-assembly behavior of Class I hydrophobins from edible mushrooms. These organisms are of particular interest because of their wide availability, renewability, and non-toxicity. Previously, De Groot et al.[93] outlined a screening procedure for the detection of *Agaricus bisporus* (edible white button mushroom) genes that code for hydrophobins. They noted that a hydrophobin, ABH1, was produced in the latter stages of development, presumably with the function of maintaining the fruiting body. Lugones et al.,[94] in an attempt to distinguish mushroom tissues in which hydrophobins are located by immunoblotting with hydorphobin-specific antibodies, reported that ABH1 was also found in the interior of the fruiting body, lining the air channels. The hydrophobic coating of air channels is thought to prevent water from entering and thereby avoid air channel collapse and/or filling with water in moist environments. De Groot et al.[55] noted that there was a high prevalence of ABH1 in the outer peel tissue of the fruiting body and that a third hydrophobin, ABH3, was found in the transition zone just below the cap. ABH1 is of particular interest to our research due to its accessible location on the outer skin of the white button mushroom.

A small number of studies have been reported on the assembly properties of hydrophobins from white button mushroom. Lugones et al.[95] studied the assembly of ABH1 onto Teflon (hydrophobic) and filter paper (hydrophilic). In summary, the authors concluded that an ABH1 coating caused Teflon to become more water wetting and that it

led to filter paper exhibiting great hydrophobicity. The protein coating remained mostly stable after washing with a boiling SDS solution, as evident by small shifts in water contact angle (WCA) after SDS exposure. Lugones et al.[96] studied the assembly of ABH3 onto Teflon and filter paper, and reported SDS-insolubility of the ABH3 membranes. ABH3-coated Teflon and filter paper exhibited similar modifications as were observed for ABH1. Also, a rodlet morphology of the protein was observed from the hydrophobic side of the film in electron microscopy analysis. It was also reported that ABH3 lowered surface tension as demonstrated with axisymmetric drop shape analysis.

The main objectives of this research are to (1) isolate ABH1 from the edible, white button mushroom and to confirm its purity, (2) develop a model of the molecular ordering that occurs upon self-assembly at different interfaces, (3) determine how the strength of an interface affects the nature of assembly, and (4) determine if an outside factor such as temperature can affect the molecular ordering and kinetics of self-assembly.

CHAPTER VIII

EXPERIMENTAL DETAIL FOR HYDROPHOBIN RESEARCH

Research Overview

It is the goal of our current research to better understand the phenomenon of self-assembly of ABH1 and to develop an idea of its affinity for interfaces with varying interfacial tensions. Scheme 6 depicts the competitive nature of self-assembly. Diagramed is the organization of ABH1 at both the air/water and substrate/water interfaces.

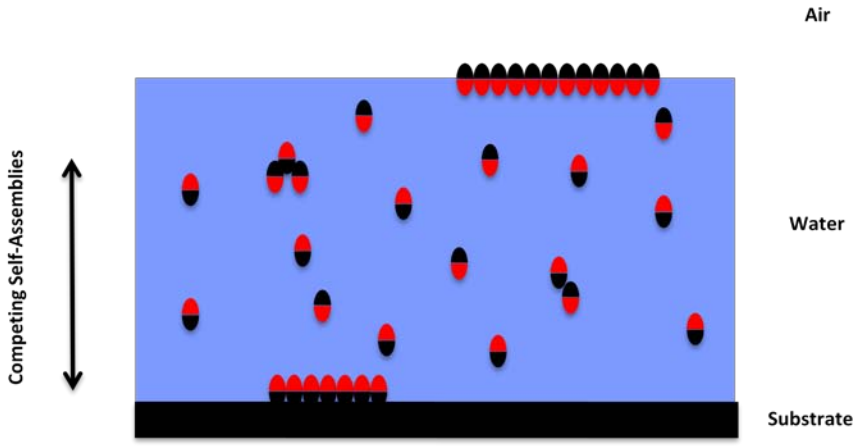

Scheme 6. The competitive nature of ABH1's self-assembly at the air/water interface versus the water/substrate interface.

Also depicted is the tendency of the protein to aggregate in solution over time. We hypothesized that the rate of self-assembly and the properties of the self-assembled structures would vary as a function of the strength of the interface (interfacial tension). The kinetics of the self-assembly process were evaluated via QCM studies with quartz crystal sensors coated with materials of differing polarity. The structure and morphology of the self-assembled structures were evaluated by atomic force microscopy, circular dichroism spectroscopy, static and dynamic light scattering, ellipsometry, surface

tensiometry, and contact angle goniometry. It was found that the strength of the interface had a profound effect on the nature of the self-assembly process and that the process is accelerated by increasing the temperature of the solution.

Materials

HPLC grade water (Fisher Scientific), Pierce BCA Protein Assay Kit (Thermo Scientific), citric acid, 99% (Aldrich), sodium dodecyl sulfate (Fisher Scientific), sodium phosphate (Fisher Scientific), 2,5-dihydroxybenzoic acid, 98% (Aldrich), TEMED (Fisher BioReagents), 40% acrylamide/bis solution, 29:1 (3.3% C) (Bio-Rad Laboratories, Inc.), trifluoroacetic acid, 99.5% (Acros Organics), hydrogen peroxide, 35wt.% (Acros Organics), 2-mercaptoethanol, 99% extra pure (Acros Organics), toluene anhydrous, 99.8% (Aldrich), TRIS crystallized free base molecular biology grade (Fisher Scientific), glycine (Fisher Scientific), glycerol (Sigma), hydrochloric acid (Fisher Scientific), Silver Stain Plus (Bio-Rad Laboratories), polystyrene pellets, 280,000 g/mol (Aldrich), PELCO mica discs, 9.9 mm diameter (Ted Pella, Inc.), and ammonium persulfate (Flinn Scientific, Inc.) were purchased and used as received. Single side polished silicon wafers were purchased from Silicon, Inc. and further scored and broken to the desired size and shape. HYFLON® AD40 L and HYFLON® AD40 L Solvent were provided by Solvay Specialty Polymers Italy SpA. ABH1 was isolated from white button mushrooms that were purchased from a local Corner Market grocery store in Hattiesburg, MS.

Methods

Isolation of ABH1

The hydrophobin protein, ABH1, was isolated from the edible mushroom *Agaricus bisporus* and purified according to previously published procedures[95, 97] with some modification. Packages of whole white button mushrooms were purchased at the market, each containing mushrooms of similar size, shape, and developmental stage. The peel tissue was removed from the fruiting body, frozen in liquid nitrogen, and then crushed to dust using a mortar and pestle. The mushroom dust was suspended in a 1% SDS solution and washed for 10 min at 100 °C under continuous, slow stirring. Next, the fungal tissue was separated from the detergent solution by filtration. The wash procedure was repeated an additional two times. The fungal tissue was then rinsed five times in room temperature DI water. The tissue was separated from the supernatant, between each rinse, by filtration. The remaining fungal tissue was lyophilized for 48 hr followed by suspension in 99.5% trifluoroacetic acid (TFA) and chilling overnight at 4 °C. TFA was then removed from the pellet using a Nalgene sterilization filter unit (115 mL, 0.2 μm pore size) and solvent from the filtrate was evaporated in a stream of N_2 gas, which left an isolation product (brown film) on the bottom of the vial.

ABH1 Solution Preparation

Solutions were prepared by suspending the desired mass of isolation product in DI or HPLC water. The ratio of mass of isolation product to volume of water was changed to obtain the desired concentration of protein.

Determination of Protein Concentration

To determine the concentrations of hydrophobin and standard bovine serum albumin (BSA) solutions, a spectrophotometric bicinchoninic acid (BCA) assay was performed. The absorbance at 562 nm was measured in a DU 800 UV-Vis spectrophotometer (Beckman).

Sodium Dodecyl Sulfate-Polyacrylamide Gel Electrophoresis (SDS-PAGE)

Electrophoresis was performed to identify proteins present in our isolation product. A 12% polyacrylamide gel was used at a run voltage of 120 V. Protein solutions (0.1-1 mg/mL) dissolved in Laemmli buffer were loaded into the wells to determine purity and stability of the hydrophobin preparation and to approximate molecular mass. Polypeptide bands were visualized by staining with Silver Stain Plus.

Matrix-Assisted Laser Desorption / Ionization - Time of Flight Mass Spectrometry (MALDI-ToF MS)

A Bruker Daltonics FLEX-PC Microflex MALDI-ToF mass spectrometer was used to determine the mass and identity of the purified protein. The acquisition operation mode was reflector with a positive voltage polarity. The matrix used was 2,5-dihydroxybenzoic acid (DHB) dissolved in 0.1% TFA. 1 μL of the protein sample (0.8 mg/mL) was spotted onto a MALDI target and mixed with 1 μL DHB solution (10 mg/mL). To further confirm the identify the purified protein, an in-gel trypsin digestion was performed to degrade the protein into peptide fragments in a controlled, specific manner.[98] MALDI-ToF MS was used to identify the resulting tryptic peptide products by their mass and predict the identity of the isolated protein by its peptide composition.[99, 100] (See APPENDIX for sequence confirmation results)

Static Light Scattering

Static light scattering (SLS) was performed on hydrophobin solutions to determine the effect of concentration on aggregation of the protein. Hydrophobin solutions were prepared at six different concentrations ranging from 43 μg/ml to 270 μg/ml in HPLC water. All solutions were filtered using PVDF, 0.22 μm Millex®-GV syringe-driven filter units. SLS was performed using an incident light of 633 nm from a Spectra Physics He-Ne laser. The angular dependence of the scattering intensities was measured using a Brookhaven BI-200SM goniometer with a TurboCorr correlator. The radius of gyration (Rg) was determined by plotting inverse scattering intensity (I^{-1}) against scattering vector (q^2). Aggregation behavior as a function of solution pH was also considered; however, changes in pH seemed to have little influence on aggregate Rg (data shown in APPENDIX).

Surface Tensiometry

Surface tension was determined for a 30 μg/mL ABH1 solution using the plate method with a Krüss K12 Processor Tensiometer, glass sample vessel, and a Wilhelmy platinum plate (PL12). Measurements were taken at room temperature over the course of 4 hr after solution preparation, and then at 24 hr. The plate was cleaned between each measurement by rinsing with DI water and dried by passing through the flame of a torch.

AFM Analysis of ABH1 Assembled at the Air/Water Interface

ABH1 solutions ranging in concentration from 2 to 22 μg/mL were deposited onto silicon wafers (~1 inch squares) that had been cleaned with piranha solution (70:30 H_2SO_4 : 30% H_2O_2). Cleaning with piranha solution results in the formation of a ~3nm thick layer of SiO_2 at the surface. The protein solutions that were deposited onto SiO_2 (20

μL at 2 and 22 μg/mL) were allowed to dry under ambient conditions. The object of these experiments was to allow the protein to assemble at the air/water interface and subsequently dry the assembly on the substrate in preparation for imaging using atomic force microscopy. Silicon offers a nanoscopically smooth surface, which allows the visualization of small biological materials that possess roughness values on the scale of only a few nanometers. The surface coverage, topography, and morphology of ABH1 coated substrates were studied using a Dimension 3000 scanning probe microscope in tapping mode in a temperature (27 °C) and humidity (40-45%) controlled room with a standard Veeco RTESP silicon probe (cantilever length: 125 μm, nominal force constant: 40 N/m, and resonance frequency: 350 kHz). Height, phase, and amplitude images were collected simultaneously. The image size ranged from 500 nm x 500 nm to 5 μm x 5 μm, while the resolution was held constant at 512 x 512 data points. The images shown were chosen to best represent the samples, as multiple scans were taken for each sample on macroscopically separated regions of the substrate. All standard image processing techniques were performed on Nanoscope version 5.30 r2 image analysis software.

Quartz Crystal Microbalance (QCM) Investigation of ABH1 at the Water/Substrate Interface

QCM was used to measure protein adsorption onto oxidized silicon (SiO_2), polystyrene (PS) and a fluoropolymer (HYFLON® AD40 L or Teflon AF)-coated quartz crystals using the Q-sense E4 system with QFM 401. PS and Teflon AF functionalized crystals were obtained pre-coated from Q-Sense. PS and HYFLON® AD40 L were spin cast onto gold QCM sensors in our laboratory and, when used in measurements, are denoted in the Results and Discussion section. The spin-coating procedure is detailed in

the next section. The QCM-D system was equilibrated with HPLC water until a baseline was observed for frequency and dissipation signals. ABH1 solutions were then coursed over the functionalized q-sensors until the frequency change reached a baseline. Next, HPLC water was coursed over the newly formed protein film to remove any weakly attached protein and establish a final baseline. All flow rates were held constant at 100 μL/min. Frequency and dissipation changes for the 3rd, 5th, and 7th overtones were analyzed. The Sauerbrey equation,[101] $\Delta m = -(C\Delta f/n)$, was used to estimate protein adsorption where Δm, C, Δf, and n are change in mass, a constant for the crystal, change in frequency, and the overtone number, respectively.

Model Studies at the Water/Substrate Interface

Piranha solution-cleaned silicon wafers were prepared and either PS (3.5 mg/mL in toluene) or HYFLON® AD40 L (3 mg/mL in HYFLON® AD40 L Solvent) was spin cast onto a subset of the cleaned wafers. Fourty microliters of PS or HYFLON® AD40 L solutions were pipetted onto the silicon wafers as they were spun at 1500 rpm for 1.5 min. The spin cast wafers were placed in desiccant until use. Each of the so prepared substrates was placed into glass Petri dishes and submerged in 8 mL of ABH1 solution. The protein concentration, incubation time, and incubation temperature were varied depending on the specific experiment. After the protein was allowed to assemble or deposit at the solution/substrate interface for a chosen length of time the substrate was removed from the solution, rinsed with DI water, and dried with a stream of N_2 gas. The samples were stored in desiccant until characterization by AFM, ellipsometry, and contact angle goniometry measurements.

Ellipsometry

Ellipsometry measurements were performed to monitor the thickness of the assembled protein layer on a Gaertner Scientific ellipsometer with an angle of incidence of 70° using a 632.8 nm He-Ne laser and Gaertner GEMP software. This technique was also used to characterize the thickness of the formed substrates before the addition of protein. The SiO_2, PS, and HYFLON® AD40 L thin films had resulting measured thicknesses of approximately 3 nm, 14 nm, and 40 nm, respectively, as determined via ELLI software using the refractive indices of each of the layers and the ellipsometry measured delta values. The refractive index of the protein layer was estimated based on that of a similar hydrophobin.[102]

Contact Angle Goniometry

Contact angle measurements were conducted to monitor the surface modification behavior of the assembled hydrophobin. The sessile drop technique was employed using a Ramé-Hart goniometer coupled with DROP-image® data analysis software. The static contact angle formed by drops of HPLC grade water (11 μL) was measured on each surface immediately after deposition.

Circular Dichroism Spectroscopy (CD)

CD spectroscopy was performed to identify secondary structure organizations of ABH1 as a factor of time and temperature. CD Spectra were obtained for wavelengths of 260-198 nm using a quartz cuvette with a 0.1 cm path length and the Jasco J-815 spectropolarimeter in continuous scanning mode (260-190 nm). Acquisition parameters included a scanning speed of 50 nm/min, 8 s response times, 1 nm bandwidth, and a 0.1 nm data pitch. Data sets were averaged over three scans and preceding solvent blanks

were subtracted. The corrected, averaged spectra were then smoothed using the *means-movement* algorithm with a convolution width of 25 in the Jasco spectra analysis program.

CHAPTER IX

KINETICS AND CONTROL OF SELF-ASSEMBLY OF ABH1 HYDROPHOBIN FROM THE EDIBLE WHITE BUTTON MUSHROOM

Chapter Overview

Hydrophobins are small fungal proteins that self-assemble at hydrophobic/hydrophilic interfaces to form stable, amyloid membranes that are resistant to denaturation. Their remarkable surface activity has driven intense research for their potential utility in biomedical and cosmetic applications. In this research, the self-assembly characteristics of the Class I hydrophobin ABH1 from *Agaricus bisporus*, the edible white button mushroom, were evaluated as a function of solution and interface properties in an attempt to gain greater mechanistic understanding. The kinetics of self-assembly were examined using dynamic quartz crystal microbalance techniques in combination with AFM, ellipsometry, contact angle goniometry, light scattering, and circular dichroism spectroscopy. It was found that the strength of interfacial tension between two phases drives the speed of protein assembly, and that the nature and location of the molecular ordering was influenced by temperature.

Protein Isolation and Characterization

SDS-PAGE and MALDI-ToF MS analysis were used to determine the identity of the isolated protein (Figure 25). In silver-stained gels, a heavy band is observed near 8928 Da., the molecular mass of unimeric ABH1 calculated from its amino acid sequence. Additional, fainter bands are observed at approximately two and three times the mass of the unimer, which are attributed to different states of aggregation of the protein. Such aggregation appears to be characteristic of hydrophobin proteins and has been reported previously.[70, 71] The protein material that is trapped at the top of the

separation gel is attributed to large molecular weight aggregates. MALDI-ToF MS analysis further confirms the purity of the isolation product. A single, large peak is observed at 8918 Da and a minor peak is visible at approximately twice this molecular weight. Trypsin digestion and analysis of the tryptic peptides confirmed the amino acid sequence of the isolated hydrophobin protein (see APPENDIX).

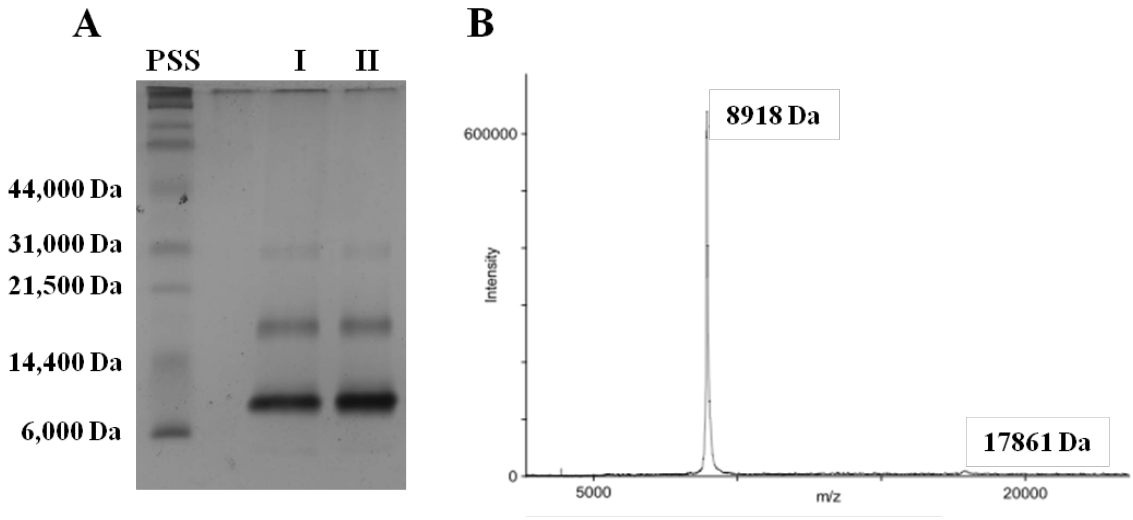

Figure 25. SDS-PAGE (A) and MALDI-ToF MS spectrum (B). Columns I and II in the SDS-PAGE represent two different isolation batches. SDS-PAGE (A) shows the approximate molecular mass of the isolated protein. Maldi-Tof spectrum (B) confirms purity and molecular mass of the product.

Previous research conducted on hydrophobin SC3 led to the postulation that unimeric hydrophobin or low molecular weight aggregates (i.e., dimers) may be required for organization at an interface.[70, 71] Hydrophobins self-assemble at interfaces as well as aggregate in solution, reducing the tension between their hydrophobic patches and the aqueous solution; therefore, as aggregation levels in the bulk of solution increase one would expect the driving force for self-assembly at an interface to consequently decrease. Static light scattering (SLS) was performed to determine the effect of concentration on aggregation behavior. SLS measures the intensity of scattered light and thereby allows

the determination of particle molecular weight; however, the method can also yield a radius of gyration (Rg), which is defined by Hiemenz and Lodge[103] as the root-mean-square, mass-weighted average distance of individual residues from a particle's center of mass. Figure 26 shows that Rg increases as a function of hydrophobin protein concentration.

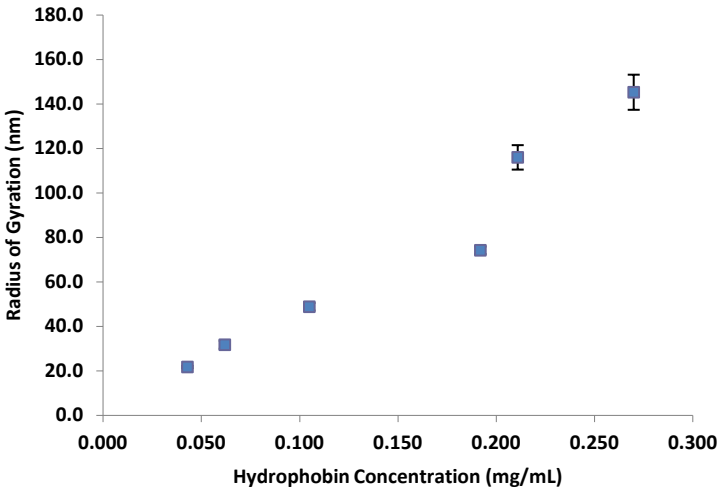

Figure 26. Static light scattering of ABH1 solutions. Data suggest that particle size increases with increasing concentration (error bars indicate ± one standard deviation). HPLC water was used as the solvent and all samples were filtered using PVDF, 0.22 µm Millex®-GV syringe-driven filter units.

Note that the smallest average Rg detected, at 20 nm, is much larger than would be expected from a single ABH1 molecule (~2.9 nm in diameter assuming a globular protein and using 8,928 Da as the molecular mass). Larger protein aggregates scatter light more effectively than unimers and dimers, making it difficult to detect the smaller species in solution even though MALDI-ToF MS analysis suggests that unimers are the predominant species present (see APPENDIX for an AFM image of light scattering samples that had been dried onto a mica substrate depicting the presence of aggregates). Light scattering does, however, indicate that lower protein concentrations yield smaller

aggregate sizes, so an ABH1 concentration of less than 80 μg/mL was targeted for all of the following analyses.

ABH1 Assembly at the Air/Water Interface

Previous literature reports document the ability of hydrophobin to reduce the surface tension of water;[65] however, the rate at which this change in surface property occurs has not been reported for ABH1. Surface tension measurements for an ABHI solution of 30 μg/mL were made immediately after the solution was prepared. The results indicate an immediate decrease in surface tension from 73mN/m for pure water to 44mN/m for ABH1 solution. The measured surface tension remained constant for 24 hr, indicative of a stable interface (data shown in APPENDIX). The observed reduction in surface tension is attributed to hydrophobin assembly into an amphipathic film at the air/water interface.[104] Surface tensiometry provides only indirect evidence of protein self-assembly, so AFM analysis of the films formed at the air/water interface was conducted to gain a greater understanding of protein organization.

A drop of hydrophobin solution was deposited onto a silicon wafer and allowed to dry under ambient conditions. The protein that had assembled at the air/water interface was thus deposited onto the SiO_2 substrate. Figure 27 shows AFM phase images of films formed from solutions of two different ABH1 solution concentrations. Rodlet features are apparent, which are indicative of self-assembled proteins rich in cross β-sheet secondary structure organization.

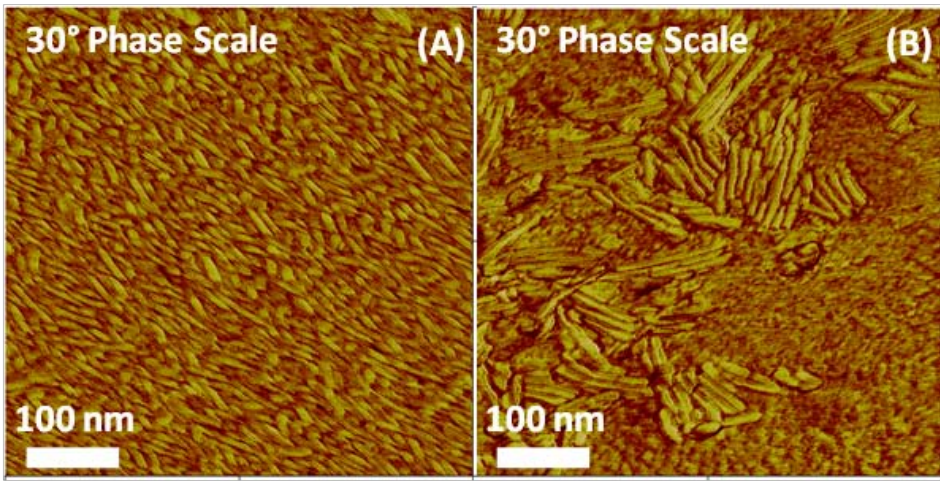

Figure 27. AFM micrographs (phase images) of an ABH1 film that was assembled at the air/water interface and deposited onto SiO_2 (A & B). The concentration of ABH1 was 2 μg/mL (A) and 22 μg/mL (B).

This type of morphology and assembly into cross β-sheet secondary structures is characteristic of hydrophobin self-assembly and that of many amyloid protein aggregates.[62] The rodlets appear aligned and aggregated, particularly in the film represented in Figure 27B. This supramoleculular organization of rodlets is attributed to the high mobility of the protein at the solution surface. The combined results from surface tensiometry and AFM analysis indicate that ABH1, in solution, moves quickly to the air/water interface and adopts a rodlet morphology as it assembles.

ABH1 Assembly or Deposition at the Water/Substrate Interface

QCM is a high-resolution mass sensing device (nanogram level sensitivity) that allows the monitoring of biopolymer deposition at the solution/surface interface.[105] Grunér et al.[106] used QCM to study the adsorption of Class II hydrophobins onto charged substrates. The authors concluded that electrostatic interactions played a role in binding to polar substrates, as the Class II hydrophobins adhered to cationic, but not to negatively charged surfaces. For our investigation, QCM was used to monitor the adsorption

behavior of ABH1 onto substrates with varying surface energies and interfacial tensions at the water/substrate boundary, which we hypothesized would influence assembly behavior. To test this hypothesis, ABH1 solutions were coursed over quartz crystal sensors that had been functionalized with SiO_2, PS, or a fluoropolymer, and the mass increase due to protein deposition was measured as a function of time. SiO_2, PS, and the fluoropolymer coated sensors have WCAs of approximately 23°, 92°, and 120°, respectively, and collectively represent a wide range of relative surface hydrophobicities. Changes in frequency (-ΔF) and dissipation (D) were monitored as a function of interface type, protein concentration, and time (see Figure 28 for a representative QCM trace), and the data were compiled in Table 7.

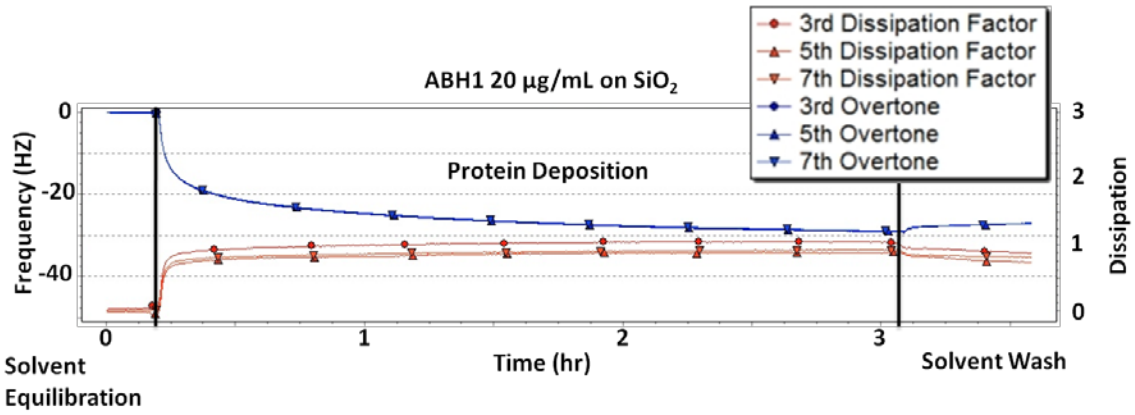

Figure 28. Representative QCM data (blue = frequency red = dissipation). Each experiment followed the protocol of equilibration in water, equilibration in protein solution and lastly, equilibration in water to remove weakly adsorbed protein. In the above experiment a 20 µg/mL solution of ABH1 was coursed over a SiO_2 substrate. The observed change in frequency and dissipation after solvent wash were -26.2 ± 0.3 Hz and 0.6 ± 0.1, respectively. The solvent wash led to little removal of protein, which indicates a stable film.

In general, larger levels of protein adsorption were observed for the two hydrophobic substrates (PS and the fluoropolymers), and protein deposition did not increase dramatically with increasing concentration of protein in the solution. For the

hydrophilic substrate, on the other hand, protein concentration in solution appeared to directly affect protein adsorption levels.

Table 7

Final Changes in Frequency and Dissipation as a Function of Protein Concentration and Interface Type

Sample	Conc. (μg/mL)	- ΔF (Hz)	D	~Protein Adsorption ($\mu g/cm^2$)
	10	16.6 ± 0.7	0.5 ± 0.2	0.29
SiO_2	20	26.2 ± 0.3	0.6± 0.1	0.46
	50	31.6 ± 0.5	1.0 ± 0.1	0.56
	10	34.2 ± 0.8	1.8 ± 0.1	0.6
PS	20	23.1 ± 0.8	1.7 ± 0.3	0.41
	50	36.5 ± 0.7	1.1 ± 0.1	0.65
	10	33.4 ± 0.1	0.8 ± 0.1	0.59
Fluoropolymer	20	38.5 ± 0.9	1.6 ± 0.4	0.68
	50	35.3 ± 1.0	1.8 ± 0.2	0.62

Note. Values shown are averaged over the overtones 3, 5, and 7 (± indicates one standard deviation). Protein adsorption was estimated using the Sauerbrey equation. PS 20 and Fluoropolymer 10 and 20 experiments were performed on gold Q-Sense crystals that had been spin coated with either PS or HYFLON® AD40 L in our laboratory. All other experiments utilized commercial pre-coated sensors.

To determine the effect of ABH1 concentration and substrate polarity on the rate of deposition, the time required for -ΔF of the third overtone to reach 15 Hz was recorded (Figure 29). This value was chosen as it represents the lowest reliable change in frequency change that all experiments reached. At low concentrations, ABH1 is absorbed

onto the low-surface energy substrates at a faster rate than onto those of high surface energy. When the ABH1 concentration was raised to 50 µg/mL, deposition onto all substrates occurred at a similar rate.

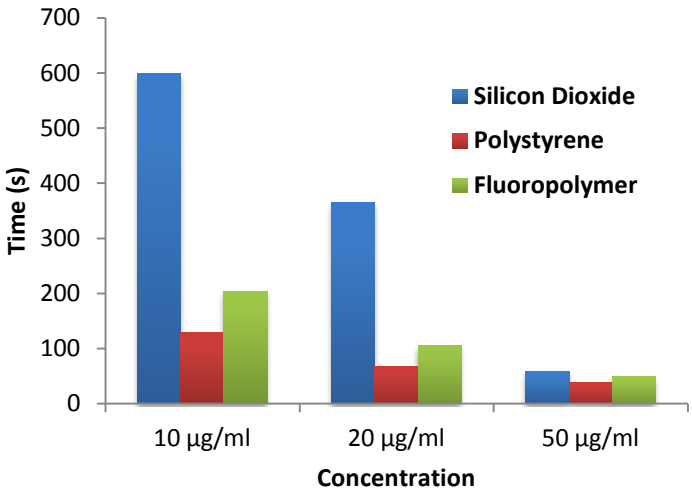

Figure 29. Time for deposition of ABH1 to cause a frequency change (-ΔF) of 15 Hz on SiO_2 (blue), PS (orange) and fluoropolymer (green) substrates as a function of concentration. At low concentrations the protein moves to hydrophobic substrates (stronger interfacial tension) at a faster rate. At high concentrations, little difference is observed.

It is generally difficult to observe hydrophobin morphology on modified quartz crystal sensors, because of the inherent roughness of the surfaces. Therefore, comparative model studies were performed on silicon wafers submerged in quiescent ABH1 solutions of similar concentration and for similar periods of time as those used in the QCM studies. For example, in a model study a SiO_2 wafer was completely submerged in a 20 µg/mL solution of ABH1, incubated for two hours at room temperature, removed from the solution, rinsed with DI water, dried with a slow stream of N_2 gas, and imaged via AFM (Figure 30) Small globular protein deposits are observed; however, the surface coverage is low (see APPENDIX for an AFM image of a silicon wafer before protein

modification). Both ellipsometry and AFM roughness analysis suggest that the average protein layer thickness is below 1 nm, a fact that further indicates a low surface coverage.

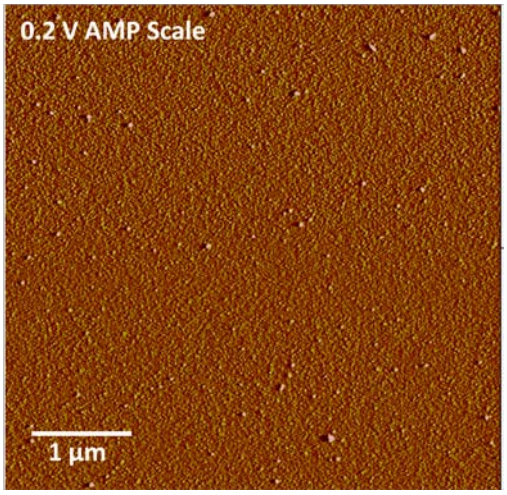

Figure 30. AFM amplitude micrograph of ABH1 deposited onto a SiO_2 substrate. Small globular deposits of protein were observed on the substrate after 2 hours of incubation in a 20 µg/mL ABH1 solution at room temperature. The 5 X 5 µm image is shown to best represent the sample, however no rodlet deposits were observed at smaller scan sizes.

In an attempt to increase the surface coverage, the incubation time was raised from 2 to 24 hr. At the longer time interval, the wafers were completely submerged in ABH1 solutions in which the concentration varied from 10 to 70 µg/mL. Figure 31 shows AFM micrographs of the substrate after immersion in solution for 24 hours at room temperature. In general, the amount of deposited protein increases with incubation time, and the deposits appear more rod-like at higher concentrations. It is important to note that the rods are larger and appear less defined than those observed in the earlier air/water interface investigations and may represent supramolecular assembled structures of smaller rodlets.

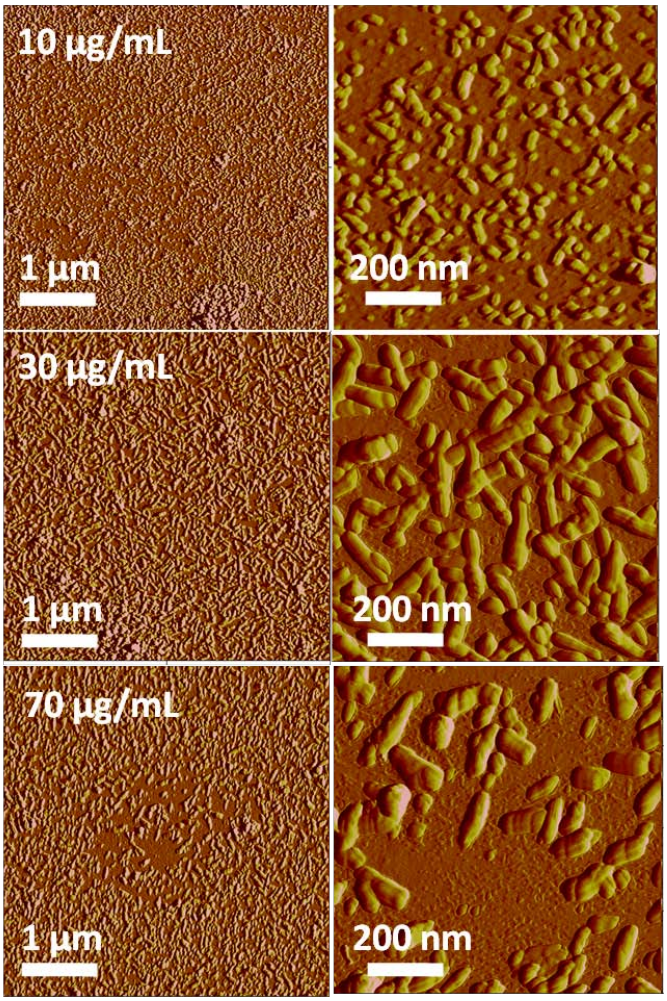

Figure 31. Amplitude AFM micrographs showing assembly of ABH1 after 24 hours at room temperature onto submerged SiO_2 substrates. The concentration was varied to in order to observe the morphology of deposition as a function of concentration. All images have a z-range scale of 0.2 V.

Longer incubation times (>24 hr) did not measurably change surface deposition layer thickness (measured by ellipsometry) or extent of coverage (observed by AFM)(Figure 32).

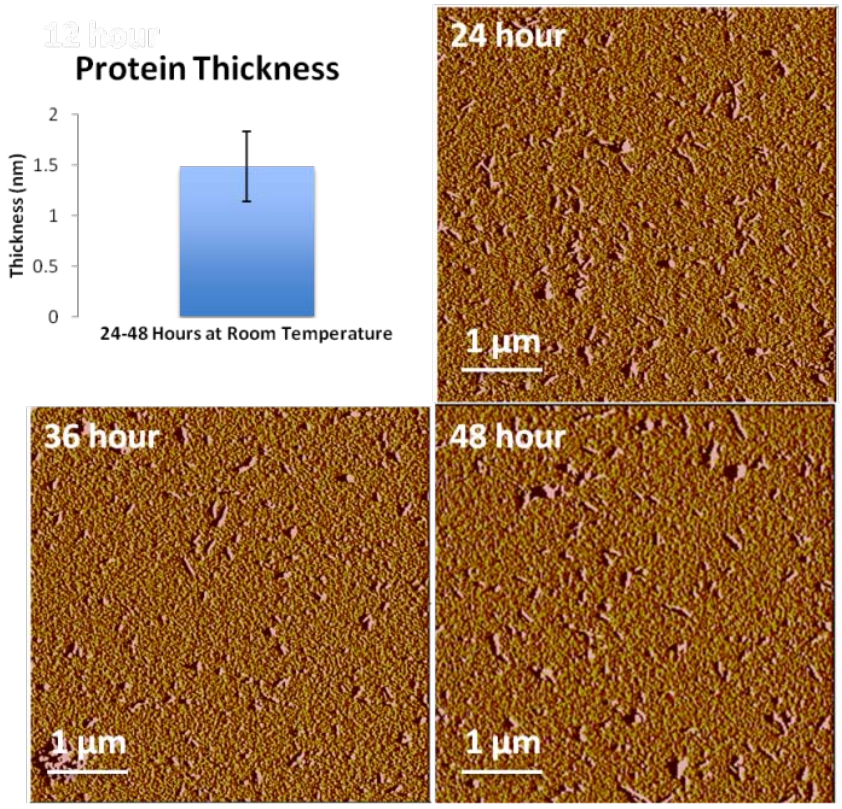

Figure 32. Amplitude AFM micrographs of ABH1 at the substrate/water interface where a silicon wafer was the substrate. Silicon wafers were submerged in 20 µg/mL solutions of ABH1 for various times to monitor assembly as a function of time. The z-range data scale was held constant at 0.2 Volts. Protein layer thickness was calculated by ellipsometry by averaging the protein thicknesses of the 24, 36 and 48 hour samples (error bar indicates ± one standard deviation).

The small average protein layer thickness, 1.5 ± 0.4 nm, estimated by ellipsometry and the estimated individual rodlet height of ~10 nm measured by AFM indicated a low coverage density (note that both ellipsometry and QCM calculations assume a smooth, completely covered surface). It is likely that the SiO_2/water interface does not provide a strong enough interfacial tension to drive protein assembly. The small amount of globular protein observed on the SiO_2 surface after submersion in ABH1 solutions for 2 hr is attributed to protein aggregates formed in the bulk of solution that deposit onto the substrate. The rod-like protein observed on the substrate after 24 hr is attributed to protein assembled at the air/water interface that is later deposited on the substrate. It is

concluded from the data that the protein first moves quickly to and organizes at the air/water interface, grows to a critical size at which it becomes insoluble, and then precipitates and deposits onto the substrate. This interpretation of our data also helps explain the larger size of the rodlets observed at the water/SiO_2 interface.

CD was performed in order to identify secondary structural changes that may occur in the bulk protein solution. Aliquots were taken from the bulk of a 50 μg/mL hydrophobin solution immediately after preparation, then after 24 and 96 hr. Figure 33 represents the collected CD spectra.

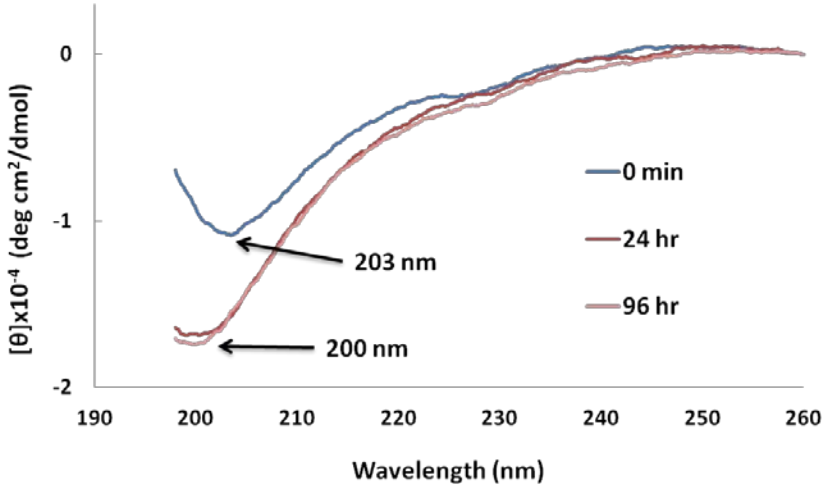

Figure 33. CD suggests ABH1 does not undergo molecular rearrangement in solution at room temperature. The similar positions of the minima indicate that the protein remains in a predominantly random coil conformation throughout the 96 hour test.

At all points measured, the protein remained in a random coil conformation in the bulk solution. AFM imaging of the protein assembled at the air/water interface clearly depicts the presence of cross β-sheet rich rodlets, however no such organization can be seen in the bulk solution. This finding suggests that, in the absence of another driving force, the protein self-assembles only at a strong polar/nonpolar interface, such as air/water, and will not assemble at the silicon oxide/water interface. With a secondary

driving force, however, it is possible to induce ABH1 self-assembly in the bulk solution. The effect of temperature on self-assembly was examined by incubating ABH1 at 60 °C, obtaining aliquots from the bulk of solution over the course of 4 hr, and examining the solutions by CD (Figure 34).

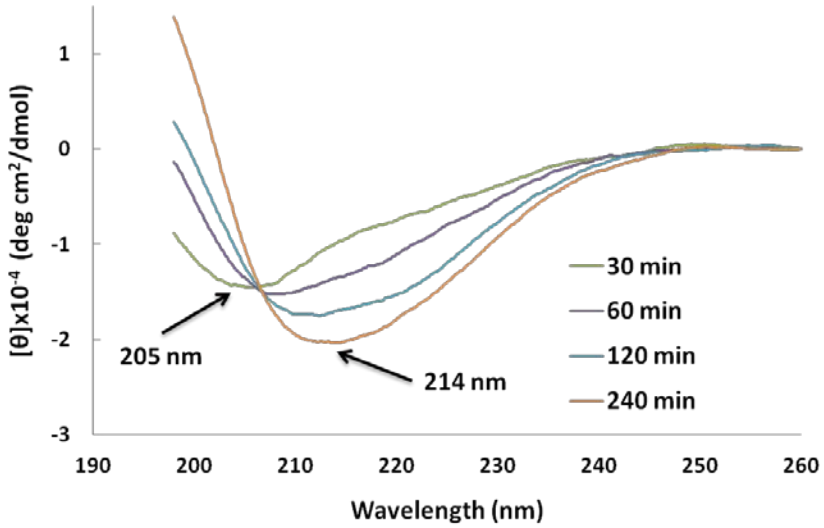

Figure 34. CD depicts the gradual increase in beta sheet secondary structure in the bulk solution at 60 °C. The shape of the curve changes as the minimum shifts from 205 nm to 214 nm, signifying protein folding into beta sheets.

A shift in the minimum is observed over the course of the 4 hr incubation from 205 to 214 nm, indicating a secondary structure shift from a predominately random coil to structures rich in β-sheets. Additionally, 18 hr after the heating cycle ended, the minimum in the CD spectra remained near 215 nm, suggesting that the β-sheet-rich assembled structures are stable in solution for extended periods of time (data not shown).

The effect of temperature on the assembly of ABH1 was further examined by AFM. Figure 35 shows images of films produced from 50 μg/mL ABH1 solutions allowed to assemble at 60 °C onto SiO_2 wafers as a function of time.

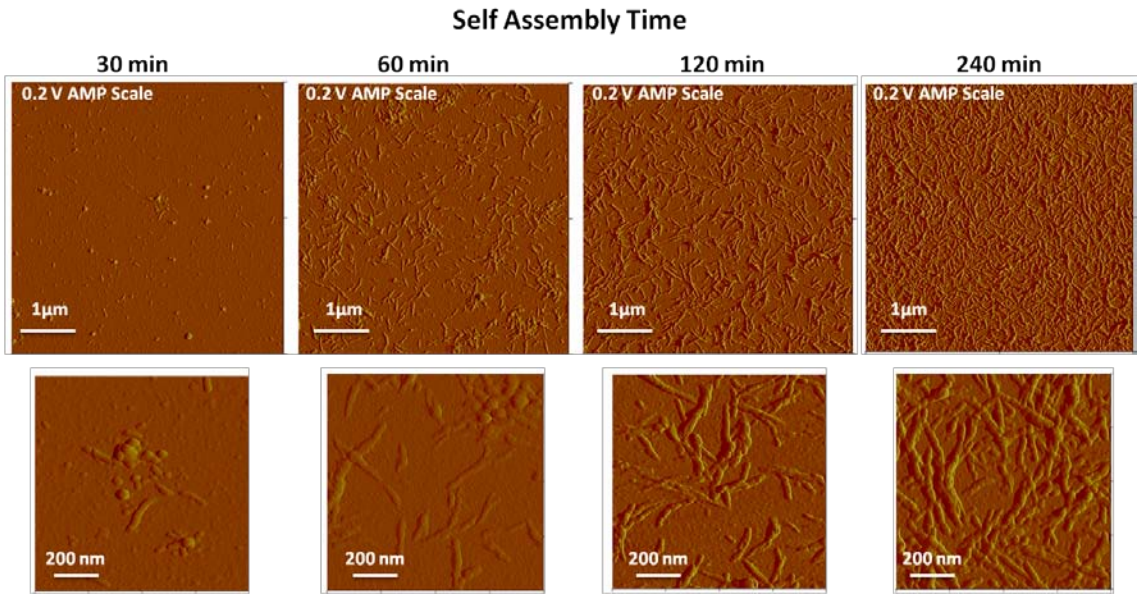

Figure 35. Amplitude AFM micrographs of self-assembled ABH1 on SiO_2 substrates that were incubated in a 50 µg/mL ABH1 solution at 60°C for 30, 60, 120 and 240 minutes. The data scale was kept constant at 0.2 Volts.

The AFM micrographs indicate that rodlet protein deposition increases as a function of time and that a high level of surface coverage is obtained after 4 hr of incubation. AFM results are consistent with those observed by CD, indicating that at elevated temperature, ABH1 organizes in the bulk of solution and ABH1 assemblies deposit onto the SiO_2 substrate. The surface modification behavior was also monitored as a function of incubation time. The WCA shifted from 23 ± 1° on the neat SiO_2 wafer to 59 ± 1° after 4 hr of incubation at 60 °C indicating that the protein layer exposed to the air interface is less hydrophilic than the SiO_2 substrate following this procedure (Figure 38).

The effect of temperature on ABH1 assembly at hydrophobic substrates is somewhat different from that observed at the SiO_2 substrate. Figures 36 and 37 show AFM micrographs of PS and HYFLON® AD40 L substrates, respectively, after incubation in 50 µg/mL ABH1 solutions at 60°C as a function of time.

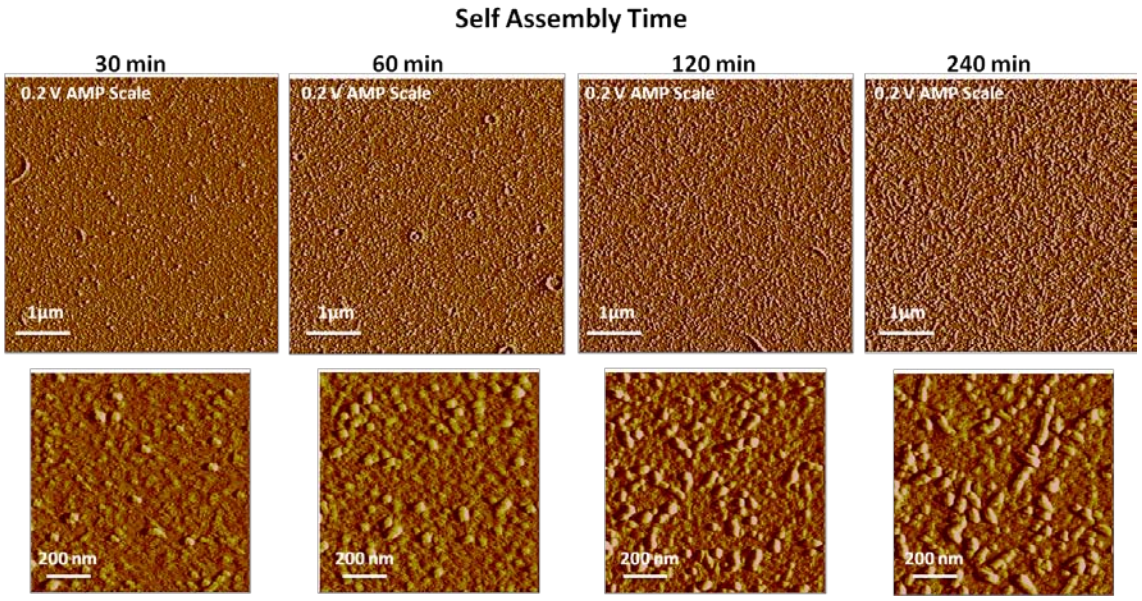

Figure 36. Amplitude AFM micrographs of deposited ABH1 on PS substrates that were incubated in a 50 µg/mL ABH1 solution at 60°C for 30, 60, 120 and 240 minutes. The data scale was kept constant at 0.2 Volts.

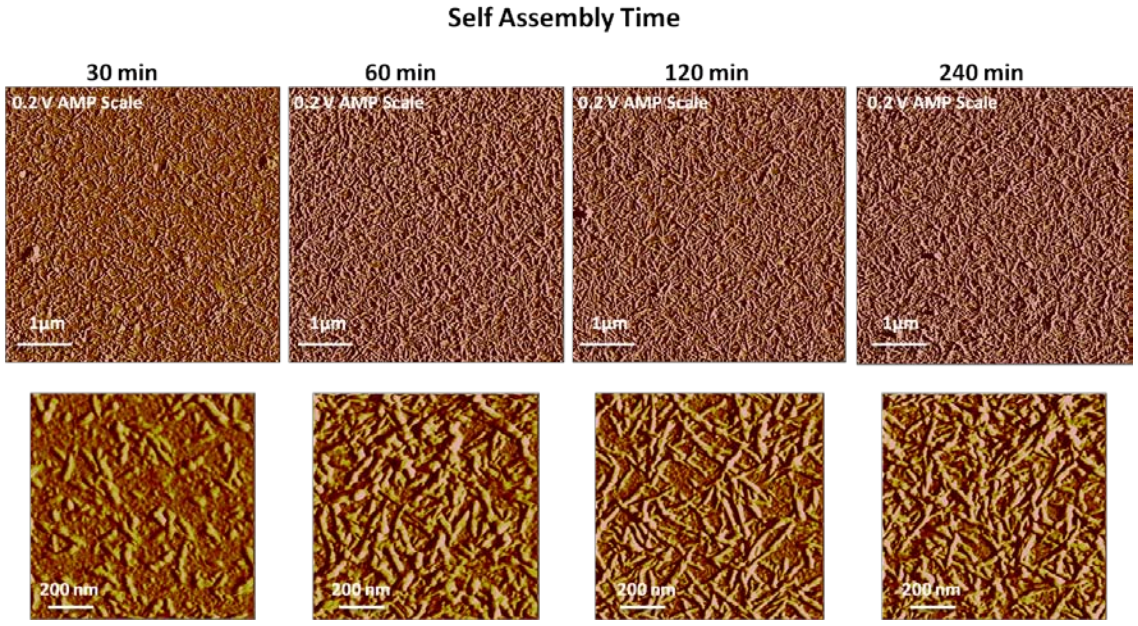

Figure 37. Amplitude AFM micrographs of self-assembled ABH1 on HYFLON® AD40 L substrates that were incubated in a 50 µg/mL ABH1 solution at 60°C for 30, 60, 120 and 240 minutes. The data scale was kept constant at 0.2 Volts.

In contrast to the solutions incubated in the presence of the SiO_2 substrate, on the hydrophobic substrate the surface is covered with globular protein deposits after only 30

min of incubation. Rodlet deposits become more evident with longer incubation times. Figure 38 represents the WCA changes observed for each of the substrates as a function of protein deposition over time (see APPENDIX for ellipsometry measured protein layer thickness over time).

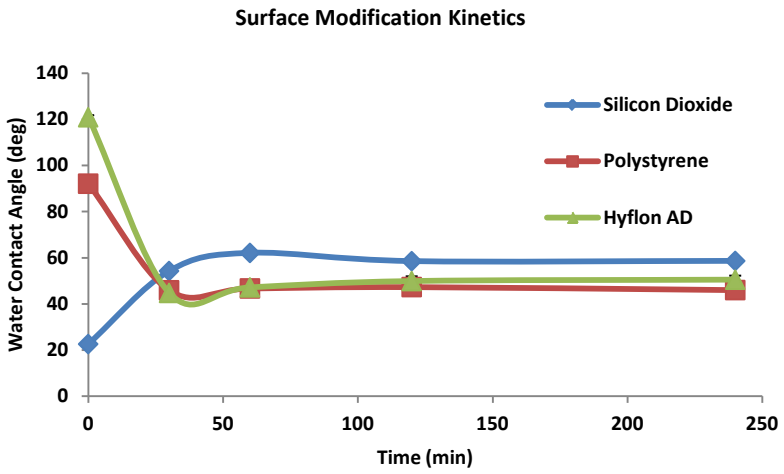

Figure 38. WCA measurements show surface modification behavior, which corresponds to assembly onto SiO_2 (blue), PS (orange) and HYFLON® AD40 L (green) at 60°C over the course of 4 hours.

ABH1 presents remarkable surface modification behavior even after short periods of time when the deposition is allowed to occur at 60 °C. The resulting water contact angle of the protein coated surface is approximately the same after a short period of incubation regardless of the starting substrate polarity or the morphology of the protein deposits. These findings indicate that the assembled protein structures formed in the bulk solution result in films with similar surface chemistries after deposition onto substrates of widely varying polarities.

Chapter Summary

The results of these studies indicate that the strength of the interfacial tension, protein concentration, time, and temperature are key factors influencing ABH1 self-

assembly, suggesting that the self-assembly process can be triggered and controlled for desired applications, such as coating of a substrate, through changes of these parameters. In aqueous solution ABH1 moves to, organizes, and orients at the air/water interface very quickly, as evidenced by results from surface tensiometry measurements and by the characteristic rod-like protein structures in AFM images of substrates onto which structures that had formed at the air/water interface were dried. QCM studies indicated that ABH1 assembles at and adheres to hydrophobic substrates, which create strong interfacial tensions with the aqueous solution, at a more rapid rate than to hydrophilic substrates. Increase in protein concentration resulted in more rapid assembly at all interfaces in the flowing QCM studies. Light scattering studies indicated increases in aggregate size with increasing protein concentration. Model AFM immersion assembly studies showed rapid assembly of ABH1 onto hydrophobic substrates, but rodlet structures were observed at the weak SiO_2/water interface only after long incubation times. CD analysis showed that ABH1 does not assemble in the bulk of solution at room temperature in quiescent solution. It was thus concluded that the rod-like structures observed on the SiO_2 surfaces in AFM images were the result of protein that had assembled at the air/water interface, followed by rodlet growth and precipitation onto the substrate. Temperature can be used to manipulate the assembly behavior of ABH1. At 60 °C, CD measurements confirmed self-assembly of the protein forming β-sheet structures in the bulk of solution. AFM studies of ABH1 deposition at elevated temperatures showed accelerated formation of fibrillar structures on the SiO_2 surfaces. After longer incubation times at elevated temperature larger fibrillar structures were observed on both hydrophilic and hydrophobic substrates. These findings indicate that ABH1 self-

assembly is accelerated at interfaces with high interfacial tensions, and the resulting protein morphology is governed by the amount of mobility the protein has at the interface. Rodlets were observed to form at room temperature, at the air/water interface, and at elevated temperatures in the bulk of solution, locations at which protein mobility is high. Scheme 7 presents a proposed model of ABH1 behavior.

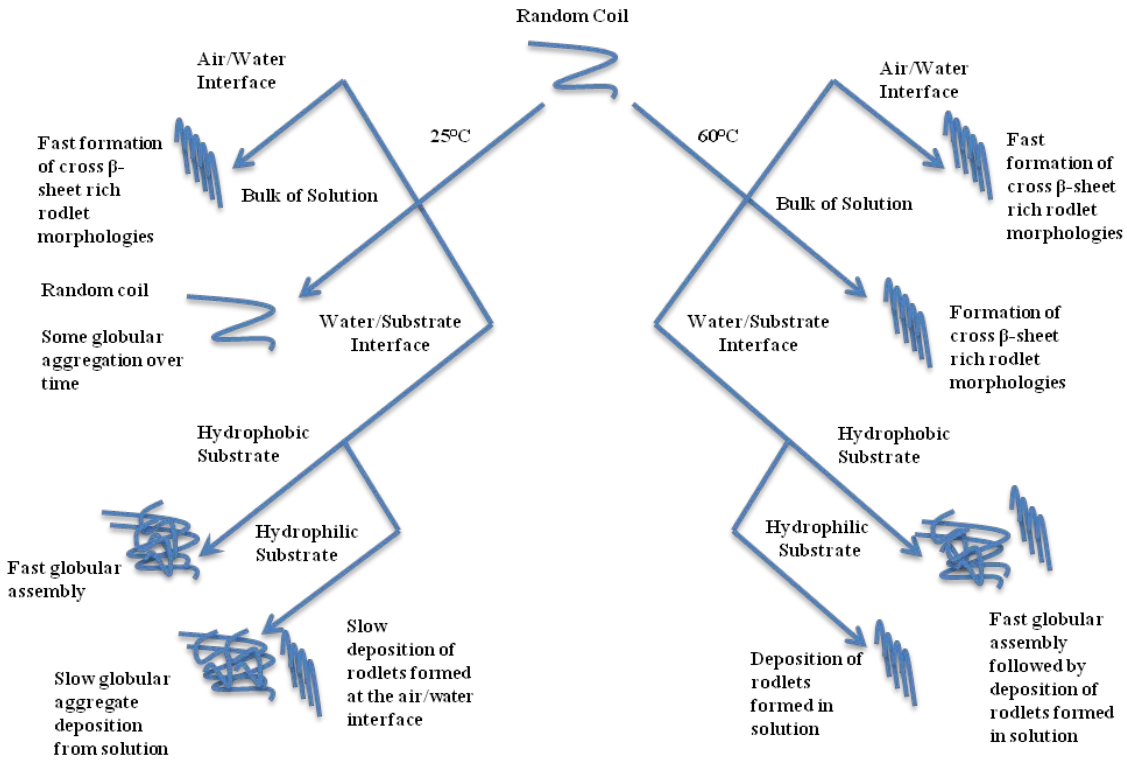

Scheme 7. Proposed assembly and deposition behavior of ABH1 as a function of temperature.

CHAPTER X
CONCLUSIONS

This work has involved (1) the design and synthesis of an amine containing poly(methacrylamide) system that presents selective toxicity to bacterial cells over eukaryotic cells and (2) the isolation and characterization of ABH1, a hydrophobin from the edible white button mushroom. The key contributions from the antimicrobial polymer research are as follows:

1. A series of methacrylamide (co)polymers with systematic variation in the ratio of primary to tertiary amine and hydrophobic content were synthesized via aqueous RAFT polymerization without the need for protecting group chemistry or extreme polymerization conditions.

2. The systematic variation in polymer composition allowed for the development of structure/activity relationships. Very low minimum inhibitory concentration (MIC) values (≤100 μg/mL) were observed against both Gram-negative *E. coli* and Gram-positive *B. subtilis* in a range of buffers for polymers having the highest primary amine content.

3. As the bulkiness of the amine increased (primary < dimethyl tertiary < diethyl tertiary) within the system so too did the amount of polymer required to kill a set concentration of bacteria. The addition of NaCl was also shown to disrupt polymer/cell interactions, reducing biocidal efficiency. However, polymers with high contents of primary amine were affected to a smaller degree.

4. Bacterial toxicity was observed both when the polymers were allowed to float freely in solution and when they were immobilized on surfaces.

5. Our strategy to create a system with fully water soluble units in hopes of reducing eukaryotic toxicity proved to be a successful plan as the polymer system induced minimal disruption to red blood cell membranes. Cell viability results also indicate that this system displays selective toxicity towards bacterial cells.

6. Two synthetic strategies to attach PAPMA were developed. The first method produced films that were stable to sonication in DMSO, but cleaved from the surface upon exposure to H_2O. The second method produced films that were stable in aqueous media.

7. The synthesis of a guanidino-containing methacrylamide was performed, and this monomer was statistically polymerized with APMA. The reaction design and execution produced a well-defined (co)polymer system.

The key contributions from the hydrophobin protein research include:

1. ABH1, a hydrophobin from the edible white button mushroom, was isolated with exceptional purity and its functionality was retained.

2. CD studies indicated that in the bulk of solution, at room temperature, ABH1 adopts a predominantly random coil conformation. ABH1 moves to, organizes, and orients at the air/water interface very rapidly (< 20 min) adopting the characteristic rod-like morphology.

3. The strength of the solution/substrate interface was shown to influence the assembly behavior of ABH1. A trend was evident in QCM investigations that, at low concentrations, ABH1 moved to non-polar substrates at a faster rate. At higher concentrations this distinction is less clear. AFM studies further suggest that ABH1 does not move quickly to polar substrates; however, given long incubation times, protein

assemblies that form at the air/water interface can precipitate from solution and deposit onto the substrate.

4. Temperature can be used to manipulate the assembly behavior of ABH1. At 60 °C, CD confirms that ABH1 has the ability to assemble, adopting β-sheet conformations, in the bulk of solution. AFM studies of deposition at elevated temperatures show that when SiO_2 is the presented substrate, rod-like ABH1 deposition onto the substrate mirrors the appearance of β-sheet assembly in the bulk of solution. When PS or Hyflon (non-polar) are the presented substrates, ABH1 moves quickly to the hydrophobic substrate interface and adopts a less ordered, globular morphology. After longer incubation times, rodlets begin to appear, mirroring the β-sheet assembly in the bulk of solution.

5. Not only is the presence of an interface important, but also the resulting protein morphology is governed by the amount of mobility the protein has at the interface. Rodlets were observed to form at room temperature at the air/water interface and at elevated temperatures in the bulk of solution, locations at which protein mobility is high.

CHAPTER XI

RECCOMENDATIONS FOR FUTURE WORK

From this work, several fundamental limitations in AMP mimic research were addressed. It was shown that a selective antimicrobial system can be developed that does not require the use of protecting group chemistry when polymerizing primary amines. Also, it was possible to produce a system that relies upon mild polymerization conditions. The greatest contribution from this research, however, is that the role of cation structure (primary versus tertiary amine) and distribution of hydrophobic moieties on antimicrobial activity is now more clearly defined. Building off the research discussed in Chapter VI, the future direction of this project could address a few additional fundamental questions.

1. Can the role of cation structure in antimicrobial mechanism be more clearly defined? Specifically, how does a gradual shift from primary amine functionality to guanidinium functionality change the mechanism of antimicrobial action?

2. Can tuning the cation structure (primary amine versus guanidinium moiety) lead to highly selective molecules that target certain bacteria types (Gram-positive versus Gram-negative)?

3. Can tuning the amine type (primary amine versus guanidinium moiety) be utilized to transform the system from antimicrobial to cell-penetrating?

As noted earlier Gabriel et al.[19] replaced the primary amine of their poly(norbornene) derivatives with a guanidinium moiety and noticed a shift in selectivity and antimicrobial mechanism. In our research, Chapter VI details the synthesis of a poly(methacrylamide) system comprised of a statistical distribution of monomers containing primary and guanidinium pendant moieties.

Currently, the (co)polymers discussed in Chapter VI are being characterized in relation to antimicrobial activity and biocompatibility; however, it is of fundamental interest to characterize these systems based on their mechanism of action. To monitor mechanistic activities, large unilamellar vesicles (LUVs) can be prepared and loaded with a fluorescent dye, calcein.[19] If the polymer disrupts or solubilizes the membrane, structural imperfections will appear in the membrane and dye will leak out, which can be monitored by a fluorescence spectrometer. If the polymer permeates through without compromising the membrane, little to no die leakage will be observed. One can also use LUVs to mimic cells with varying phospholipid content. The zwitterionic lipid 1-palmitoyl-2-oleoyl-3-phosphacidylcholine (POPC) and the anionic lipid 1-palmitoyl-2-oleoyl-phosphatidylglycerol (POPG) can be combined at different ratios to mimic the cell membranes of *E. coli* and *S. aureus*.[107] While both Gram-positive and negative bacterial cell membranes possess an overall negative charge, Gram-negative bacteria have a higher content of zwitterionic lipids.[20] RBC membranes can also be mimicked by LUVs as they are comprised of mostly zwitterionic phospholipids.

Dynamic light scattering (DLS) can also be used to monitor the interaction between the polymers and the LUVs.[107] This type of study supplements the dye-leakage tests by further investigating the biocidal mechanism. As mentioned previously, some antimicrobial polymers act by causing the aggregation of target cells; therefore, the combination of dye-leakage experiments and DLS measurements will yield many clues that will help to formulate a mechanism of action.

The work also included the isolation of ABH1 from the edible white button mushroom, and its purity was confirmed. The development of a model for the molecular

ordering that occurs upon self-assembly of ABH1 at different interfaces was accomplished and the strength of the interface was shown to affect the nature of assembly. Perhaps the most interesting conclusion from this work is that the molecular ordering of ABH1 can be manipulated by changes in temperature. With this new knowledge, the design of applications for ABH1 will be easier, as its behavior and characteristics have been clearly outlined. In regards to the future direction of research, there are a few fundamental questions that are of interest.

1. Can ABH1 be produced recombinantly and retain its ability to self-assemble at interfaces?

2. Can ABH1 mediate the attachment of bacteria to surfaces?

3. What are the limits of mechanical stability of formed ABH1 coatings?

The recombinant production of ABH1 was explored via a collaborative project between Sabine Heinhorst, Ph.D., and Sarah E Morgan, Ph.D., at The University of Southern Mississippi, in which Lacey Harris, an undergraduate researcher, developed a technique to clone ABH1 and express it in *E. coli*.[108] This project concluded before optimization of isolation had been performed. Also, it is unknown if the recombinantly produced ABH1 has the capability to self-assemble in a similar manner as the naturally occurring ABH1. The ability to recombinantly produce functional ABH1 hydrophobin protein would better allow for its mass production. One drawback with a mushroom isolation procedure is that large quantities of mushroom tissue is required to yield sufficient amounts of protein (10 g mushroom peel ≈ 70 mg hydrophobin isolation product). Future studies should strive to optimize the previously developed recombinant

procedure and to investigate the produced proteins' ability to self-assemble at and modify interfaces.

As a second direction for future research, it would be interesting to investigate if ABH1 has the ability to reduce biofilm formation of polymer substrates. Bacteria, such as *S. epidermidis*, have been shown to have a unique affinity for hydrophobic polymer surfaces. *S. epidermidis* is everywhere and typically shows little virulence to humans upon everyday contact, but it forms antibiotic resistant biofilms on hydrophobic polymer surfaces,[74] which is likely due to the hydrophobic effect.[75] Once these biofilms are formed, the infection is almost impossible to treat. Pringle and Fletcher[76] tested freshwater bacteria attachment to solid surfaces and found that all bacteria studied had a higher affinity for hydrophobic surfaces. ABH1 would serve to reduce the hydrophobicity of polymer substrates, potentially reducing the prevalence bacterial attachment.

In nature it is thought that hydrophobin layers help to prevent bacterial infections from entering the inner fruiting body tissue.[55] This could be attributed to either the lack of permeability and/or to the chemical and structural characteristics of the membrane. It would be of fundamental interest to determine if pH has an effect on microbial attachment to the ABH1 layer. As mentioned previously, hydrophobins have also been shown to have the ability to either prevent or promote secondary protein adsorption via electrostatic interactions.[89-92] Bacterial cells typically possess a net negative charge due to their specific phospholipid membrane compositions. ABH1 has an isoelectric point (pI) of 4.4; therefore, at pH 7.4 both the bacteria and the protein layer should possess net negative charges, which could serve as a repulsive force. As the pH changes, so too will

the charge characteristics of the protein, potentially leading to a shift in bacterial attachment mediation. A procedure for understanding bacterial adhesion can be modified from previously published procedures.[109] Common bacteria such as *S. aureus*, *S. epidermis*, and *E. coli* could be suspended in buffered solutions. Hydrophobin coated surfaces could then be incubated with bacterial solutions and the number of cells that adhere could be monitored by optical microscopy. It would also be possible to monitor bacterial attachment to both polymer substrates and hydrophobin coated polymer substrates via a quartz crystal microbalance (QCM) investigation.

Finally, the practical applicability of hydrophobins could be limited by the mechanical stability of formed coatings. Through an industrial partnership with Essilor USA, it was discovered that ABH1 coatings could be removed from substrates via mechanical washing with soapy water and a sponge. The goal of future research should be to explore the mechanical stability further in an attempt to quantify the forces required to remove the coating.

APPENDIX A

SUPPLEMENTARY INFORMATION FOR

HYDROPHOBIN RESEARCH

Table 8

Theoretical Predictions for Peptide Segment Masses After Enzymatic Digestion by the Protease Trypsin

Mass (Da)	Position	Modifications	Missed Cuts
8928.2060	1-89	Cys-Pam (9070.2)	1
8517.9419	5-89	Cys-Pam (8659.94)	0
429.28	1-4	None	0

Note. The intact polypeptide has a calculated mass of 8928 Da with a possible cysteine-polyacrylamide adduct at a mass of 9070 Da. Trypsin cleaves ABH1 after the fourth amino acid, which should cause a down shift in the above peaks to 8518 Da and 8660 Da, respectively.

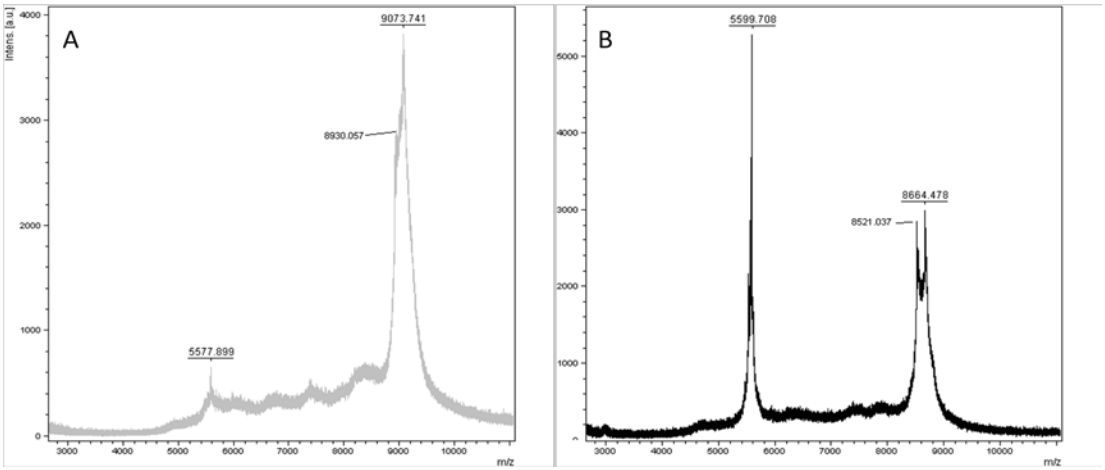

Figure 39. Maldi-ToF MS spectra of ABH1 (A) before and (B) after in gel trypsin digestion. This data agrees with the expected theoretical results shown in Table 8.

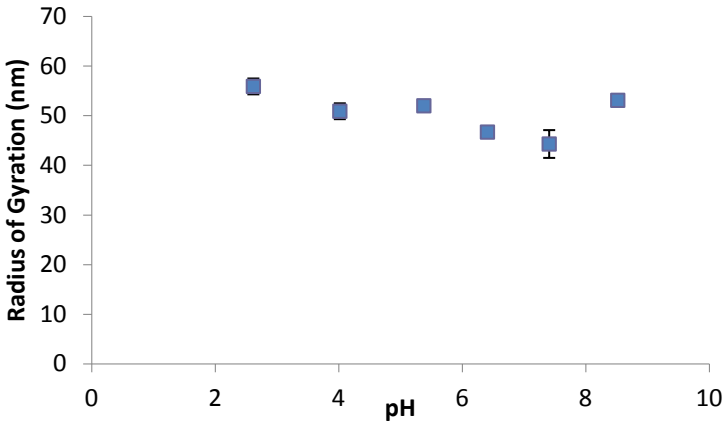

Figure 40. Static light scattering data suggest no change in aggregation behavior as a function of pH. ABH1 was dissolved in a universal buffer (sodium phosphate/citric acid) to create a pH range from approximately 3 to 8. Ionic strength was not held constant. The concentration of protein was held constant at 45 µg/mL. ABH1 aggregate size seems to be smaller in water than in buffer.

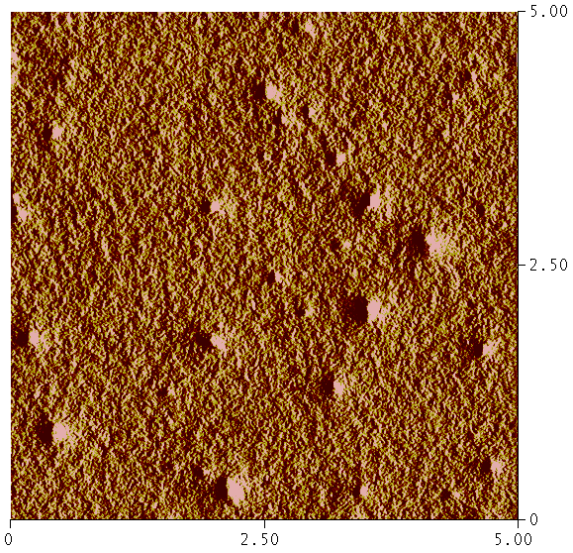

Figure 41. AFM amplitude image of ABH1 solution (75 µg/mL) light scattering sample that had been dried onto freshly cleaved mica. The globular protein aggregates in the image match SLS determined particle size.

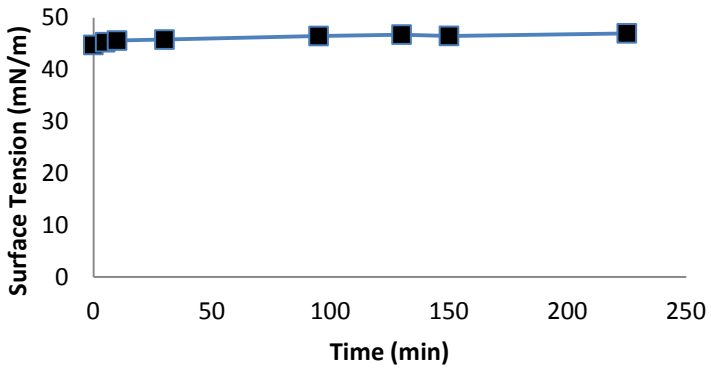

Figure 42. Surface tension measurements over the course of 4 hours. The ABH1 concentration was 30 µg/mL. Measurement of pure HPLC water yielded a surface tension value of approximately 74 mN/m. ABH1 reduced the tension of the air/water interface on a timescale faster than we could monitor. The interface remained stable over 24 hours.

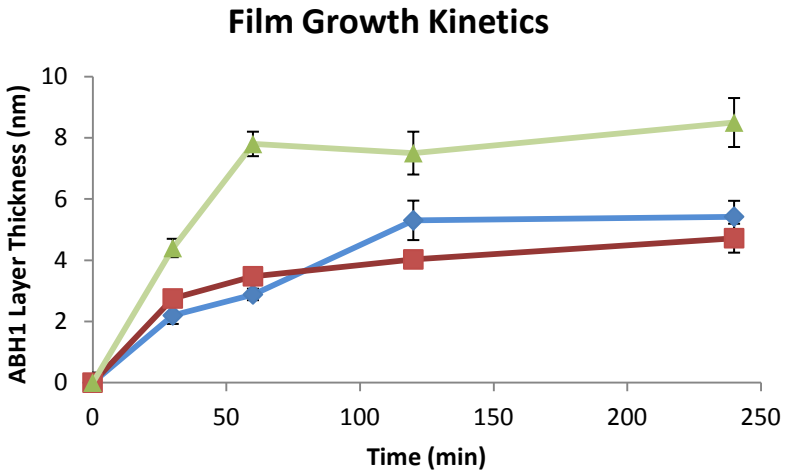

Figure 43. Film growth kinetics for ABH1 assembly onto SiO_2 (blue), PS (orange) and HYFLON® AD40 L (green) at 60°C over the course of 4 hours. Thickness was measured by ellipsometry.

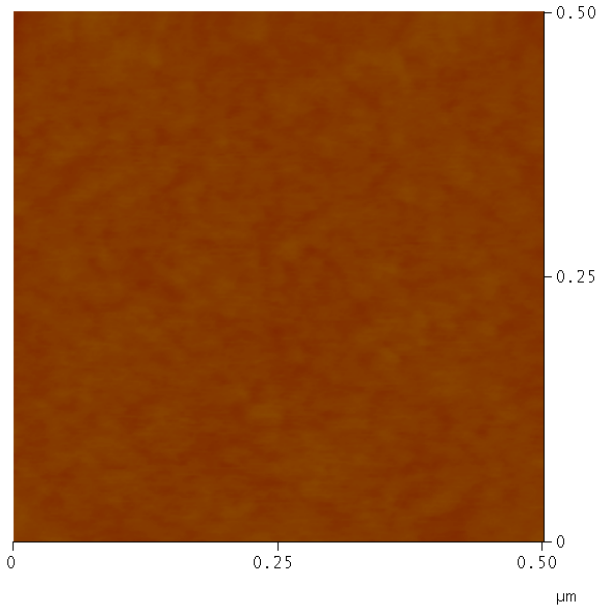

Figure 44. AFM height image of a silicon wafer after cleaning in piranha solution shows nanoscopically smooth surface. The z-scale is 20 nm.

REFERENCES

1. Klevens, R. M.; Edwards, J. R.; Richards, C. L., Jr.; Horan, T. C.; Gaynes, R. P.; Pollock, D. A.; Cardo, D. M., Estimating health care-associated infections and deaths in U.S. hospitals, 2002. *Public Health Rep.* **2007,** *122*, 160-166.
2. Zasloff, M., Antimicrobial peptides of multicellular organisms. *Nature* **2002,** *415* (6870), 389-395.
3. Yeaman, M.; Yount, N., Mechanisms of antimicrobial peptide action and resistance. *Pharmacol. Rev.* **2003,** *55* (1), 27-55.
4. Brogden, K. A., Antimicrobial peptides: Pore formers or metabolic inhibitors in bacteria? *Nat. Rev. Microbiol.* **2005,** *3*, 238-250.
5. Teuber, M.; Bader, J., Action of polymyxin B on bacterial membranes. Binding capacities for polymyxin B of inner and outer membranes isolated from *Salmonella typhimurium* G30. *Arch. Microbiol.* **1976,** *109*, 51-58.
6. Mavri, J.; Vogel, H., Ion pair formation of phosphorylated amino acids and lysine and arginine side chains: a theoretical study. *Proteins: Struct., Funct., Bioinf.* **1996,** *24* (4), 495-501.
7. Welling, M.; Lupetti, A.; Balter, H.; Lanzzeri, S.; Souto, B.; Rey, A.; Savio, E.; Paulusma-Annema, A.; Pauwels, E.; Nibbering, P., ^{99m}Tc-labeled antimicrobial peptides for detection of bacterial and *Candida albicans* infections. *J. Nucl. Med.* **2001,** *42* (5), 788-794.
8. Welling, M.; Paulusma-Annema, A.; Balter, H.; Pauwels, E.; Nibbering, P., Technetium-99m labelled antimicrobial peptides discriminate between bacterial

infections and sterile inflammations. *European Journal of Nuclear Medicine and Molecular Imaging* **2000,** *27* (3), 292-301.

9. Hancock, R.; Chapple, D., Peptide antibiotics. *Antimicrob. Agents Chemother.* **1999,** *43* (6), 1317-1323.
10. Chitnis, S.; Prasad, K., Seminalplasmin, an antimicrobial protein from bovine seminal plasma, inhibits peptidoglycan synthesis in *Escherichia coli*. *FEMS microbiology letters* **1990,** *72* (3), 281-284.
11. Xiong, Y.; S. Bayer, A.; Yeaman, M., Inhibition of intracellular macromolecular synthesis in *Staphylococcus aureus* by thrombin-induced platelet microbicidal proteins. *The Journal of infectious diseases* **2002,** *185* (3), 348-356.
12. Wieprecht, T.; Dathe, M.; Beyermann, M.; Krause, E.; Maloy, W.; MacDonald, D.; Bienert, M., Peptide hydrophobicity controls the activity and selectivity of magainin 2 amide in interaction with membranes. *Biochemistry* **1997,** *36* (20), 6124-6132.
13. Dathe, M.; Wieprecht, T., Structural features of helical antimicrobial peptides: their potential to modulate activity on model membranes and biological cells. *Biochimica et Biophysica Acta (BBA)-Biomembranes* **1999,** *1462* (1-2), 71-87.
14. Choi, S.; Isaacs, A.; Clements, D.; Liu, D.; Kim, H.; Scott, R. W.; Winkler, J. D.; Degrado, W. F., De novo design and in vivo activity of conformationally restrained antimicrobial arylamide foldamers. *Proc. Natl. Acad. Sci. U. S. A.* **2009,** *106*, 6968-6973.

15. Tew, G. N.; Scott, R. W.; Klein, M. L.; De, G. W. F., De Novo Design of Antimicrobial Polymers, Foldamers, and Small Molecules: From Discovery to Practical Applications. *Acc. Chem. Res.* **2010,** *43*, 30-39.

16. Gabriel, G. J.; Tew, G. N., Conformationally rigid proteomimetics: a case study in designing antimicrobial aryl oligomers. *Org. Biomol. Chem.* **2008,** *6*, 417-423.

17. Rennie, J.; Arnt, L.; Tang, H.; N¸sslein, K.; Tew, G. N., Simple oligomers as antimicrobial peptide mimics. *J. Ind. Microbiol. Biotechnol.* **2005,** *32* (7), 296-300.

18. Ilker, M. F.; Nuesslein, K.; Tew, G. N.; Coughlin, E. B., Tuning the hemolytic and antibacterial activities of amphiphilic polynorbornene derivatives. *J. Am. Chem. Soc.* **2004,** *126*, 15870-15875.

19. Gabriel, G. J.; Madkour, A. E.; Dabkowski, J. M.; Nelson, C. F.; Nusslein, K.; Tew, G. N., Synthetic mimic of antimicrobial peptide with nonmembrane-disrupting antibacterial properties. *Biomacromolecules* **2008,** *9*, 2980-2983.

20. Al-Badri, Z. M.; Som, A.; Lyon, S.; Nelson, C. F.; Nusslein, K.; Tew, G. N., Investigating the Effect of Increasing Charge Density on the Hemolytic Activity of Synthetic Antimicrobial Polymers. *Biomacromolecules* **2008,** *9*, 2805-2810.

21. Dathe, M.; Nikolenko, H.; Meyer, J.; Beyermann, M.; Bienert, M., Optimization of the antimicrobial activity of magainin peptides by modification of charge. *Febs. Letters* **2001,** *501* (2-3), 146-150.

22. Lienkamp, K.; Madkour, A.; Musante, A.; Nelson, C.; Tew, G., Antimicrobial polymers prepared by ROMP with unprecedented selectivity: A molecular construction kit approach. *J. Am. Chem. Soc.* **2008,** *130* (30), 9836-9843.

23. Mowery, B. P.; Lee, S. E.; Kissounko, D. A.; Epand, R. F.; Epand, R. M.; Weisblum, B.; Stahl, S. S.; Gellman, S. H., Mimicry of antimicrobial host-defense peptides by random copolymers. *J. Am. Chem. Soc.* **2007,** *129*, 15474-15476.

24. Epand, R. F.; Mowery, B. P.; Lee, S. E.; Stahl, S. S.; Lehrer, R. I.; Gellman, S. H.; Epand, R. M., Dual mechanism of bacterial lethality for a cationic sequence-random copolymer that mimics host-defense antimicrobial peptides. *J. Mol. Biol.* **2008,** *379*, 38-50.

25. Venkataraman, S.; Zhang, Y.; Liu, L.; Yang, Y.-Y., Design, syntheses and evaluation of hemo-compatible pegylated-antimicrobial polymers with well-controlled molecular structures. *Biomaterials* **2010,** *31*, 1751-1756.

26. Kuroda, K.; DeGrado, W. F., Amphiphilic Polymethacrylate Derivatives as Antimicrobial Agents. *J. Am. Chem. Soc.* **2005,** *127*, 4128-4129.

27. Palermo, E. F.; Kuroda, K., Chemical structure of cationic groups in amphiphilic polymethacrylates modulates the antimicrobial and hemolytic activities. *Biomacromolecules* **2009,** *10* (6), 1416-1428.

28. Palermo, E. F.; Sovadinova, I.; Kuroda, K., Structural Determinants of Antimicrobial Activity and Biocompatibility in Membrane-Disrupting Methacrylamide Random Copolymers. *Biomacromolecules* **2009,** *10* (11), 3098-3107.

29. Palermo, E. F.; Vemparala, S.; Kuroda, K., Cationic Spacer Arm Design Strategy for Control of Antimicrobial Activity and Conformation of Amphiphilic Methacrylate Random Copolymers. *Biomacromolecules* **2012,** *13* (5), 1632-1641.

30. Mizutani, M.; Palermo, E. F.; Thoma, L. M.; Satoh, K.; Kamigaito, M.; Kuroda, K., Design and Synthesis of Self-Degradable Antibacterial Polymers by Simultaneous

Chain-and Step-Growth Radical Copolymerization. *Biomacromolecules* **2012,** *13* (5), 1554-1563.

31. Palermo, E. F.; Kuroda, K.-I., Structural determinants of antimicrobial activity in polymers which mimic host defense peptides. *Appl. Microbiol. Biotechnol.* **2010,** *87*, 1605-1615.
32. Knauf, M. J.; Bell, D. P.; Hirtzer, P.; Luo, Z. P.; Young, J. D.; Katre, N. V., Relationship of effective molecular size to systemic clearance in rats of recombinant interleukin-2 chemically modified with water-soluble polymers. *J. Biol. Chem.* **1988,** *263* (29), 15064-16070.
33. Alidedeoglu, A. H.; York, A. W.; McCormick, C. L.; Morgan, S. E., Aqueous RAFT polymerization of 2-aminoethyl methacrylate to produce well-defined, primary amine functional homo-and copolymers. *J. Polym. Sci., Part A: Polym. Chem.* **2009,** *47* (20), 5405-5415.
34. Alidedeoglu, A. H.; York, A. W.; Rosado, D. A.; McCormick, C. L.; Morgan, S. E., Bioconjugation of D-glucuronic acid sodium salt to well-defined primary amine-containing homopolymers and block copolymers. *J. Polym. Sci., Part A: Polym. Chem.* **2010,** *48* (14), 3052-3061.
35. Li, Y.; Lokitz, B. S.; McCormick, C. L., Thermally Responsive Vesicles and Their Structural "Locking" through Polyelectrolyte Complex Formation. *Angew. Chem. Int. Ed.* **2006,** *45*, 5792-5795.
36. Vasilieva, Y. A.; Thomas, D. B.; Charles, W.; McCormick, C. L., Direct controlled polymerization of a cationic methacrylamido monomer in aqueous media via the RAFT process. *Macromolecules* **2004,** *37* (8), 2728-2737.

37. Convertine, A. J.; Benoit, D. S. W.; Duvall, C. L.; Hoffman, A. S.; Stayton, P. S., Development of a novel endosomolytic diblock copolymer for siRNA delivery. *J. Controlled Release* **2009,** *133* (3), 221-229.

38. Vasilieva, Y. A.; Scales, C. W.; Thomas, D. B.; Ezell, R. G.; Lowe, A. B.; Ayres, N.; McCormick, C. L., Controlled/living polymerization of methacrylamide in aqueous media via the RAFT process. *J. Polym. Sci., Part A: Polym. Chem.* **2005,** *43*, 3141-3152.

39. Tyagi, A. K.; Malik, A., Antimicrobial potential and chemical composition of Mentha piperita oil in liquid and vapour phase against food spoiling microorganisms. *Food Control* **2011,** *22*, 1707-1714.

40. Gulati, N.; Rastogi, R.; Dinda, A. K.; Saxena, R.; Koul, V., Characterization and cell material interactions of PEGylated PNIPAAM nanoparticles. *Colloids Surf., B* **2010,** *79* (1), 164-173.

41. Guo, W.; Hensarling, R.; LeBlanc, A.; Hoff, E.; Braranek, A.; Patton, D., Rapid Synthesis of Polymer Brush Surfaces via Microwave-Assisted Surface-Initiated Radical Polymerization (μW-SIP). *Macromol. Rapid. Commun.* **2012,** *33*, 863-868.

42. Hensarling, R.; Doughty, V.; Chan, J.; Patton, D., Clicking Polymer Brushes with Thiol-Yne Chemistry: Inside and Out. *J. Am. Chem. Soc.* **2009,** *131*, 14673-14675.

43. Van, d. W. P.; Moret, E. E.; Schuurmans-Nieuwenbroek, N. M. E.; Van, S. M. J.; Hennink, W. E., Structure-Activity Relationships of Water-Soluble Cationic

Methacrylate/Methacrylamide Polymers for Nonviral Gene Delivery. *Bioconjugate Chem.* **1999,** *10*, 589-597.

44. Lowe, A. B.; McCormick, C. L. In *Stimuli Responsive Water-Soluble and Amphiphilic Copolymers*, ACS Publications: 2001; pp 1-13.
45. Palermo, E. F.; Lee, D. K.; Ramamoorthy, A.; Kuroda, K., Role of Cationic Group Structure in Membrane Binding and Disruption by Amphiphilic Copolymers. *J. Phys. Chem. B* **2011,** *115*, 366-375.
46. Oren, Z.; Shai, Y., Selective lysis of bacteria but not mammalian cells by diastereomers of melittin: structure-function study. *Biochemistry* **1997,** *36* (7), 1826-1835.
47. Plank, L.; Harvey, J., Generation time statistics of Escherichia coli B measured by synchronous culture techniques. *J. Gen. Microbiol.* **1979,** *115* (1), 69.
48. Product Information Sheet for ATCC HTB-22. http://www.atcc.org/attachments/17392.pdf.
49. Henriques, S. T.; Melo, M. N.; Castanho, M. A. R. B., Cell-penetrating peptides and antimicrobial peptides: How different are they? *Biochem. J.* **2006,** *399*, 1-7.
50. Treat, N. J.; Smith, D. D.; Teng, C.; Flores, J. D.; Abel, B. A.; York, A. W.; Huang, F.; McCormick, C. L., Guanidine-Containing Methacrylamide (Co) polymers via a RAFT: Toward a Cell-Penetrating Peptide Mimic. *ACS Macro Letters* **2011,** *1*, 100-104.
51. Wessels, J., Hydrophobins, unique fungal proteins. *Mycologist* **2000,** *14* (4), 153-159.

52. Schuren, F. H.; Wessels, J. G., Two genes specifically expressed in fruiting dikaryons of Schizophyllum commune: homologies with a gene not regulated by mating-type genes. *Gene* **1990,** *90* (2), 199-205.

53. Wessels, J.; De Vries, O.; Asgeirsdottir, S. A.; Schuren, F., Hydrophobin Genes Involved in Formation of Aerial Hyphae and Fruit Bodies in Schizophyllum. *Plant Cell* **1991,** *3* (8), 793-799.

54. Wosten, H. A.; de Vocht, M. L., Hydrophobins, the fungal coat unravelled. *Biochim. Biophys. Acta.* **2000,** *1469* (2), 79-86.

55. De Groot, P. W.; Roeven, R. T.; Van Griensven, L. J.; Visser, J.; Schaap, P. J., Different temporal and spatial expression of two hydrophobin-encoding genes of the edible mushroom *Agaricus bisporus*. *Microbiology* **1999,** *145 (Pt 5)*, 1105-1113.

56. Scholtmeijer, K.; Wessels, J. G.; Wosten, H. A., Fungal hydrophobins in medical and technical applications. *Appl. Microbiol. Biotechnol.* **2001,** *56* (1-2), 1-8.

57. Wosten, H.; De Vries, O.; Wessels, J., Interfacial Self-Assembly of a Fungal Hydrophobin into a Hydrophobic Rodlet Layer. *Plant Cell* **1993,** *5* (11), 1567-1574.

58. Wang, X.; Shi, F.; Wosten, H. A.; Hektor, H.; Poolman, B.; Robillard, G. T., The SC3 hydrophobin self-assembles into a membrane with distinct mass transfer properties. *Biophys. J.* **2005,** *88* (5), 3434-3443.

59. Hektor, H. J.; Scholtmeijer, K., Hydrophobins: proteins with potential. *Curr. Opin. Biotechnol.* **2005,** *16* (4), 434-439.

60. Morgan, S. E.; Li, J.; Benson, S. D.; Misra, R.; Cannon, G. C., Nanoprobe evaluations of hydrophobin-modified hair. *Polymer Preprints* **2005,** *46* (2), 517-518.

61. Misra, R.; Li, J.; Cannon, G. C.; Morgan, S. E., Nanoscale reduction in surface friction of polymer surfaces modified with Sc3 hydrophobin from Schizophyllum commune. *Biomacromolecules* **2006,** *7* (5), 1463-1470.

62. Gebbink, M. F.; Claessen, D.; Bouma, B.; Dijkhuizen, L.; Wosten, H. A., Amyloids--a functional coat for microorganisms. *Nat. Rev. Microbiol.* **2005,** *3* (4), 333-341.

63. Janssen, M. I.; van Leeuwen, M. B.; Scholtmeijer, K.; van Kooten, T. G.; Dijkhuizen, L.; Wosten, H. A., Coating with genetic engineered hydrophobin promotes growth of fibroblasts on a hydrophobic solid. *Biomaterials* **2002,** *23* (24), 4847-4854.

64. Wosten, H. A., Hydrophobins: multipurpose proteins. *Annu. Rev. Microbiol.* **2001,** *55*, 625-646.

65. Martin, G. G.; Cannon, G. C.; McCormick, C. L., Sc3p hydrophobin organization in aqueous media and assembly onto surfaces as mediated by the associated polysaccharide schizophyllan. *Biomacromolecules* **2000,** *1* (1), 49-60.

66. Vries, O.; Fekkes, M.; Wösten, H.; Wessels, J., Insoluble hydrophobin complexes in the walls of Schizophyllum commune and other filamentous fungi. *Archives of Microbiology* **1993,** *159* (4), 330-335.

67. de Vocht, M. L.; Reviakine, I.; Wosten, H. A.; Brisson, A.; Wessels, J. G.; Robillard, G. T., Structural and functional role of the disulfide bridges in the hydrophobin SC3. *J. Biol. Chem.* **2000,** *275* (37), 28428-28432.

68. Butko, P.; Buford, J. P.; Goodwin, J. S.; Stroud, P. A.; McCormick, C. L.; Cannon, G. C., Spectroscopic evidence for amyloid-like interfacial self-assembly of hydrophobin Sc3. *Biochem. Biophys. Res. Commun.* **2001,** *280* (1), 212-215.

69. Wang, X.; de Vocht, M. L.; de Jonge, J.; Poolman, B.; Robillard, G. T., Structural changes and molecular interactions of hydrophobin SC3 in solution and on a hydrophobic surface. *Protein Sci.* **2002,** *11* (5), 1172-1181.

70. Stroud, P. A.; Goodwin, J. S.; Butko, P.; Cannon, G. C.; McCormick, C. L., Experimental evidence for multiple assembled states of Sc3 from Schizophyllum commune. *Biomacromolecules* **2003,** *4* (4), 956-967.

71. Wang, X.; Graveland-Bikker, J. F.; de Kruif, C. G.; Robillard, G. T., Oligomerization of hydrophobin SC3 in solution: from soluble state to self-assembly. *Protein Sci.* **2004,** *13* (3), 810-821.

72. de Vocht, M. L.; Scholtmeijer, K.; van der Vegte, E. W.; de Vries, O. M.; Sonveaux, N.; Wosten, H. A.; Ruysschaert, J. M.; Hadziloannou, G.; Wessels, J. G.; Robillard, G. T., Structural characterization of the hydrophobin SC3, as a monomer and after self-assembly at hydrophobic/hydrophilic interfaces. *Biophys. J.* **1998,** *74* (4), 2059-2068.

73. Wang, X.; Permentier, H. P.; Rink, R.; Kruijtzer, J. A.; Liskamp, R. M.; Wosten, H. A.; Poolman, B.; Robillard, G. T., Probing the self-assembly and the accompanying structural changes of hydrophobin SC3 on a hydrophobic surface by mass spectrometry. *Biophys. J.* **2004,** *87* (3), 1919-1928.

74. Mack, D., Molecular mechanisms of Staphylococcus epidermidis biofilm formation. *J. Hosp. Infect.* **1999,** *43 Suppl*, S113-S125.

75. Doyle, R. J., Contribution of the hydrophobic effect to microbial infection. *Microbes. Infect.* **2000,** *2* (4), 391-400.

76. Pringle, J. H.; Fletcher, M., Influence of Substratum Wettability on Attachment of Freshwater Bacteria to Solid Surfaces. *Appl. Environ. Microbiol.* **1983,** *45* (3), 811-817.

77. Donlan, R. M., Biofilm formation: a clinically relevant microbiological process. *Clin. Infect. Dis.* **2001,** *33* (8), 1387-1392.

78. Scholtmeijer, K.; Janssen, M. I.; Gerssen, B.; de Vocht, M. L.; van Leeuwen, B. M.; van Kooten, T. G.; Wosten, H. A.; Wessels, J. G., Surface modifications created by using engineered hydrophobins. *Appl. Environ. Microbiol.* **2002,** *68* (3), 1367-1373.

79. Wang, R.; Yang, Y.; Qin, M.; Wang, L.; Yu, L.; Shao, B.; Qiao, M.; Wang, C.; Feng, X., Biocompatible Hydrophilic Modifications of Poly (dimethylsiloxane) Using Self-Assembled Hydrophobins. *Chem. Mater.* **2007,** *19* (13), 3227-3231.

80. Bilewicz, R.; Witomski, J.; Van der Heyden, A.; Tagu, D.; Palin, B.; Rogalska, E., Modification of electrodes with self-assembled hydrophobin layers. *J. Phys. Chem. B* **2001,** *105* (40), 9772-9777.

81. Hippeli, S.; Elstner, E. F., Are hydrophobins and/or non-specific lipid transfer proteins responsible for gushing in beer? New hypotheses on the chemical nature of gushing inducing factors. *Z. Naturforsch* **2002,** *57* (1-2), 1-8.

82. Kuhnle, A.; Exner, C.; Bollshweiler, C.; Subkowski, T.; Baus, U.; Lemairi, H.; Karos, M. Aqueous monomer emulsions containing hydrophobin. Patent: **2009**.

83. Exner, C.; Baus, U.; Holoch, J.; Bollchweiler, C.; Subkowski, T.; Karos, M.; Lemairi, H. Hydrophobin as a coating agent for expandable or expnded thermoplastic polymer particles. Patent: **2006**.

84. Subkowski, T.; Lemairi, H.; Karos, M.; Hammer, S.; Karl, J.; Posselt, D. Use of proteins as an antifoaming constituent in fuels. Patent: **2007**.

85. Montag, T.; Baus, U.; Karos, M.; Subkowski, T.; Schwendemann, V.; Baur, R.; Mendera, C.; Bollchweiler, C.; Lemairi, H. Method for coating fibre substrate surfaces. Patent: **2007**.

86. Bimbo, L. M.; Makila, E.; Raula, J.; Laaksonen, T.; Laaksonen, P.; Strommer, K.; Kauppinen, E. I.; Salonen, J.; Linder, M. B.; Hirvonen, J., Functional hydrophobin-coating of thermally hydrocarbonized porous silicon microparticles. *Biomaterials* **2011,** *32* (34), 9089-9099.

87. Sarparanta, M. P.; Bimbo, L. M.; Makila, E. M.; Salonen, J. J.; Laaksonen, P. H.; Helariutta, A.; Linder, M. B.; Hirvonen, J. T.; Laaksonen, T. J.; Santos, H. A., The mucoadhesive and gastroretentive properties of hydrophobin-coated porous silicon nanoparticle oral drug delivery systems. *Biomaterials* **2012,** *33* (11), 3353-3362.

88. Aimanianda, V.; Bayry, J.; Bozza, S.; Kniemeyer, O.; Perruccio, K.; Elluru, S. R.; Clavaud, C.; Paris, S.; Brakhage, A. A.; Kaveri, S. V., Surface hydrophobin prevents immune recognition of airborne fungal spores. *Nature* **2009,** *460* (7259), 1117-1121.

89. Corvis, Y.; Walcarius, A.; Rink, R.; Mrabet, N. T.; Rogalska, E., Preparing catalytic surfaces for sensing applications by immobilizing enzymes via hydrophobin layers. *Anal. Chem.* **2005,** *77* (6), 1622-1630.

90. Takahashi, T.; Maeda, H.; Yoneda, S.; Ohtaki, S.; Yamagata, Y.; Hasegawa, F.; Gomi, K.; Nakajima, T.; Abe, K., The fungal hydrophobin RolA recruits polyesterase and laterally moves on hydrophobic surfaces. *Mol. Microbiol.* **2005,** *57* (6), 1780-1796.

91. Wang, Z.; Lienemann, M.; Qiau, M.; Linder, M. B., Mechanisms of protein adhesion on surface films of hydrophobin. *Langmuir* **2010,** *26* (11), 8491-8496.

92. von Vacano, B.; Xu, R.; Hirth, S.; Herzenstiel, I.; Ruckel, M.; Subkowski, T.; Baus, U., Hydrophobin can prevent secondary protein adsorption on hydrophobic substrates without exchange. *Anal. Bioanal. Chem.* **2011,** *400* (7), 2031-2040.

93. De Groot, P. W.; Schaap, P. J.; Sonnenberg, A. S.; Visser, J.; Van Griensven, L. J., The Agaricus bisporus hypA gene encodes a hydrophobin and specifically accumulates in peel tissue of mushroom caps during fruit body development. *J. Mol. Biol.* **1996,** *257* (5), 1008-1018.

94. Lugones, L.; Wosten, H.; Berkenkamp, K.; Sjollema, K.; Zagers, J.; Wessels, J., Hydrophobins line air channels in fruiting bodies of Schizophyllum commune and *Agaricus bisporus*. *Mycol. Res.* **1999,** *103* (05), 635-640.

95. Lugones, L. G.; Bosscher, J. S.; Scholtmeyer, K.; de Vries, O. M.; Wessels, J. G., An abundant hydrophobin (ABH1) forms hydrophobic rodlet layers in Agaricus bisporus fruiting bodies. *Microbiology* **1996,** *142*, 1321-1329.

96. Lugones, L. G.; Wosten, H. A.; Wessels, J. G., A hydrophobin (ABH3) specifically secreted by vegetatively growing hyphae of Agaricus bisporus (common white button mushroom). *Microbiology* **1998,** *144 (Pt 8)*, 2345-2353.

97. Gunning, A.; De Groot, P.; Visser, J.; Morris, V., Atomic Force Microscopy of a Hydrophobin Protein from the Edible Mushroom Agaricus bisporus. *J. Colloid Interface Sci.* **1998,** *201* (2), 118-126.

98. Trypsin Gold, Mass Spectrometry Grade Technical Bulletin. http://www.promega.com/resources/protocols/technical-bulletins/101/trypsin-gold-mass-spectrometry-grade-protocol/ (accessed September 25, 2012).

99. Hydrophobin [Agaricu bisporus] CAA62331. http://www.ncbi.nlm.nih.gov/protein/CAA62331 (accessed September 25, 2012).

100. PeptideMass. http://web.expasy.org/peptide_mass/ (accessed September 25, 2012).

101. Sauerbray, G. Z., Use of vribrating quartz for thin film weighing and microweighing. *Phys.* **1959,** *155*, 206-222.

102. Tchuenbou-Magaia, F.; Norton, I.; Cox, P., Hydrophobins stabilised air-filled emulsions for the food industry. *Food Hydrocolloids* **2009,** *23* (7), 1877-1885.

103. Hiemenz, P.; Lodge, T., *Polymer Chemistry*. 2nd ed.; Boca Raton: CRC Press: **2007**.

104. Wosten, H. A. B.; van Wetter, M.-A.; Lugones, L. G.; van der Mei, H. C.; Busscher, H. J.; Wessels, J. G. H., How a fungus escapes the water to grow into the air. *Current Biology* **1999,** *9* (2), 85-88.

105. Marx, K. A., Quartz crystal microbalance: a useful tool for studying thin polymer films and complex biomolecular systems at the solution-surface interface. *Biomacromolecules* **2003,** *4* (5), 1099-1120.

106. Grunér, M. S.; Szilvay, G. R.; Berglin, M.; Lienemann, M.; Laaksonen, P.; Linder, M. B., Self-assembly of Class II Hydrophobins on Polar Surfaces. *Langmuir* **2012,** *28* (9), 4293-4300.

107. Gabriel, G. J.; Pool, J. G.; Som, A.; Dabkowski, J. M.; Coughlin, E. B.; Muthukumar, M.; Tew, G. N., Interactions between Antimicrobial Polynorbornenes and Phospholipid Vesicles Monitored by Light Scattering and Microcalorimetry. *Langmuir* **2008,** *24,* 12489-12495.

108. Harris, L. The isolation and characterization of ABH1 hydrophobin protein from Agaricus bisporus. Honors College Thesis, The University of Southern Mississippi, Hattiesburg, MS, **2009**.

109. West, S. L.; Salvage, J. P.; Lobb, E. J.; Armes, S. P.; Billingham, N. C.; Lewis, A. L.; Hanlon, G. W.; Lloyd, A. W., The biocompatibility of crosslinkable copolymer coatings containing sulfobetaines and phosphobetaines. *Biomaterials* **2004,** *25* (7-8), 1195-1204.